AD-A062 862 GENERAL RESEARCH CORP MCLEAN VA F/G 19/1
AN OBSCURING AEROSOL DISPERSION MODEL. VOLUME I. DEVELOPMENT AN--ETC(U)
DEC 78 R ZIRKIND DAAK02-76-C-0366
UNCLASSIFIED CR-231-VOL-1 NL

1 OF 2
ADA
062862

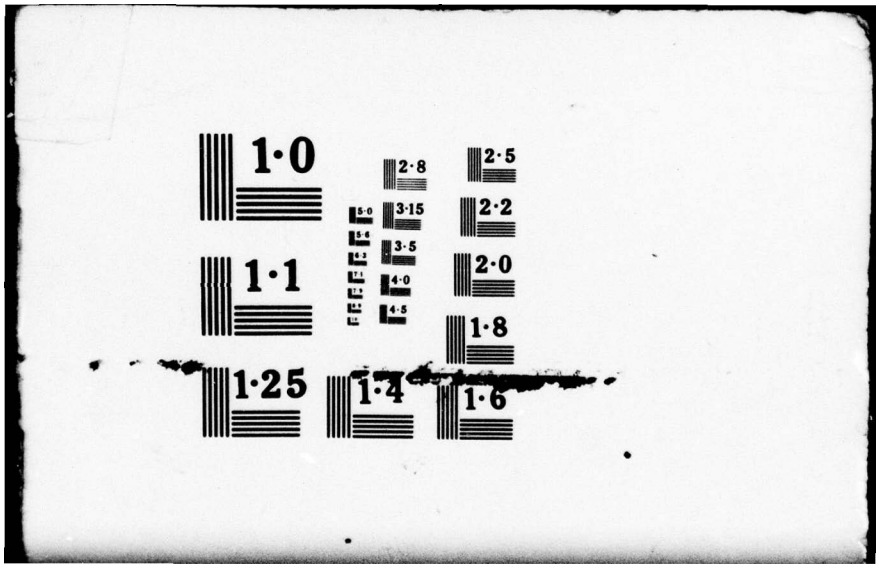
1·0
1·1
1·25
1·4
1·6
1·8
2·0
2·2
2·5
2·8
3·15
3·5
4·0
4·5

LEVEL II

Final Report CR-231

2 SC

An Obscuring Aerosol Dispersion Model

VOLUME I
DEVELOPMENT & EXPOSITION

By

Ralph Zirkind

Prepared for:

U.S. Army ERADCOM
Night Vision and EO Laboratory
Fort Belvoir, Virginia
Contract No. DAAK02-74-C-0366

OPERATIONS ANALYSIS GROUP

GENERAL RESEARCH CORPORATION

A SUBSIDIARY OF FLOW GENERAL INC.

7655 Old Springhouse Road, McLean, Virginia 22102

December 1978

Final Report CR-231

An Obscuring Aerosol Dispersion Model

VOLUME I
DEVELOPMENT & EXPOSITION

By

Ralph Zirkind

Prepared for:

U.S. Army ERADCOM
Night Vision and EO Laboratory
Fort Belvoir, Virginia
Contract No. DAAK02-74-C-0366

OPERATIONS ANALYSIS GROUP

GENERAL RESEARCH CORPORATION

A SUBSIDIARY OF FLOW GENERAL INC.

7655 Old Springhouse Road, McLean, Virginia 22102

December 1978

UNCLASSIFIED

SECURITY CLASSIFICATION OF THIS PAGE (When Data Entered)

REPORT DOCUMENTATION PAGE

READ INSTRUCTIONS BEFORE COMPLETING FORM

1. REPORT NUMBER (6)
2. GOVT ACCESSION NO.
3. RECIPIENT'S CATALOG NUMBER

4. TITLE (and Subtitle)
AN OBSCURING AEROSOL DISPERSION MODEL. Volume I. DEVELOPMENT & EXPOSITION. (2nd)

5. TYPE OF REPORT & PERIOD COVERED (9)
Final Rept. July 77 - Nov 78

6. PERFORMING ORG. REPORT NUMBER

7. AUTHOR(s) (10)
Ralph Zirkind

8. CONTRACT OR GRANT NUMBER(s) (15)
DAAKØ2-76-C-Ø366

9. PERFORMING ORGANIZATION NAME AND ADDRESS
General Research Corporation
Westgate Research Park
McLean, Virginia, 22102

10. PROGRAM ELEMENT, PROJECT, TASK AREA & WORK UNIT NUMBERS (16)
62709A; 1L162709DH95, OV, 023CJ; 65713A, 1X765713DF26, OV, 009CJ

11. CONTROLLING OFFICE NAME AND ADDRESS (11)
Director (DELNV-VI)
Night Vision and Electrooptics Laboratory
Fort Belvoir, Virginia 22060

12. REPORT DATE (17) ØØ2, ØØ
December 78

13. NUMBER OF PAGES

14. MONITORING AGENCY NAME & ADDRESS(if different from Controlling Office) (14) CR-231-VOL-1

15. SECURITY CLASS. (of this report)
Unclassified

15a. DECLASSIFICATION/DOWNGRADING SCHEDULE

16. DISTRIBUTION STATEMENT (of this Report)
Distribution of this document is unlimited. (12) 126p.

17. DISTRIBUTION STATEMENT (of the abstract entered in Block 20, if different from Report)

18. SUPPLEMENTARY NOTES

19. KEY WORDS (Continue on reverse side if necessary and identify by block number)
Obscurants
Smoke Model
Aerosol Properties

20. ABSTRACT (Continue on reverse side if necessary and identify by block number)
This report presents the development and exposition of a non-Gaussian aerosol dispersion model and, the effect of the aerosol cloud on electrooptical systems. Explicitly, algorithms are provided to calculate both the transmitted and backscattered (glare) radiation components.

Finally, a validation of the model was performed with good to excellent agreement. This validation included the space-time history of cloud geometry and aerosol concentration.

DD FORM 1 JAN 73 1473 EDITION OF 1 NOV 65 IS OBSOLETE

UNCLASSIFIED

SECURITY CLASSIFICATION OF THIS PAGE (When Data Entered)

410 304 78 12 21 010 LB

SUMMARY

An approach to the effect of smoke or obscuring aerosols, on battlefield electrooptical systems is presented here; that is, a first generation model is constructed to be consistent with an earlier developed GRC target acquisition model for CARMONETTE or any combat simulation model. The attack taken here is to consider smoke as a transient modification to the natural terrain height, i.e., the spatial coordinate (x,y,z) become [x,y,z+Z(t)].

The approach philosophy was to initially generate a simple semi-empirical model that includes all the necessary ingredients to permit, if necessary, the generation of a model of greater sophistication and accuracy. The model is not the classical approach (Gaussian); however, the model validates extremely well with field tests.

In Volume 1 a technical discussion is presented and includes smoke generation mechanisms, smoke dispersal, radiation propagation and validation tests of the proposed smoke model. In Volume 2 we present the model structure in a step-by-step procedure.

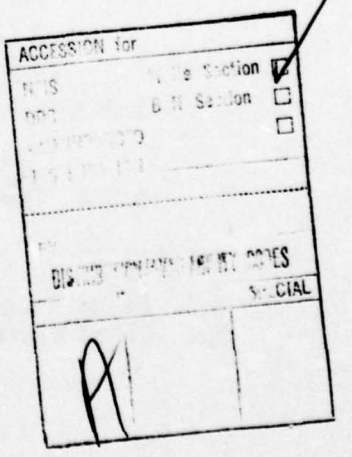

Table of Contents

APPENDIXES

FIGURES

TABLES

BACKGROUND

This report is a formalization and extension of an earlier working paper[1] prepared for the U.S. Army Night Vision Laboratory on a model to describe the smoke cloud, aerosol concentration and optical properties of the cloud where the smoke is generated by various smoke munitions.

The diffusion of smoke and other pollutants have been studied for the past forty years, both theoretically and experimentally. Since the primary transport mechanism is atmospheric turbulence, the overall activity has been directed in solving the turbulent diffusion equation and measuring the cloud parameters in terms of solution(s) to the latter equation, i.e, in terms of mean values and their variances. The difficulty with the application of this approach is that (1) the use of the "turbulent" diffusion equation to find the mean concentration and mean cloud dimensions is normally based on 3 minute averaging periods or longer and (2) the boundary condition for the near ground source is inadequate. Of the two issues the former may be more critical since in most cases of interest the smoke generation is over in at most several minutes and fluctuation statistics are not satisfied by the suggested sampling time.

Also, there is some question, from purely a mathematical standpoint whether the Sutton-Calder solution (parabolic diffusion equation) is appropriate in place of a hyperbolic one (Monin-Oboukov).

Hence, for the present purpose, namely <u>to generate a simple model that can be utilized in a combat simulation model</u> an empirical approach

---

[1] Zirkind, R., "An Initial Approach to a Smoke Model," General Research Corporation Working Paper, July 1977.

is adopted throughout its formulation so that the degradation effects of smoke on military systems can be readily calculated.

This volume is basically divided into two parts: Part 1 will be devoted to the concepts related to the model; and Part 2 will deal with the model proper, its formulation and several validation tests. Whenever ancillary data are required these will be provided in one of several appendices.

The writer wishes to express his appreciation to A. Linz and R. Bergeman, Night Vision Laboratory, for their encouragement during the initial study phase, Seymour Berler, DIA, for his interest and agency support, and L. Obert, NVL COTR, for review of this report.

1. INTRODUCTION

1.1 OBJECTIVE

The primary goal is to develop a methodology for the introduction of a smoke model into CARMONETTE that will handle both passive battlefield and active battlefield electrooptical systems, visual and infrared. This includes target acquisition devices, missile seekers and laser systems.

1.2 APPROACH

We consider here smoke as an artificially controlled, obscuring aerosol cloud which can reduce the transmittance along the line of sight between the observer and the target. In addition, backscatter or self emission from the cloud may reduce the apparent contrast at the sensor input.

Thus for passive and active systems operating in visible (photopic), near infrared (NIR), mid infrared, or far infrared (LWIR) wavelengths we must consider the wavelength dependence of the optical properties of smokes. It should be noted that there are a variety of smokes* with different optical characteristics. In order to establish the macroscopic effects of a smoke cloud, the spatial distribution of the aerosols is required as a function of time. The latter depends in a complex way on the terrain, meteorological conditions, character of smoke munitions employed, etc. The subject is treated in a statistical fashion.

From a combat simulation viewpoint, smoke in the line of sight is equivalent to a time dependent loss of intervisibility. The approach

*Smokes and obscuring aerosols are used in an equivalent sense.

suggested here is to examine the proposition that a smoke cloud or screen be treated as a time dependent terrain feature, that is the incremental increase in the spatial coordinates, see schematic diagram.

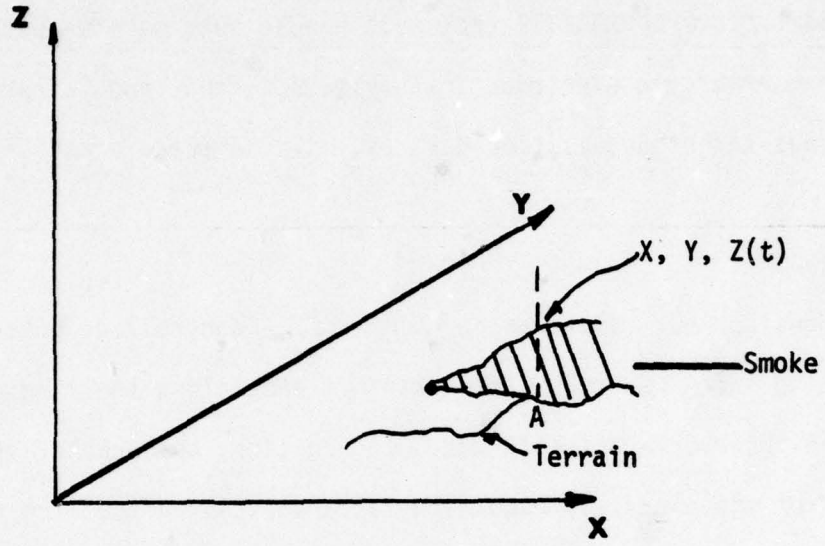

The terrain coordinates at "A" are (x,y,z) and with smoke became (x,y, z(t)); i.e., not unlike vegetation.

The advantages of this approach are (1) inputting a time dependence for smoke effects is compatible with the CARMONETTE war game, (2) the integration of smoke with terrain may be a significant aid for "intelligence preparation for the battlefield" and (3) the concept handles intervisibility for various weapons, i.e., ground-ground, ground-air, air-ground, air-air, and target acquisition systems.

Briefly then, we require the formulation of the following:

(1) The general properties of smoke munitions

(2) Temporal-spatial history of a smoke plume and

(3) The radiation transfer properties of the plume.

The amount of data on each of the above is limited particularly as the degree of detail increases: (1) for hygroscopic smokes, the quantity of energy released is required to determine the smoke plume temperature history; (2) a valid description of the smoke plume is vital for the prediction of thermal systems and the turbulence effects on laser systems; and (3) the particulate distribution will affect the radiation transfer properties.

In the latter instance, the transmittance and glare may be estimated; however, the inhomogeneities generated by random distributed smoke munitions can seriously affect thermal systems operations beyond pure transmittance and, must be taken into account.

2. BASIC CONCEPTS

2.0 INTRODUCTION

We will discuss here a number of basic concepts needed to support the smoke model that is to be presented later and, of course, its limitation. These concepts cover sources, cloud dynamics, and optical properties.

2.1 SOURCES

The smoke munitions used by various countries can be categorized as (1) non-exothermic aerosol generators and (2) exothermic aerosol generators. A primary example of the latter is white phosphorus. Next we can divide these into instantaneous (short burn time) and finite burn time.* Finally, we may have "point" sources and finite line sources. The latter is accomplished by detonating several munitions or submunitions in a linear array, a linear array of smoke pots or, a linear line of spray. For completeness several standard munitions are given in Appendix A.

2.2 YIELD

There are a variety of chemical compositions that may be used for smoke generation namely white and red phosphorus (WP/RP), hexachlorethane + Zn (HC), fog/diesel oil, $TiCl_4$(FM), chlorosulfonic acid + SO_3(FS), sulfuric acid + SO_3(Oleum), and anthracene mixtures. The products may

*We wish to make a distinction between reaction time to convert the munition fill into smoke and smoke cloud persistence. Here we utilize the time to convert primary material into smoke.

range from mists of oil droplets, metallic chlorides ($ZnCl_2$, $TiCl_4$, NH_4Cl, etc.) to acid droplets like sulfuric acid or phosphoric acid (H_3PO_4). The interaction of these aerosol products with atmospheric moisture varies considerably; that is, they may absorb moisture and grow or react chemically like phosphorus pentoxide to form a phosphoric acid and, thereby increase in weight. This property has been parameterized as the smoke yield where the yield is defined by the expression

$$Y = \frac{\text{weight of smoke generated}}{\text{weight of smoke fill}} \cdot \eta^* \qquad (2.1)$$

It should be noted that the significance lies in the fact smoke concentration is given by gms of smoke/unit volume.

Johnson and Forney (see Appendix B) show that the yield is dependent on the relative humidity (RH) for those aerosols affected by atmospheric moisture. The expressions for several smokes are given below where the constant applies for RH ≤ bracket value:

$$\begin{aligned} Y(\text{fog oil}) &= 1 \\ Y(WP) &= .003\ (RH - 40)^{1.67} + 2.9 \\ Y(ZnCl_2) &= .051\ (RH - 50)^{.85} + 1 \\ Y(AlCl_3/H_2SO_4) &= .016\ (RH - 20)^{1.25} + 1.4 \end{aligned} \qquad (2.2)$$

The use of Y = 1 for fog oil is appropriate with the possible exception at high relative humidity since the oil may adsorbed moisture.

Clearly the yield is related to the hygroscopic properties of the condensation nuclei produced by the reactions of the smoke material. The nuclei have radii between 0.2 - 0.5 μm with a mode of ~0.25 μm and, subsequently the smoke particles will grow to a mean value of ~1.2 μm.

*η is munition efficiency and is assumed to be equal to 1.

The use of relative humidity rather than absolute humidity in eq. (2.2) is further substituted in measurements by Novikov et al.[2] In Fig. 1 we present the ratio of liquid mass/solid mass vs relative humidity and absolute water content for $Fe_4Cl/AlCl_3$/phosphoric acid aerosols. From Fig. 1 we can deduce that the yield is better represented as a function of relative humidity since the ordinate is proportional the yield minus one. The relative humidity effect should be reflected in the optical properties of the smoke cloud.

2.3 SMOKE CLOUD

To familiarize the reader we will present here an abbreviated overview of concepts related to the diffusion of smoke and other pollutants by the atmosphere. For more general discussion we suggest refs 3, 4, 5.

2.3.1 Stability Parameter

The behavior of the smoke cloud is determined primarily by the turbulent properties of the atmosphere within which the smoke is being generated and therefore, is with the exception of phosphorus a momentum exchange process. In the case of phosphorus or other strong exothermic smokes, the rate of heat generated by the associated exothermic reactions is the initial dominant mechanism, i.e., for about 200 secs or less. For the present we will discuss the momentum dominant smoke cloud.

---

[2] Novikov, Yu. I. et al, Advances in Aerosol Physics, No. 2, 90, Israel Program for Scientific Translations, 1970.

[3] Pasquill, F., Atmospheric Diffusion, Van Nostrand, London 1962.

[4] Briggs, G. A., Plume Rise, ESSA, Oak Ridge, Tenn, 1969 (TID-25075).

[5] Meteorology and Atomic Energy (D. H. Slade, ed), AEC, 1968 (TID-24190).

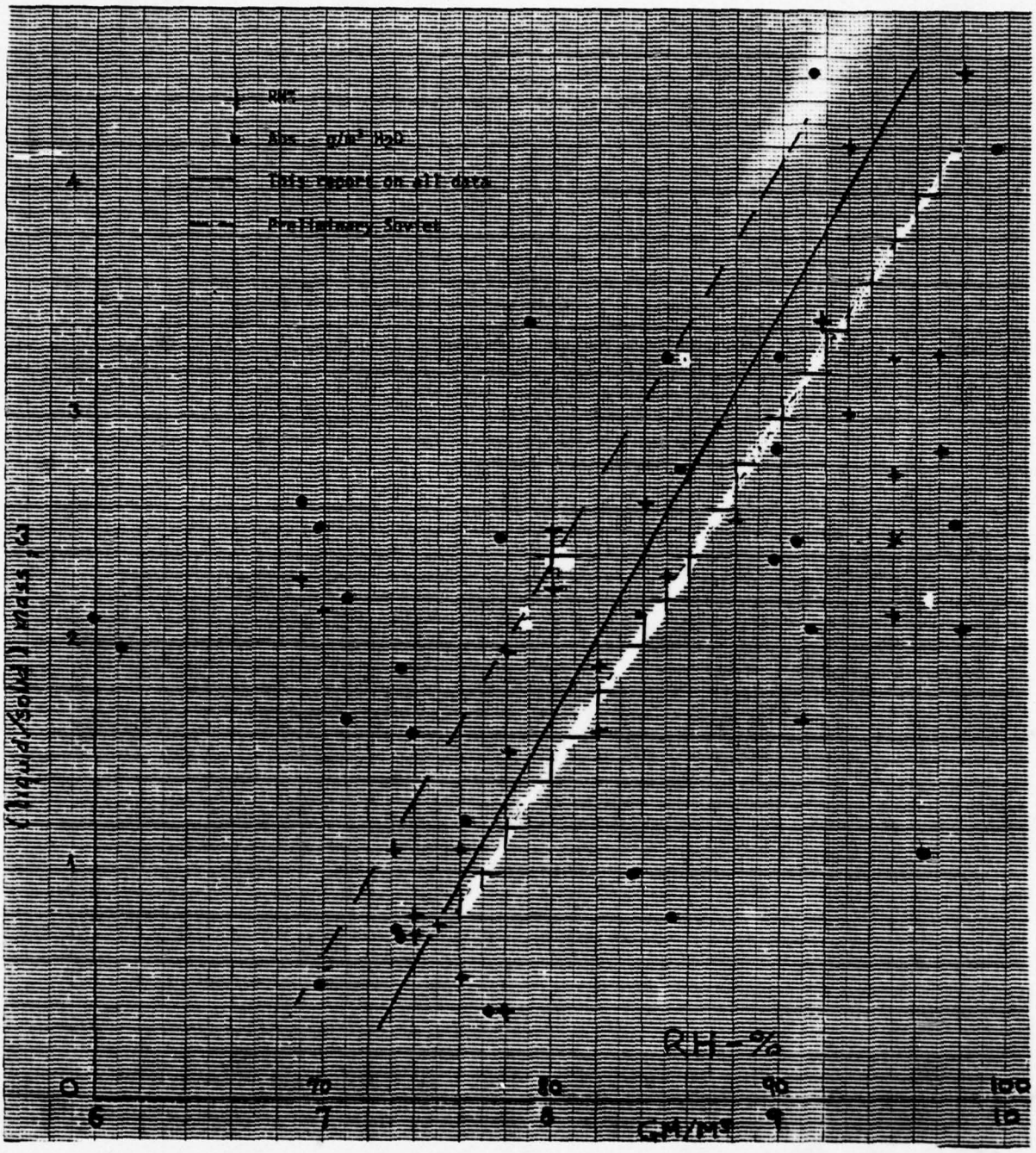

Fig. 1 (Liquid/Solid) Aerosol Mass vs Relative Humidity (%), Absolute Water Density

-- $\omega = .175(RH) - 11.62$

— $\omega = .18\ (RH) - 12.72$

To categorize the atmospheric capability to diffuse a smoke cloud Pasquill, British Meteorological Office, introduced a stability classification which depends on net radiation flux near the surface and wind speed. Clearly the former is dependent upon diurnal variations, cloudiness, soil moisture, etc. The three basic stability classes are (1) unstable, (2) neutral and (3) stable which can be further refined to several subclasses of unstable and stable conditions. Neutral conditions exist with cloudy skies or high wind speeds. Hence the Pasquill classification system runs from A (extremely unstable) to G (extremely stable) with D = neutral, see Table 1 and Appendix C.

Table 1

Pasquill Stability Categories

Surface wind speed at 10 m ($m\ sec^{-1}$)	Insolation			Night	
	Strong	Moderate	Slight	Thinly overcast or ≥4/8 low cloud	≤3/8 cloud
2	A	A-B	B	—	—
2-3	A-B	B	C	E	F
3-5	B	B-C	C	D	E
5-6	C	C-D	D	D	D
>6	C	D	D	D	D

It should be noted that the classical stability definition is given by by the atmospheric lapse rate relative to the adiabatic lapse rate, i.e.,

$$\text{Potential temperature, } \theta(T) = \Delta T + \Gamma$$

where $\Delta T = T(10m) - T(0.5m)$ and $\Gamma = .098^{\circ}C/10m$. When $\theta(T) \gtreqless 0$ the condition is stable, neutral and unstable respectively. An atmospheric

stability parameter is given by

$$\tilde{s} = \frac{g}{T} \frac{\partial \theta}{\partial z} \qquad \text{(I)}$$

where g and T are gravitational acceleration (m/sec^2) and ambient ground temperature (°K) respectively. This parameter is used later in eq. (3.15d).

From ref (6) we reproduce for completeness Table 2 wherein a continuous representation of the Pasquill classification is given. Here Class A = -3, Class G = 3 and the neutral condition = 0.

Table 2

Key Used to Estimate the Continuous Stability Classification*

Mean wind speed ($m\ sec^{-1}$)	Day			Transient period		Night	
	Incoming solar radiation					Thinly overcast or 4/8 low cloud	Cloud ≤3/8
	Strong	Moderate	Slight	Day→	←Night		
<2	−3.5~−3.0	−3.0~−2.2	−2.5~−2.0	−1.5~−0.5	0.5~1.5	1.5	2.5
2~3	−3.0~−2.2	−2.2~−2.0	−2.0~−1.0	−1.0~−0.3	0.5~1.0	1.5~0.6	2.5~1.6
3~5	−2.2~−1.5	−2.0~−1.0	−1.0~−0.5	−1.0~−0.3	0.3~0.5	0.6~0.3	1.6~0.5
5~6	−1.5~−1.0	−1.0~−0.3	−0.5~−0.2	−0.4~−0.2	0.2~0.4	0.3~0.1	0.5~0.3
6~8	−1.0~−0.3	−0.3~−0.1	−0.2~ 0	−0.3~−0.1	0.1~0.2	0.1~0	0.3~0.1
>8	−0.3	−0.1	0	0		0	0.1

* Note: 1) See Turner (1969) for overall explanations.

To appreciate the statistical variations in Pasquill Categories we provide in Table 3, the values for 291 stations throughout the U.S. and several stations in Hawaii and Puerto Rico where the column legends are self explanatory.

[6] Shir, C.C. and Shieh, L. F., Jour. Appl. Met., Mar 1974, p. 189.

Table 3

Statistical Summary of Percent Frequencies of Pasquill Stability Categories

	A	B	C	Unstable (A+B+C)	Neutral (D)	Stable (E+F+G)
Annual:Mean	1.0	6.6	11.2	18.8	47.7	33.4
Mode	1	4	11	19	54	28
Std. Dev.	1.1	3.0	2.2	5.2	12.2	7.3
Range	0-5	1-16	5-19	6-33	13-77	15-54
314 stns.						
Winter:Mean	0.0	2.6	7.1	9.7	57.5	32.7
Mode	0	1	6	7	66	26,30,32
Std. Dev.	0.2	2.5	2.9	5.1	15.0	10.4
Range	0-1	0-14	2-18	2-28	14-88	10-66
291 stns.						
Spring:Mean	1.0	6.2	11.2	18.4	52.2	29.3
Mode	1	4,6	11	14	62	23
Std. Dev.	1.2	3.0	2.5	5.7	12.6	7.3
Range	0-6	1-16	5-21	6-36	13-79	12-53
291 stns.						
Summer:Mean	2.6	11.3	16.4	30.2	36.1	33.7
Mode	1	9	16	34	32	38
Std. Dev.	2.3	4.0	2.5	5.8	12.5	7.7
Range	0-13	2-21	9-29	13-49	12-73	11-49
291 stns.						
Autumn:Mean	0.5	6.2	10.2	16.9	44.5	38.5
Mode	0	6	9	18	38	42
Std. Dev.	0.8	3.7	2.6	6.2	13.9	8.1
Range	0-5	1-19	3-19	4-34	9-75	18-57
291 stns.						

Table 4

Prevalence of Pasquill Stability Categories over the Netherlands*

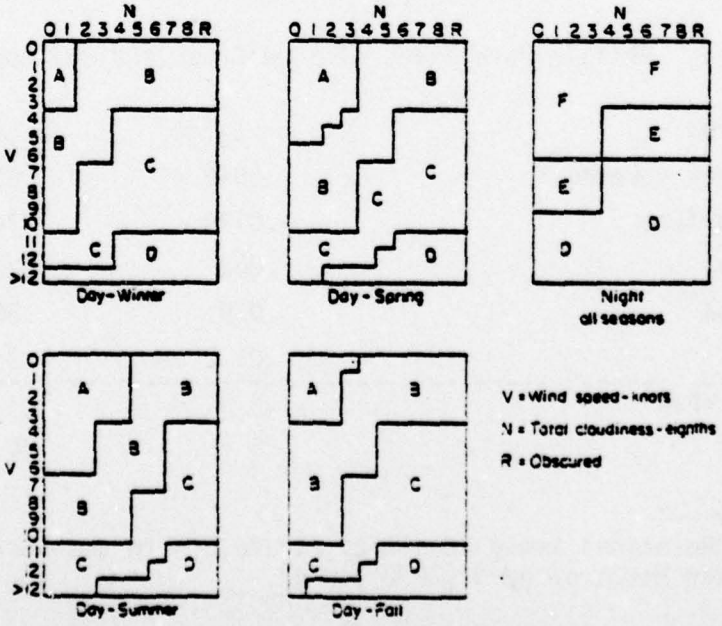

*Reproduced from G. H. Strom, "Atmospheric Dispersion of Stack Effluents" p. 257; Air Pollution (A.C. Stern, Ed) 2nd Ed. Academic Press, 1968.

The above discrete or continuous Pasquill system suffers from the absence of surface roughness dependence. Golder[7] established a relation between the Monin-Obukov length, L, and Pasquill stability namely,

$$1/L = \pm [d \ln (1.2 + 10/Z_o)]^2 \, 10^{f(s)}, \tag{2.3}$$

and

$$f(s) = -a/(1 + b|s|^c)$$

where s = stability class defined in Table 2.

a = 4, b = 1.3, c = 0.85, d = 0.21659 and

Z_o = is the surface roughness in meters.

The surface roughness, Z_o, varies from ~10^{-3}m (sand) to ~.10 m (tall vegetation). Kung and Lettau have found an empirical relation between Z_o and plant height, h_c, i.e.,

$$\log Z_o = -1.24 + 1.19 \log h_c \tag{2.4}$$

Several values of Z_o, h_c are given in Table 5.

Table 5. Profile Parameters of Some Crops and Buildup Areas

Crop	Z_o(m)	h_c(m)
Plane, snow covered	.0049	.03
Grassy surface	.0173	.10
Low grass	.032	.20
High grass	.039	.30
Wheat	.04	1.3
Suburban area	.4	
Urban	6	24

[7] Golder, D. "Relations Among Stability Parameters in the Surface Layer," Boundary Layer Meteorology 3 (1972), p 47.

The Monin-Obukov length is defined by the relationship

$$L = \frac{u* \frac{\partial \bar{u}}{\partial z}}{\frac{g}{\bar{T}} \cdot \frac{\partial \bar{T}}{\partial z}} \quad (m) \tag{2.5}$$

where $u*$ = friction velocity ($<<\bar{u}$) (m/sec)

g = acceleration of gravity (m/sec^2)

$\bar{T}$ = mean temperature ($z \leq 10m$)

$\bar{u}$ = mean wind speed ($z \leq 10m$)

The effect of surface roughness is to reduce in some instances the stability class; i.e., say B→C or D→E, see Fig. 2.

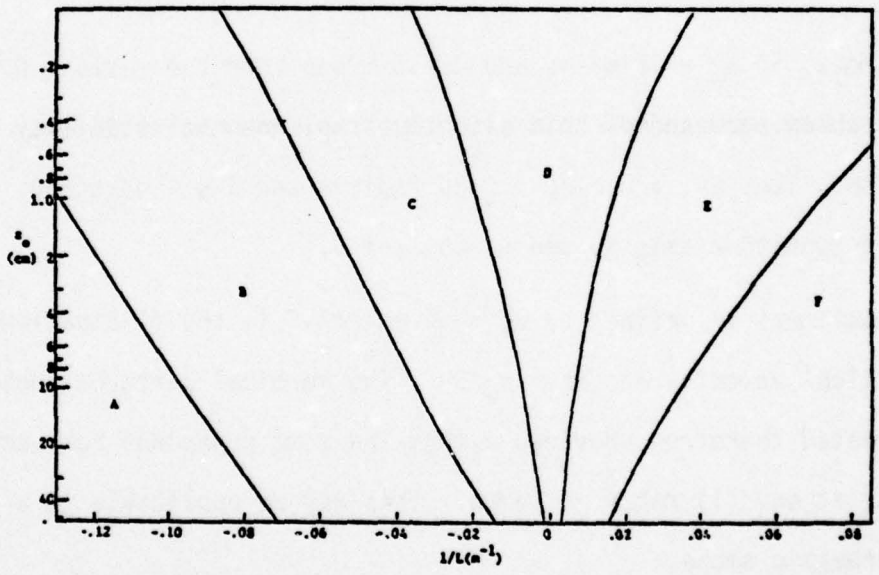

Fig. 2. 1/L as a Function of Pasquill Classes and Z_o

Evidently a factor that plays a major role in stability is the standard deviation of vertical component of turbulence, σ_w. This can be represented by an approximate expression,

$$\sigma_w \text{ (cm/sec)} \approx 12.3 \ (u_1 - 1)$$

where u_1 = wind speed (m/sec) at 1 meter altitude.

The inclination of the wind speed is defined by $(\sigma_w/\bar{u})$ and, therefore,

$$\frac{\sigma_w}{\bar{u}} = \frac{12.3(u_1 - 1)}{\bar{u}} .$$

For example, if σ_w = .5 m/sec and $\bar{u}$ = 5 m/sec then the ratio = 0.1 radians which corresponds to a slightly stable→neutral stability condition. That is, for $\sigma_w/\bar{u} > 0.25$ radians and $\bar{u} \leq 4$ m/sec an unstable condition exists, see p. 66, ref 3.

Gustiness is defined by $\sqrt{\overline{w'^2}/\bar{u}^2}$ where w' is the fluctuations in the vertical velocity and, is $\sim \sigma_w/\bar{u}$. The vertical perturbations can be estimated therefrom provided $u_1(t)$, the time dependent horizontal velocity at one (1) meter is known. This may be applicable to a non-exothermic smoke.

For the present work we adopt the simple stability definitions given in Table 1.

2.3.2 Solution to Diffusion Equation

We now present a brief discussion of the Gaussian solutions to the diffusion equation so that these may be compared to the empirical diffusion expressions used here.

The notation for the following discussion is given below as follows:

x = direction of mean wind velocity vector

y = perpendicular to x

z = perpendicular to plane $(x\text{-}y)$

$\bar{u}$ = time mean wind speed in $\vec{x}$ (m/sec)

$\bar{v}$ = time mean wind speed in $\vec{y}$ (m/sec)

$\bar{w}$ = time mean wind speed in $\vec{z}$ (m/sec)

t = time (sec)

V = volume (m^3)

Q_s = smoke munition fill weight (gm)

Q = smoke weight (gm)

C = concentration (g/m^3)

X = plume/cloud length (m)

Y = plume/cloud width (m)

Z = plume/cloud height (m)

K_i = turbulent coefficient (cm^2/sec) ($i = x,y,z$)

(a) Instantaneous Sources*

Consider a smoke source at the origin of a rectangular coordinate system (0,0,0) at time, $t = 0$, then with a wind in the x-direction having a wind mean speed, $\bar{u}$, the mean concentration of smoke will be defined by

$$\bar{C}(x,y,z,t) = \frac{Q}{8(\pi Kt)}3/2 \quad \exp -([x - \bar{u}t]^2 + y^2 + z^2/4Kt) \qquad (2.6)$$

*See discussion in Section 2.5.

Similarly for an instantaneous infinite line source we can write

$$\bar{C}(x,z,t) = \frac{Q}{4\pi Kt} \quad \exp - [(x - \bar{u}t)^2 + z^2/4Kt] \qquad (2.7)$$

Clearly, these solutions are travelling Gaussian distributions with increasing entrainment of air to dilute the smoke concentration. Further, for the infinite line source the diffusion is independent of "y". Graphically, the result is depicted in Fig. 3.

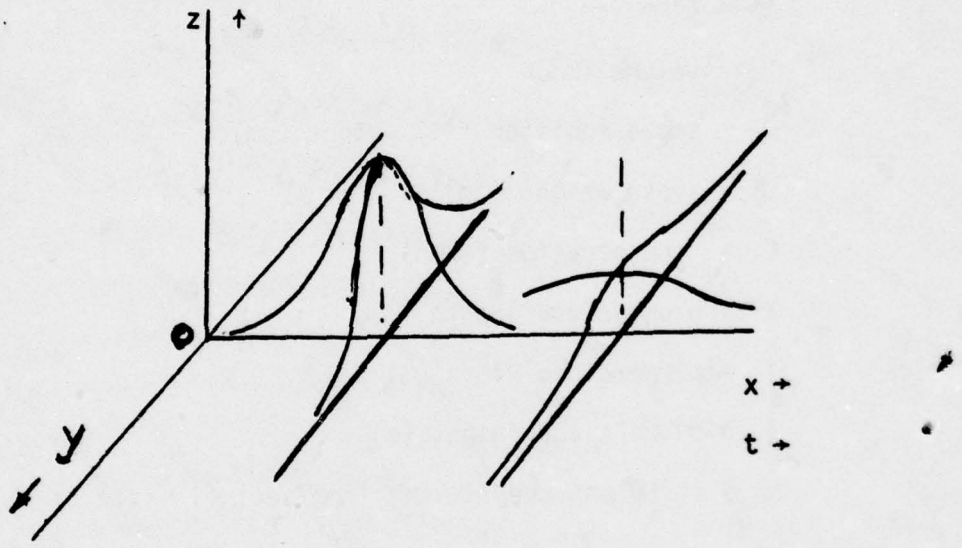

Fig. 3. Schematic of Gaussian Solutions

(b) Continuous Sources

For the point source one obtains an expression of the time-mean concentration in the form

$$\bar{C} = \frac{Q}{4\pi Kr} \left[1 - \phi\left(\frac{r}{\sqrt{4Kt}}\right)\right] \qquad (2.8)$$

where Q is the release of smoke in (gm/sec) and ϕ is the normal probability integral function. When a wind is introduced then

$$\bar{C} \simeq \frac{Q}{4\pi Kr} \exp -\left[\frac{\bar{u}\,(y^2+z^2)}{4Kx} \right] \tag{2.9}$$

In the above solutions, turbulence was considered to be isotropic, i.e., $K = K_x = K_y = K_z$, if we assume no downward transport at surface, $K_z d\bar{c}/dz \to 0$ and conservation of downwind flux, we obtain for a continuous point source.

$$\bar{C} = \frac{Q}{4\pi r (K_y K_z)^{\frac{1}{2}}} \exp -\left[\frac{\bar{u}}{4x} \left(\frac{y^2}{K_y} + \frac{z^2}{K_z} \right) \right] \tag{2.10}$$

For a continuous line source of infinite length with constant mean wind, $\bar{u}$, perpendicular to y-axis and constant K_z, the concentration is found to be

$$\bar{C}(x,z) \simeq \frac{Q}{(2\pi K_z x)^{\frac{1}{2}}} \exp -\left[\frac{\bar{u} z^2}{4K_z x} \right] \tag{2.11}$$

where K_z can be found from

$$\bar{u} = \bar{u}_1 (z/z_1)^{p*} \quad \text{and}$$

$$K_z = K_1 z^{(1-p)**}$$

Subscript 1 refers to the value at 1 meter. Further the exponent "p" has values $0<p<1$; for strong lapse $p \simeq 0.1$, $p \sim 0.8$ for extreme stability and $p \simeq 1/7$ for neutral stability and smooth ground surface.

---

* This is called the power profile law.
**This is called the conjugate profile law.

Calder proposed a definition of $\bar{u}$ in a alternate form namely,

$$\bar{u} = u_* \, q \, (Z/Z_0)^{\alpha} \tag{2.12}$$

where Z_0, q, α are constants and u_* is the friction velocity. Here the value of "Z" is the mean cloud height which is to be established from preliminary observational estimates and is required before q and α may be evaluated.

The eddy diffusion coefficient is defined by the expression

$$K_z = k \, u_* \, Z_0 \, (Z/Z_0)^{\beta} \tag{2.13}$$

where k is the Karman constant ≈ 0.4 and Z_0 is the roughness length in centimeters.

Numerical solutions to the diffusion equation are presented in graphical form in ref 8. In addition, there is a thorough discussion of the classical Sutton treatment which is based upon fluctuation theory and his solutions reduce to the above if $K/\bar{u}$ = constant.

2.3.3 Observations on Diffusion Solution

Irrespective of the origin of the solutions, i.e., (1) Roberts - presented above, (2) Sutton, Calder, etc., they all suffer from major deficiencies, (a) they are steady state solutions; and (b) the cloud-ground plane interaction is inadequate. For example, Shir (6) points out that the effects of surface roughness can influence the concentration distribution significantly. Similarly, Hildebrand (9) states as recently as 1977 "there has not yet been a systematic verification of the Gaussian

---

[8] Haltiner, G. J. and Martin, F.L., Dynamical and Physical Meteorology, McGraw-Hill, New York, 1957.

[9] Hildebrand, G., J.A.M. 1977.

solution of the equation for differing atmospheric conditions." Nevertheless, for sustained operations, i.e., where smoke pots or generators are utilized whose duration ≥ 30 mins, use of the Calder-Sutton equation may be a fair approximation.

2.3.4 Thermal Effects

In the above discussion we have not indicated any dependence on thermal effects due to munition material. The magnitude of the effects will vary from minor (smoke pots) to major (white phosphorus) and thereby alter, to varying degrees, the smoke cloud dynamics. We will now examine several effects.

The temperature differential, $T_{smoke}-T_{ambient\ air}$, determines the buoyancy or rise and, therefore the rise will be less for an inversion (stable) than for lapse (unstable) condition.

For non-explosive or, weak to non-exothermic reactive smoke munitions (material) the resultant initial rise is insignificant about 1-2 meters subsequently the cloud dynamics is purely mechanical, i.e., momentum exchange only.

For explosive munitions where the HE will release about $5x10^5$ watts/# the rise for a standard shell (105/155mm) may be $\leq$ 5 meters. Again this may be considered as an initial rise upon which is superimposed the normal rise. When a white phosphorus round is utilized the strong exothermic reaction will sustain the rise since the heat content stays for a long period and, therefore, strongly interacts with the mechanical forces.

This topic has received modest attention with respect to modelling of smoke generated by explosive munitions.

Lastly, the ABC-M3A3 pulse jet smoke generator is a complex device because it emits about sixty (60) puffs of hot oil per second. To a first approximation one may assert that a continuous source representation is adequate and valid. The excess exhaust temperature is expended by the expanding jet and, therefore, the cloud rise is not unlike any smoke pot.

2.4 OPTICAL PROPERTIES

The optical properties of the different product aerosols and obscurants vary with wavelength and composition, see Appendix E. As noted earlier, the metal chlorides and phosphorus compounds are hygroscopic and, therefore, behave differently* in the visible, near infrared and infrared. Laboratory or field observations performed at low relative humidity $\leq$ 40% may be entirely inaccurate if corrections are not made when the relative humidity exceeds 50%. The errors arise from two sources (1) the particle size distribution will change; and (2) the optical properties will change similar to those observed for ambient atmospheric aerosols. The effect of the distribution function is primarily of interest to a detail radiation transfer calculation whereas the other error can lead to underestimates of transmittance or overestimates of backscatter.

2.5 OBSERVATIONS

From the above discussion the formulation of an analytical model for smoke clouds generated by munitions and the ability to establish the degradation induced in military optical systems is froth with uncertainties and difficulties. The latter is partially applicable to a semi-empirical approach.

*Good scatterers in infrared and also absorbers.

To illustrate, consider the generation of a smoke cloud by artillery shells. In Fig. 4(a) we show the progress of cloud in the "x" - direction" of a 105mm WP fired statically and dynamically. First we see that the dynamic curve is significantly different than for the static case which can be associated with the dispersion of the smoke material. In Fig. 4(b) we see that there are large variations in the near surface dispersal of the smoke fill material and smoke cloud.

Currently, the model described in the next section considers the mortar and artillery as an instantaneous source which extrapolates to a diameter of 9.1 meters and a height* of 2.73 meters at time zero. The AMSAA/JTCG model defines the source as a function of fill weight, e.g., the value for the 155mm is ~9 meters and height ~2.7-5 meters whereas for lesser weight munitions the values are somewhat less. Although the latter numbers are consistent, the AMSAA model suggests that the entire cloud, assuming a Gaussian distribution function, is contained within 4x the latter numerical values and this may not validate the data available from static tests like the model proposed here. Operationally the live shots are important. This fact must be evaluated in the model proposed here.

The saving feature is that great precision is not crucial; only sound estimates for operational usage are necessary to establish system performance and smoke munition effectiveness. To meet these requirements a smoke model will be described in the following sections.

*For non-white phosphorus munitions.

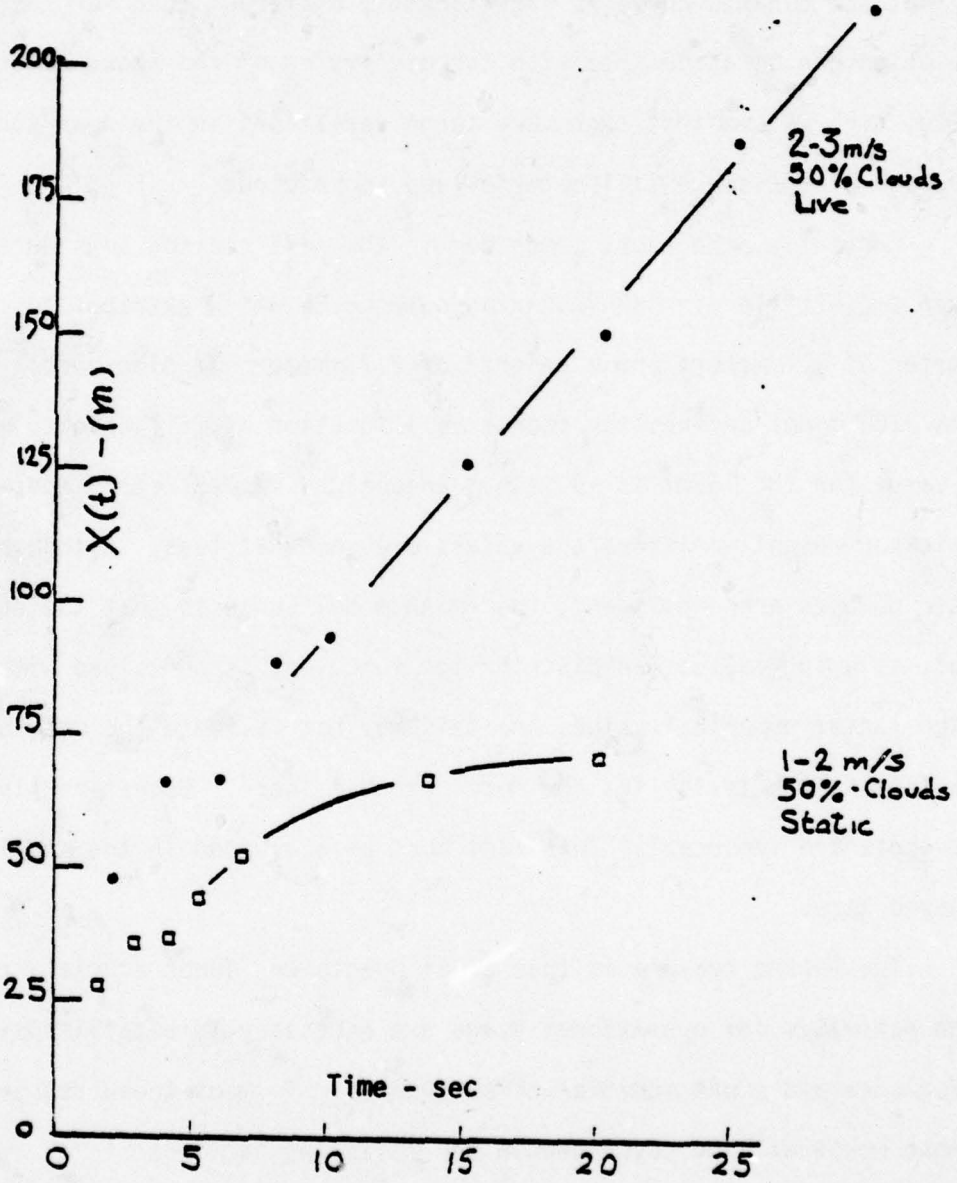

Fig. 4(a). Axial Dispersion of 105mm (WP) Shell, Static and Dynamic Firings (11)

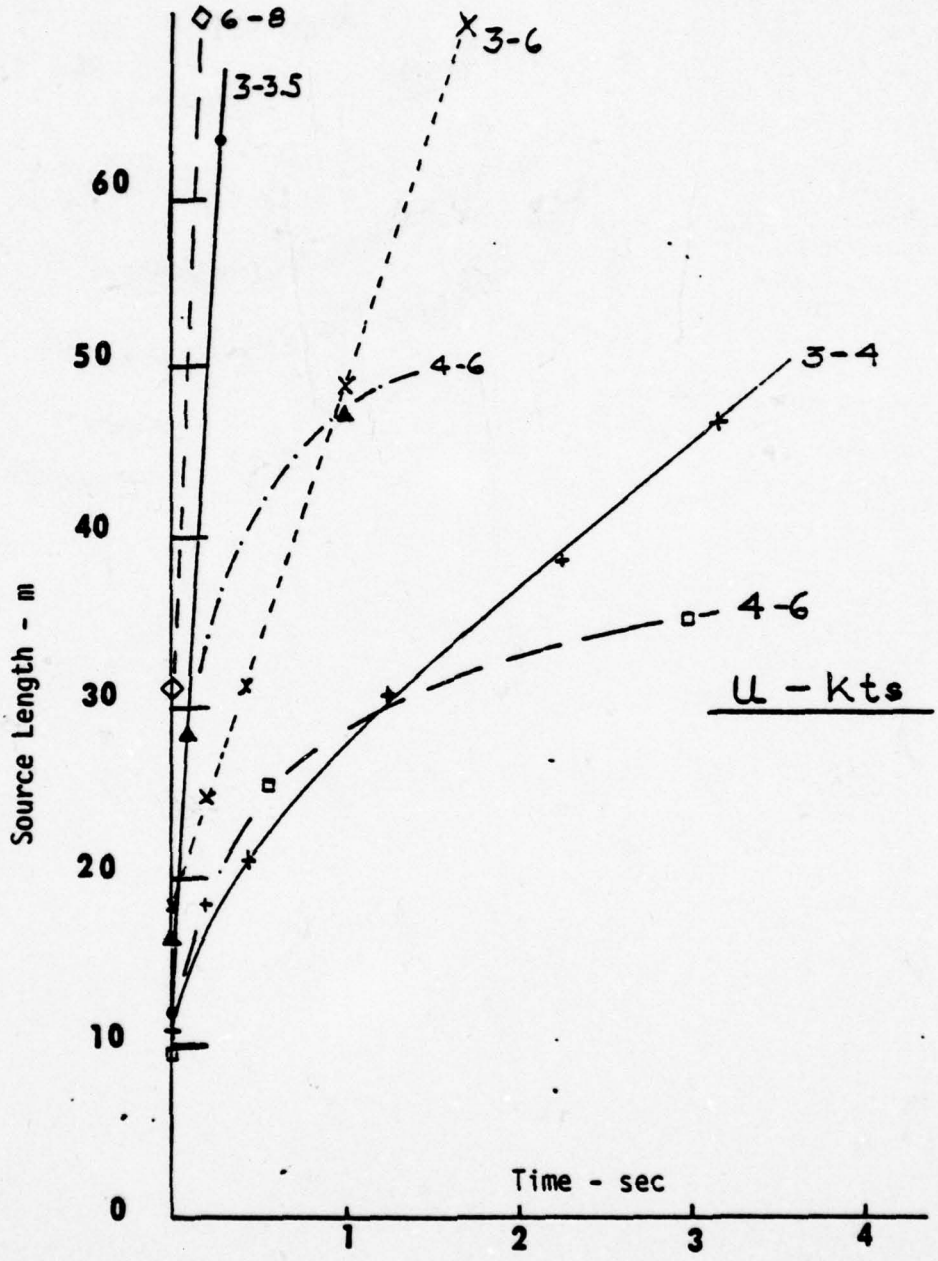

Fig. 4(b). Variation of Source Length vs Time:
(1) WP-155mm; (2) Different Speeds (11)

3. MODEL DEVELOPMENT

3.1 GENERAL

In this section we will present the formulation of a smoke model which can be utilized in a combat simulation model. The intent is to address all features including any shortcomings since the model described below is viewed by this writer as a first generation. Considerable research is required to eliminate uncertainties in the following items: input data; smoke cloud structure; and obscuring aerosol optical properties.

3.2 SMOKE CLOUD STRUCTURE

Since we are concerned with the time history of a smoke cloud produced by a military munition(s) we have drawn upon the experimental results reported by Rae (10). The smoke source was a single generator (oil fog) which is a non-exothermic, non-chemical source. For wind speeds greater than 2m/sec the tests showed that the cloud height and width can be defined for the conditions specified in Table 6 where x is the product of mean time wind speed, $\bar{u}$ (m/sec) and time, t(sec).

Table 6

SMOKE CLOUD DIMENSIONS

Turbulence State	Width (m)	Height (m)
High (Lapse)	9.14 + .419x	2.73 + .137x
Moderate (Slightly unstable)	9.14 + .238x	2.73 + .073x
Low (Stable)	9.14 + .146x	2.73 + .046x

[10] Rae, R. W., "Smoke Screenings of Vehicle Routes,"(U) CAORDE Memo 19, June 1954 (Conf).

Some data shows that the slope of the smoke cloud is a constant ($z/x \leq 0.09$) for wind speeds > 4.5 m/sec and approximately 0.17 at ~2 m/sec. The results in Table 6 have been expanded by interpolation to cover the range of Pasquill stability parameters and, are listed in Table 7.

Table 7

CLOUD SIZE PARAMETERS FOR NON-EXOTHERMIC MUNITIONS

Stability Category		Width, $\bar{y}$ (m)	Height, $\bar{z}$ (m)*	Remarks
Pasquill	Turner			
A	-3	9.1 + .419x	2.73 + .137x	Sunny day
B	-2	9.1 + .328x	2.73 + .11x	Day, broken clouds
C	-1	9.1 + .238x	2.73 + .073x	Overcast day/night
D	0	9.1 + .20x	2.73 + .06x	Neutral
E	1	9.1 + .18x	2.73 + .055x	Evening/early am
F	2	9.1 + .146x	2.73 + .046x	Evening/early am

*See Appendix G for discussion of plume height for $\bar{u} < 5$ m/sec.

It should be noted that Soviet measurements with a heated smoke pot* ($\Delta T \simeq 2°C$), for a terrain roughness, $Z_o = 0.4$ cm, give the following cloud slopes:

$$\tan \alpha \simeq -.85 \left(\frac{1}{L}\right) + .07 \qquad \frac{1}{L} < 0 \text{ (unstable)}$$
$$\simeq .07 \qquad \frac{1}{L} \geq 0 \text{ (neutral-stable)} \qquad (3.1)$$

where $\alpha = \tan^{-1}(\bar{z}/X)$. This result may be compared to the values in Table 7 with the aid of eqs. (2.3) and (3.1).

*$\Delta T = (T - T_{ambient})$

When Z_o = 0.4 cm and the Pasquill stability class is A-B the value of $L^{-1} \leq -.07(m^{-1})$, and the cloud slope ≈ 0.11. Since the Z_o from Table 7 may differ somewhat, the value of 0.11 is a good average value (0.09 - 0.17) for category B. This indicates a good correlation between Pasquill-Turner and Monin-Obukov stability definitions.

To describe the geometric shape of the smoke cloud we select a semicone for the near ground, point source, non-exothermic smoke munition. Thus, the volume as a function of time, V(t), is given by the expression

$$V(t) = \frac{\pi}{6} \; x(t)\left[\frac{y(t)}{2}\right]^2 \qquad (3.2)$$

At this point we introduce the effect of a strong exothermic chemical reacting smoke munition like white or red phosphorus. Here the thermal effect overrides the momentum exchange mechanism for the dispersion of the smoke aerosol as the smoke cloud temperature differential, ΔT, is non-negative for a long period. Further if $(\Delta T)_{cloud} > 0$ the cloud has buoyancy and this buoyancy will vary with the atmospheric gradient. Let us now consider the thermal history of the smoke cloud and estimate its temporal values.

The overall heat release from white phosphorus is estimated to be 800 kcal/kg. Hence the incremental temperature in the smoke cloud, assuming it to be an "air" volume is given by the simple relation

$$Q_H = mc_p\Delta T \qquad (3.3)$$

where m, C_p and Q_H are the cloud mass (gms), the specific heat of air and the quantity of heat available respectively

For a 10 meter sphere we find, where m = ρ(density) × V(volume),

$$T = Q_H/c_p\rho V \approx 10°C$$

At later times ΔT will decrease inversely with the volume, e.g., when the radius increases to ~20 meters the ΔT ~0.5°C, and therefore some residual buoyancy remains if unstable or neutral air conditions exist. On the other hand for an inversion condition (stable) the lift effect would stabilize. We will consider the effect, for a more practical case, in greater detail.

Consider a continuous source then the heat balance equation for combustion is

$$C \cdot Q_c = S \cdot \rho c_p \Delta T_c \tag{3.4}$$

where C = concentration (gm/m^3)

Q_c = heat released ($cal \cdot m^{-1} \cdot sec^{-1}$)

S = gms of smoke $\cdot\, m^{-1} \cdot sec^{-1}$

ΔT_c = *temperature increase*

ρ = smoke density

Similarly, the heat released by reactive processes including atmospheric moisture reaction is

$$C \cdot Q_r = S \cdot \rho c_p \Delta T_r \tag{3.5}$$

where $$Q_r = \frac{4\pi}{3} (\rho_f \cdot r_f^3 N_f - \rho_i r_i^3 N_i) L \tag{3.6}$$

and, ρ_i = particle density

r_i = particle radius

N_i = no. of particles formed/sec/meter

L = 600 cal/gm

Now the number of particles, N remain unchanged and, therefore

$$N_f = N_i = \nu \cdot S/(4\pi\rho r^3/3) \tag{3.7}$$

where ν = fraction of hygroscopic material.

Hence we can write for eq. (3.6) the following

$$Q_r = SL \frac{\rho_f r_f^3}{\rho_i r_i^3} - 1 \tag{3.8}$$

The effect of relative humidity, R% < 100, on a hygroscopic aerosol can be expressed as

$$\frac{R}{100} = 1 + \frac{3.2 \times 10^{-5}}{Tr_f} - 8.6 \frac{m}{Wr_f^3} \tag{3.9}$$

where m = initial mass in grams

W = molecular wt of smoke particle

The second term on the r.h.s. is evidently small and, therefore we have for r_f,

$$r_f = \frac{8.6\ m}{w(1 - \frac{R}{100})} = 8.6\ \frac{4\pi}{3} \rho\, r_i^3/W(1 - \frac{R}{100}) \tag{3.10}$$

Substituting eq. (3.10) into (3.8) gives

$$Q_r = \nu \cdot S \cdot L \left[\frac{\rho_f}{W} \left(\frac{35.9}{1 - \frac{R}{100}} \right) - 1 \right] \tag{3.11}$$

and, the total ΔT is given in eq. (3.12),

$$\Delta T = \frac{C}{\rho c_p} \left[\frac{Q_c}{S} \eta + \nu \cdot L \left(\frac{\rho_f}{W} \frac{35.9}{(1 - \frac{R}{100})} - 1 \right) \right] \tag{3.12}$$

where Q_c/S = 200

η = combustion efficiency, smoke wt/fill weight

c_p = 0.24 cal/gm°C

ρ = 1.29 x 10^3gm/m^3

ν = (Y-2.9)/Y

ρ_f = 1.83 (phosphoric acid)

W = 98 (phosphoric acid)

If we substitute the appropriate constants then for R = 80% and η = .9 we obtain

$$\Delta T = \frac{C}{(.24)(1.29 \times 10^3)}\left[180 + (.5)(600)\left(\frac{1.83}{98}\frac{35.9}{.2} - 1\right)\right] \simeq 2.8C(°C) \quad (3.13)$$

For an uniform concentration, the ΔT is uniform throughout the smoke cloud otherwise, the spatial distribution will define the variation in ΔT. Since ΔT varies with relative humidity in a non-linear fashion, we have calculated ΔT, see Fig. 5. If the yield curve changes upward as suggested by Johnson and Forney, the ΔTs will be differenct, see Fig. 5.

Hence if C ≃ 0.1 gm/m^3 then in the above case $\Delta T \simeq .28°C$ a relative unimportant value; if L = 100 and CL = 10 gm/m^2 then C = .1 gm/m^3.

<u>To a first approximation the mean concentration can be determined by dividing the smoke weight by the volume,</u>

$$\bar{C}\,(x,y,z,t) = Q/V \quad (3.14)$$

i.e., we assume here the concentration is uniform and decreases with time. Although this approximation suffers from at least two shortcomings,

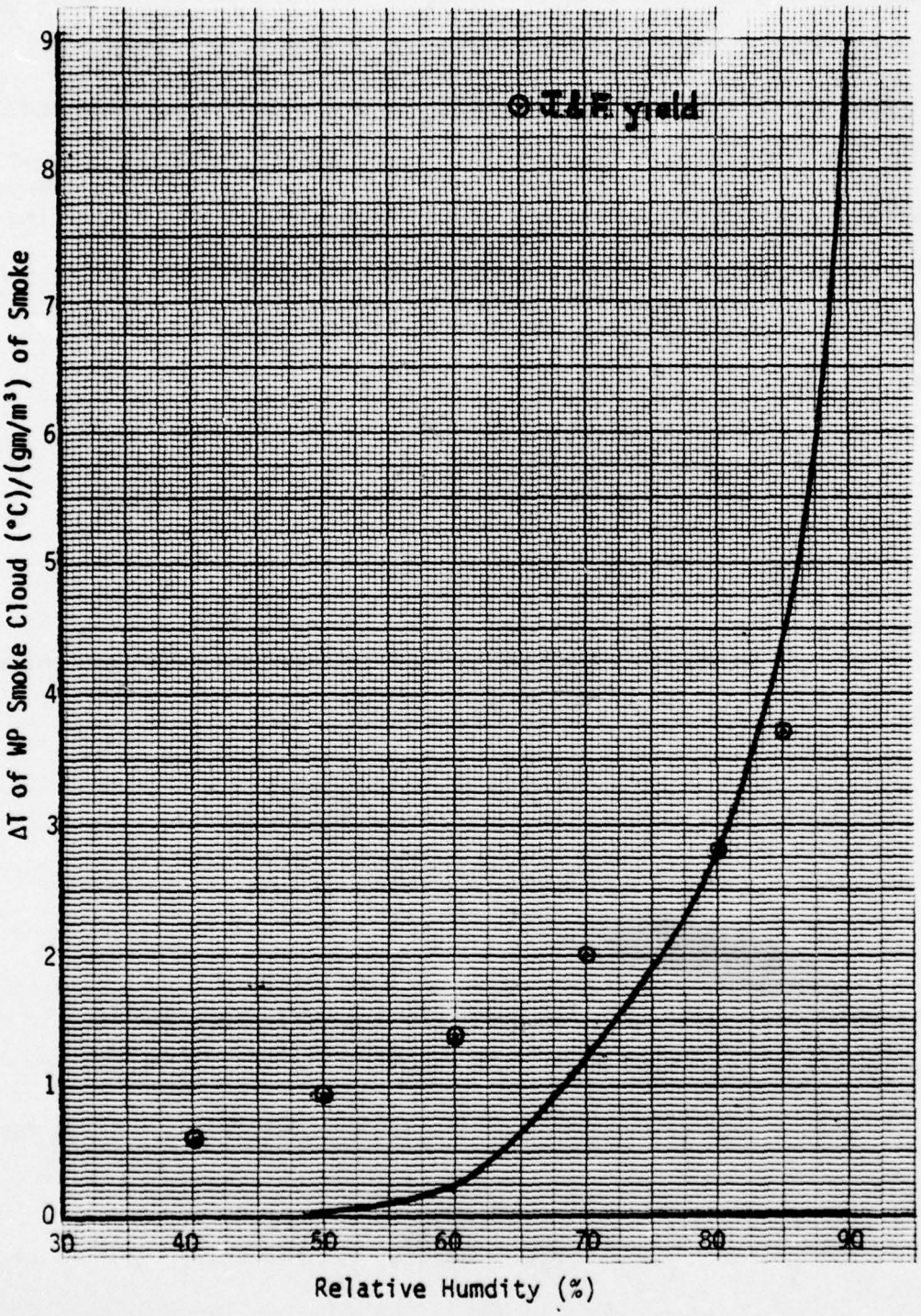

Fig. 5. Cloud ΔT as a Function of Relative Humidity

i.e., (1) the mean concentration has a spatial variation and (2) local inhomogeneity may exist, it can serve to provide an initial value for eq. (3.12). Further the shortcomings will be examined later.

We return now to the strong exothermic chemical munition and determine the dimensions of the resultant smoke cloud. Here the thermal effect overrides the momentum exchange mechanism for the dispersion of the smoke aerosols. Since the cloud temperature differential is non-negative we consider the plume rise to be defined by the following expression

$$Z = \bar{z} + \Delta h \tag{3.15a}$$

where $\bar{z}$ = momentum rise and,

Δh = rise due to heat addition

For Δh we accept a modified result recommended by Briggs (4) when the stability category is unstable, namely

$$\Delta h = \frac{1.6F^{1/3}x^{2/3}}{\bar{u}} (F^{1/6}) \tag{3.15b}$$

where $F = 3.7 \times 10^{-5} H$ and

H = calories/sec*

The additional factor $F^{1/6}$ accounts for the difference between the mean height and actual cloud top.

When a neutral condition exists the recommended expression for Δh is

$$\Delta h = \frac{1.6F^{1/2}x^{*2/3}}{\bar{u}} \left[.4 + .64\left(\frac{x}{x^*}\right) + 2.2\left(\frac{x}{x^*}\right)^2\right]\left[1 + .8\left(\frac{x}{x^*}\right)\right]^{-2} \tag{3.15c}$$

*For WP, H = (800 cal/gm) x WP fill wt(gm) ÷ 1 sec burn time.

where $x^* = 0.52F^{.4}h_s^{.6}$

h_s = source height = 1 meter

The maximum rise is estimated to be $3x^* \leq x \leq 5x^*$.

For a stable category (3.15b) is good to $x = 2.4\bar{u}/\bar{s}^{\frac{1}{2}}$ where $\bar{s}$ is defined by eq. I, p 11. The maximum value of Δh is defined by

$$\Delta h(max) = 2.9 \left(\frac{F}{\bar{u}\bar{s}}\right)^{1/3} \qquad (3.15d)$$

Since $z > y$ the smoke cloud shape is assumed to be defined as a quarter of an ellipsoid, i.e., the volume is given by

$$V(t) = \pi/6 \cdot x \cdot y \cdot Z \qquad (3.16)$$

The value of H for various munitions is uncertain; that is, the rate of burn and conversion are unknown and, therefore the number of calories produced per sec is uncertain. Theoretical estimates based upon phosphorus particle size and rate of oxidization would suggest ≃2 sec except for the several larger fragments. The latter implies a dependence on explosive charge and casing thickness, a fact to be established by experiment.* Dolce and Metz (11) state "the end of the weapon (155 mm shell) phase is the time when the flowing orange hemisphere becomes a white cloud, which is generally about 1 second after burst." The conversion of the initial oxide aerosol to phosphoric acid droplets occurs at distances ≤ 20 meters. Hence for the present, until

---

[11] Dolce, T.J. and Metz, D.F., "An Analysis of the Smoke Cloud Data from August 1975 Jefferson Proving Ground Smoke Test," AMSAA Tech Report 201, Sept 1977.

*Private communications from Dee, Edgewood Arsenal (April 1978) suggests for a 81 mm mortar about 80% of the phosphorus was oxidized in ≤ 2 sec and the remainder ≤ 10 secs. Note: the source was ~5 meters in radius.

more data are available we assume the conversion is ≃1 sec for all WP munitions irrespective of their fill weight with the exception of the L8A1, phosphorus wicks (WPW), wedges, etc. The latter must be treated as sources with a finite duration of emission, e.g., the L8A1 burns about 30 secs and the WPW (2.75" rocket head) burns about 4 to 5 minutes. Further, by virtue of their deployment they create a linear distributed source.

Earlier we noted that the temporal-spatial distribution defined by a "Gaussian" function was not an accurate description of the concentration in a smoke cloud particularly generated by military smoke. For the vertical distribution we are aware that this distribution depends on the lapse rate, wind speed and frictional velocity, $u*$. The horizontal distribution of the concentration, $C(x)$, depends on the wind speed, surface roughness and a stability length, e.g., L, the Monin-Obukov parameter.

To obtain a qualitative picture of the (x,z) distributions assuming that the y distribution is uniform we examined the data from several experiments. First we reduced the results from a Dugway Test* where a linear array of 6-155mm white phosphorus shells were statically detonated. The concentration vs x is shown in Fig. 6 and, the extrapolation to $x = 0$ is given in Fig. 7.

The latter corresponds to the approximate expression

$$C(o,o,o,t) = C_o \exp(-.0203t) \qquad (3.17)$$

where $C_o \simeq 24.81$ gm/m^3. The latter is consistent with initial conditions.

One fact that this indicates is that the mortar, artillery, etc. munitions cannot be treated as a puff since the residual concentration is ~9 gm/m^3 @ 60 secs. Further, the effect of initial dispersal has not been considered.

*Dugway Trial, DPI-002 T34, Nov 19, 1977.

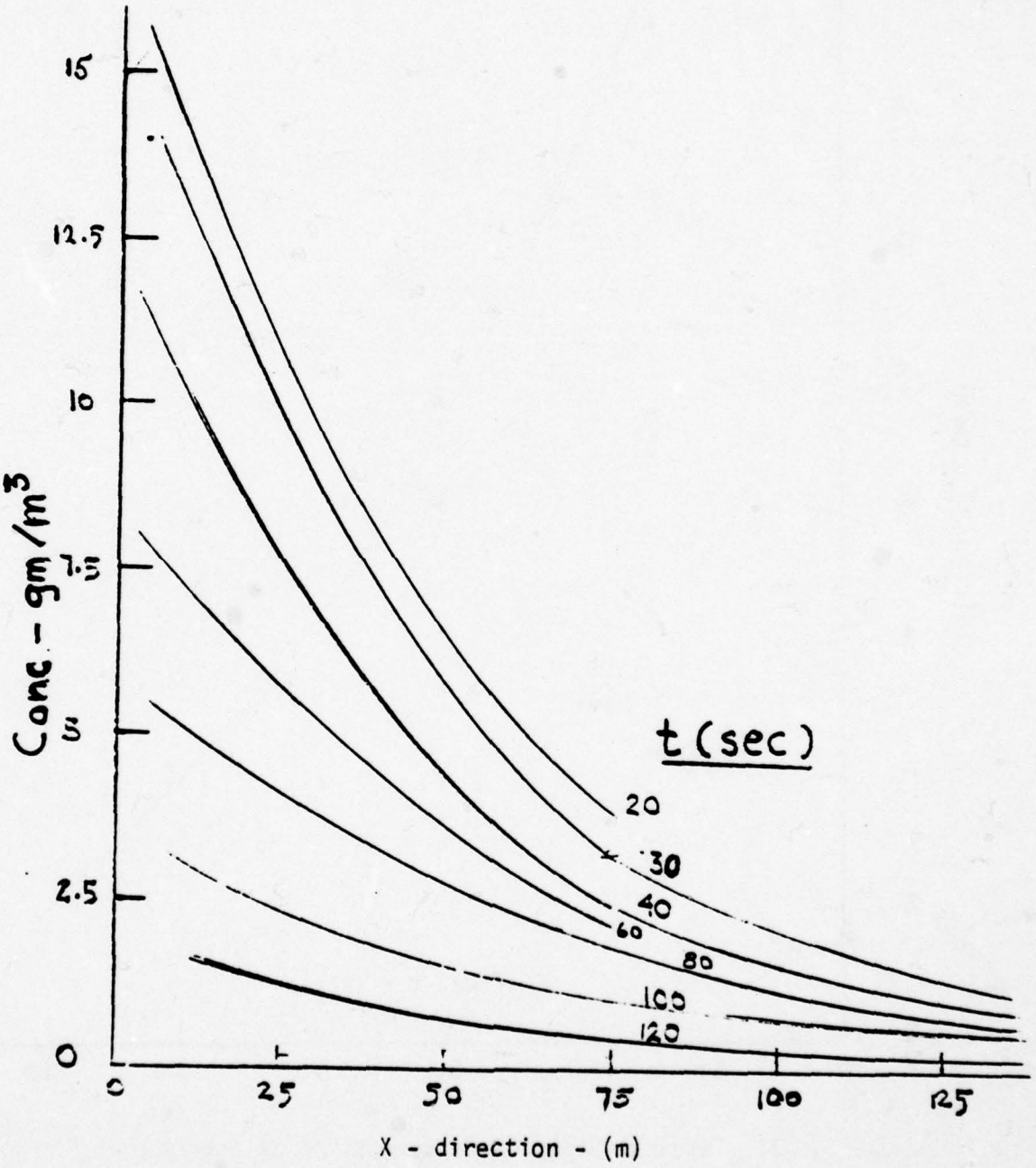

Fig. 6 Concentration Distribution Along X Axis
for Several Different Times

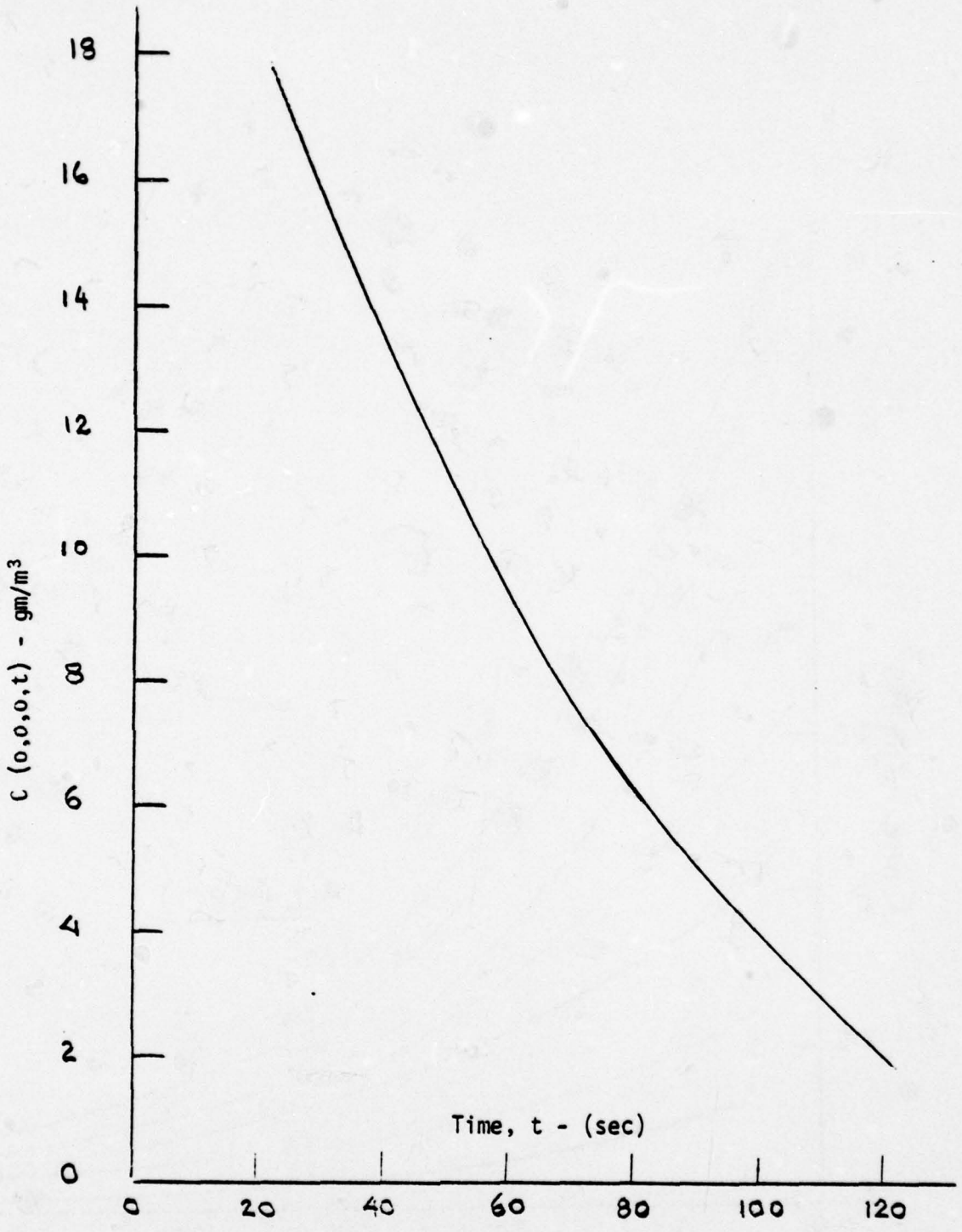

Fig. 7. Temporal Decay of Concentration at Source

The concentration C(x,o,o,t) appears to be defined by a relation

$$C(x,o,o,t) = C(o,o,o,t)\left[1-Ae^{f(x-\bar{u}t)}\right] \qquad (3.18)$$

where A and $f(x-\bar{u}t)$ are a numeric and a function of x respectively and, $C(x,o,o,t)\rightarrow(\sim 0.1)$ at $x = \bar{u}t$. This dependence is clearly related to a single analyzed event where the stability class was slightly unstable. For a similar surface situation Kazanski and Monin (12) using a continuous array found the concentration distribution to be inversely proportional to (x/L) which will agree with an explosive source for $t>>t_o$, i.e., quasi - steady state. For stable conditions, L increases with stability hence the decay rate will increase with x. Similarly, for unstable conditions $|1/L|$ decreases going from A→D stability class and therefore the decay will decrease with x as we go from stability class A→D.

For the vertical distribution we have determined for a cloud height H that the dependence can be categorized as follows:

$$\begin{aligned}
&\text{(unstable)} \quad C(z) = C(x,o,o,t)\,[1.25e^{-Z/H}-.25] \\
&\text{(neutral)} \quad C(z) = C(x,o,o,t)\,[1.35e^{-Z/H}-.35] \qquad (3.19) \\
&\text{(stable)} \quad C(z) = C(x,o,o,t)e^{1.52/H} \text{ for } Z \le .2H \\
&\qquad\qquad = C(x,o,o,t)\,[2.25e^{-\frac{(Z-.2H)}{H}}-.9] \text{ for } Z \le .2H
\end{aligned}$$

For the horizontal distribution we suggest the following:

a. For early times $t \le 20$ secs

$C(x,o,o,t) = C(o,o,o,o)[.8(1.2 - x/\bar{u}t)]$

where $x_o = \bar{u}t$

---

[12] Kazanski, A.B., and Monin, A.S., "The Form of Smoke Jets," Izv. Akad. Nanka SSSR Seriya Geofizika, 1957, p 1020.

b. For $t > 20$

$$C(x) \simeq C(o,o,o,o)(1 - x/x_o) \qquad x/x_o < .2$$

$$C(x) \simeq C(o,o,o,o)(1.1 - e^{(x/\bar{u}t - 1)}) \qquad x/x_o \geq .2$$

For a linear array equally spaced instantaneous point sources, e.g., n-munitions spaced "d" meters apart where $d > y$ $(t=5)$ they can be treated as individual sources, Fig. 8. From Fig. 8 we note the overlap

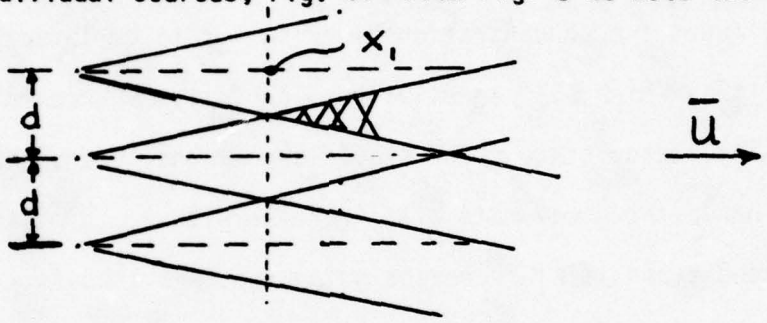

Fig. 8. Multi-Munition Schematic

occurs at time $t = (d - 9.1)/A\bar{u}$ where A is the constant given in Table 6, $y = 9.1 + Ax$. Beyond this, the lateral path length for $n = 2$ will decrease by the amount

$$\Delta = d \cdot (x_2 - x_1)/x_1 \tag{3.20}$$

where x_1 is the value of x at time of intersection and x_2 the value of x at the point of interest. For n munitions we can write immediately

$$\Delta = (n-1)(d)(x_2 - x_1)/x_1 \tag{3.21}$$

When the wind speed is at an angle, θ, appropriate adjustment is required.

The overlap zones are significant for radiation transport (optical properties) laser propagation and some cases of backscatter. However, for $C \cdot L$ computation one may treat the sources as additives, $\sum_i C_i L_i$.

For a linear continuous source of length, ℓ, where Q grams of smoke material of yield Y are released, the quantity of smoke produced per unit length per sec is $(Q \cdot Y)/(\ell \cdot t)$ gms/m-sec.

The concentration to a first approximation is defined by the relation

$$C(x,y,z,t) = \frac{Q \cdot Y}{t \cdot \ell} \frac{2}{\frac{\pi}{6} \bar{u} \cdot \bar{z}(x,t)(1+k)} \quad (gm/m^3) \qquad (3.22)$$

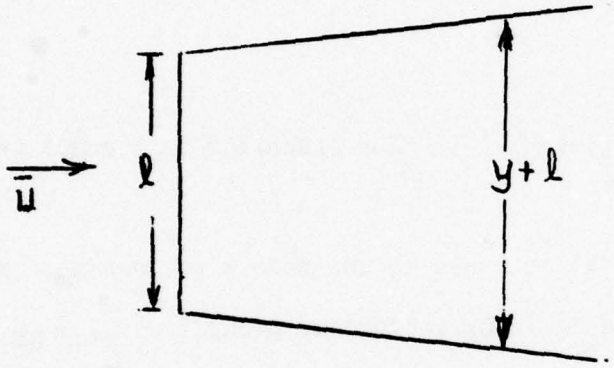

where $\bar{u}$ = mean speed (m/sec)

$\bar{z}$ = smoke cloud height @ "x" ($\bar{z}$ or Z)

k = incremental length of smoke width @ "x"

For the case when wind speed is normal to the smoke line, $k = \bar{y}/\ell$, and when $\bar{u}$ is at angle, θ, to the smoke $k = y\sin\theta/\ell$. The spatial distributions in the x and z may have a form similar to eqs. (3.18) and (3.19).

For a distributed source, a combination of point and/or linear arrays may be applied with appropriate accounting of the time coordinates; that is, if we have linear arrays at x_i, x_j and x_k then any x is $(x-x_i)$, $(x-x_j)$ and $(x-x_k)$ and the relative time is $t_1 = (x-x_i)/\bar{u}$, etc. A program for distributed steady sources like smoke pots and generators is given in Appendix D.

When a moving ground generator is utilized a vectorial representation is applied; that is, the generator velocity, v, is added vectorially to the wind velocity, u, hence for a headwind, a line source is produced with a resultant mean wind speed of $\bar{u} + \bar{v}$. The value of x is found by

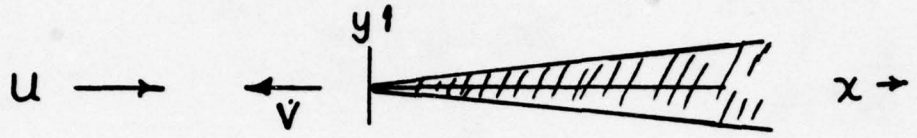

applying the expression, $x = [|\vec{u}| + |\vec{v}|]t$. The expansion in y and z are defined by Table 7.

When the generator moves at an angle to the mean wind then the resultant speed would be found again by vector addition.

3.3 OPTICAL CHARACTERISTICS

The overall treatment of the optical characteristics of the smoke cloud and its interaction with optical/infrared radiation is considered here. Again the approach, for modelling purposes, is to provide a simplified version of radiation transport to determine the smoke effects on optical systems. First we will consider the aerosol, then the transmittance and finally the effects on systems.

3.3.1 Aerosol Properties

The notation used here is given below

$\sigma(\lambda)$ = spectral cross section (m^2) or (cm^2)

$\alpha(m)$ = mass coefficient (m^2/gm), spectral (λ) or spectral band ($\Delta\lambda$) is implied

N = no. of particles/m^3 or per cc

$\alpha(\lambda) = N\sigma(\lambda)$ = volume coefficient (m^{-1})

Subscripts

e,s,a, = extinction, scattering, absorption

Definition

extinction = scattering + absorption

The aerosols produced for obscuring purposes vary from pure scatterers (fog oil) to particles (phosphoric acid) which are highly absorbing in the infrared. Actually the obscuration results from the high particle density which is produced; that is, for a concentration of 0.1 gm/m^3 the number density is of the order of 10^5/cc which is ~$10^2$to 10^3 greater than that found in clouds or haze. This fact explains the larger attenuation for shorter path lengths when particle sizes are comparable.

The smoke aerosol, like the atmospheric aerosol, may absorb moisture (chlorides) or is deliquescence like phosphoric acid and, therefore its optical properties will depend on relative humidity. In Fig. 9 the mass extinction coefficient vs wavelength for white phosphorus (WP) is given. From Fig. 9 we see that the extinction in the visible is significantly greater than in the infrared and, the latter varies significantly over the region of several microns wide. For this case, integration over wavelength is necessary; that is, an average extinction coefficient cannot be utilized. In regions of varying absorption it has been established that Beer's law is not valid. Simply speaking, standard methodology should be applied namely, to integrate the product of (spectral intensity x system spectral response x spectral transmittance) over the wavelength region of interest. In the event a polydispersed aerosol mixture is produced which is the usual situation then the mean value is derived by integrating the coefficient as a function of particle size over the size distribution.

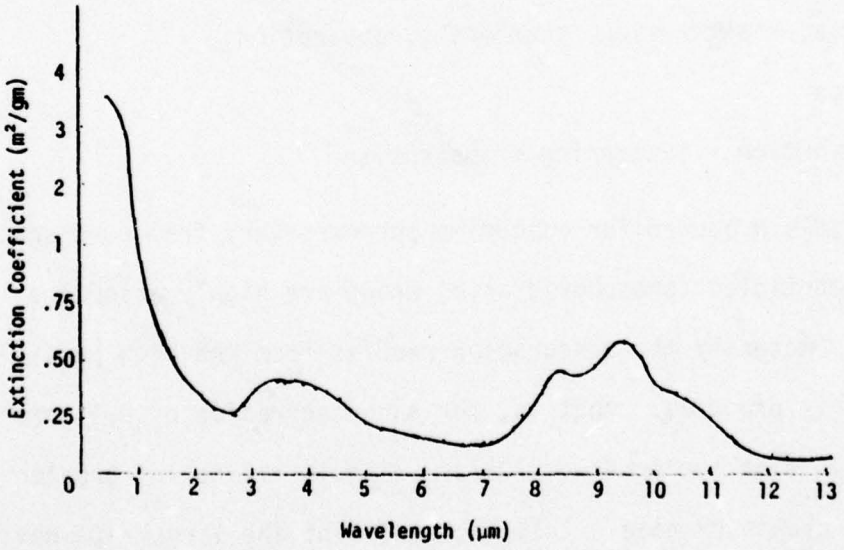

Fig. 9. Extinction Coefficient of RP/WP
(Ref 2, App E, ED-SP-77002)

For the above reasons we have tended here to depend upon experimental data to provide the mass (m^2/gm) and volume (m^{-1}) optical parameters (extinction, etc) for the different smokes. A precaution must be exercised to properly account for relative humidity: the coefficients will increase particularly at elevated values.

In Appendix E we present current detailed values of the optical parameters for different smokes. Some nominal broadband values are given in Table 8.

For some applications there is a need to utilize the angular dependence of scattering. For small particles or, when the particle radius $\leq \lambda/2\pi$ (λ = wavelength of radiation) then the scattering is defined by $(1 + \cos^2\theta)$, i.e., Rayleigh, otherwise the scattering is highly asymmetric and predominantly in the forward direction, Mie scattering. To obtain the scattering cross-section we integrate over all solid angles, i.e.,

$$\sigma_s = \int \sigma_s(\theta) d\Omega,$$

and, therefore for Rayleigh scattering the scattered intensity flux is equally divided between the forward and backward direction. For Mie scattering the backscatter is relatively small, (10^2 - 10^3) less than the forward component. By convention, one normally writes $\sigma_s(\theta)$ as $P(\theta)/4\pi$.

In Fig. 10 we present a result for phosphoric acid at wavelengths 3.39μm and 10.6μm. The effect of wavelength and scattering angle are self evident. To demonstrate different properties we also plotted the value for $ZnCl_2$ (HC smoke) at wavelength of 10.5 μm.*

*Private communication from R. Frickel, CSL, Aberdeen Proving Ground, MD.

Table 8. $\sigma_e(m)$, Average Extinction Coefficient**

Item Composition	Average Coefficient (m^2/gm)			
	Visible	0.7-1.2μm	3-5μm	8-12μm
1. WP & RP*	3.32	2.30	0.32	0.36
2. HC	4.91	3.00	0.31	0.1
3. MK 24	5.67	3.80	0.75	0.18
4. Foreign	3.73	3.50	0.85	0.18
5. Foreign	4.39	2.60	0.41	0.10
6. Eber Mix	4.72	3.40	0.32	0.10
7. Anthracene	6.32	3.00	0.18	0.05
8. Y-2 (Yershov)	6.18	2.90	0.11	0.03
9. KA	7.86	3.90	0.61	0.28
10. A5				0.21
11. Fog Oil	4.0	3.40	0.2	<0.1

*FS ≈ WP

**Johnson, M.C. and Forney, P.D., "The Effectiveness of Obscuring Smoke," ORG, Edgewood Arsenal, (Unpublished update).

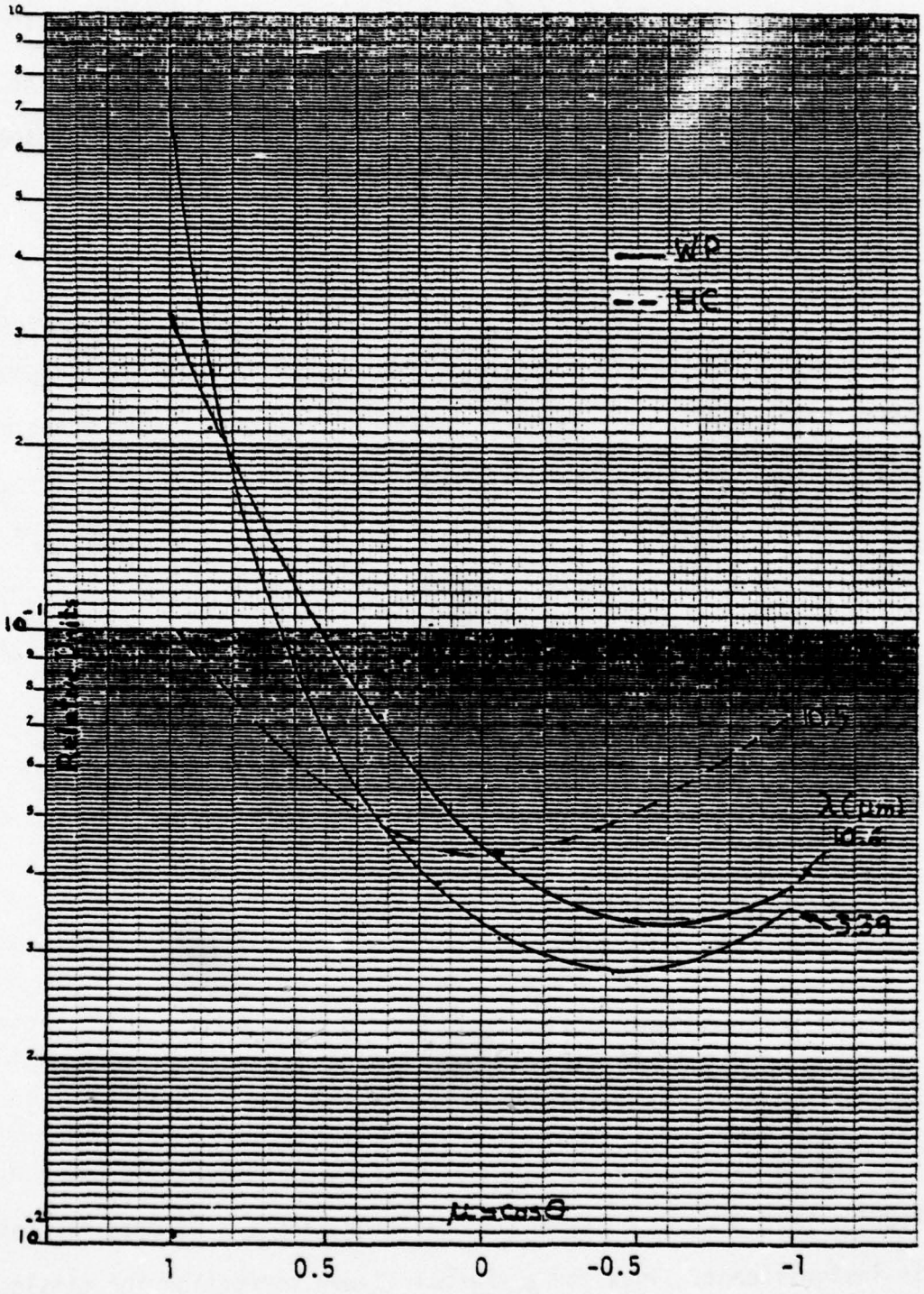

Fig. 10. Phase Function in Relative Units

3.3.2 Radiation Transport

Here we will present the necessary formulations to determine the effect of smoke on the propagation of the target or background spectral intensity.

3.3.2.1 Attenuation

The spectral attenuation is defined by $\exp[-\alpha_e(\lambda)R]$ where $\alpha_e(\lambda)$ is the spectral extinction coefficient and R is the length of the propagation path. This simple expression is appropriate when (1) scattering is omitted and (2) the receiver field-of-view is small. For a collimated source a first order correction is $[1 + \alpha_s R \cdot \bar{\Phi}]$ where $\bar{\Phi}$ is the receiver f-o-v/180°. Zuev (13) gives a more general expression for single scattering, namely $[1 + \alpha_s R \cdot D]$ where D is a function of source angle, θ, receiver angle, ϕ and particle size parameter $\rho = 2\pi r/\lambda$, see Fig. 11.

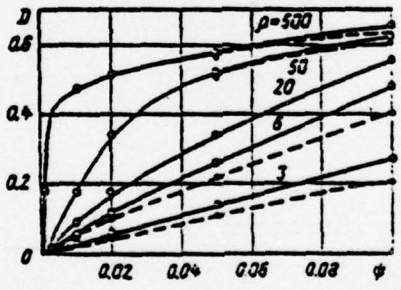

FIGURE 11. Curves of D as a function of receiver aperture for various ρ and half-cone angles θ of the source emissions. Solid curves pertain to $\theta = \pi/2$ and dashed curves to $\theta = \pi/6$.

For smoke the mean particle size is ~2 μm hence at 10 μm, $\rho \equiv 2\pi r/\lambda = 1.256$. When $\theta = \pi/2$, a Lambertian radiator, and $\phi \leq 10$ mrad the value of D is insignificant. Thus for a thermal viewer correction for single scattering is unimportant. If $\lambda = 1.0$ μm and a 10° field of view system is used then the correction factor is sizeable.

---

[13] Zuev, V.E., Propagation of Visible and Infrared Radiation in the Atmosphere, Halstead Press, John Wiley & Sons.

Clearly, we imply that the $\alpha_e(\lambda)$ is treated as discussed earlier.

Hence we will use for the transmitted radiation the following

$$I = I_0[1 + \alpha_s R \cdot D(\rho,\theta,\phi)]e^{-\alpha_e R}$$

3.3.2.2 Backscatter

Here we must define two concepts of backscatter. First the backscatter applicable to laser radiation corresponds to the scattering at 180°, $P(\pi)$. This can be obtained from plots like Fig. 10. The second concept is germane to solar backscatter or other sources, e.g., flare illumination, which may cause glare in the receiving sensor, see Fig. 12.

Under the assumption that single scattering is valid, i.e., when $\alpha_s/\alpha_e \leq 0.8$ and multiple scattering can be neglected, then the spectral steradiancy (brightness) is defined by

$$N_\lambda(e) = N_s(\lambda)\tau_i(\lambda) \cdot \frac{\alpha_s(\lambda)}{\alpha_e(\lambda)} \cdot \frac{P(\theta)}{4\pi} \cdot \frac{\cos i}{\cos i + \cos e} \qquad (3.23)$$

where N_s = source steradiancy

$P(\theta)$ = differential scattering cross section/unit area/steradian

$\theta = \pi - (i + e)$, degrees

i,e = angle of incidence, exitance

τ_i = atmospheric spectral transmittance from source to cloud surface

The received radiance is $N_\lambda(e) \times \tau_e(\lambda)$ where $\tau_e(\lambda)$ is the spectral transmittance from the cloud surface to the receiver. For an uncollimated source, i and θ will include a finite set of values and, therefore $N_\lambda(e)$ will require integration over the receiver field-of-view. For the sun, we treat it as a collimated source.

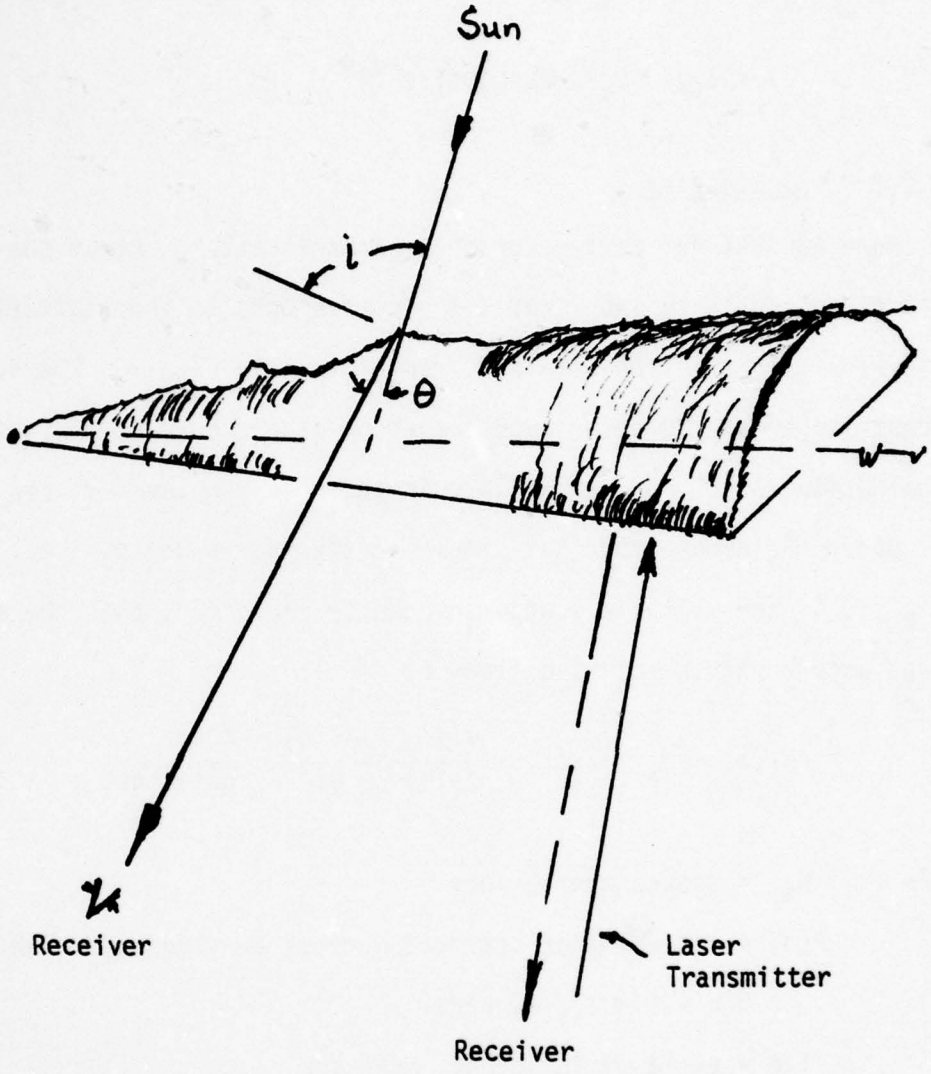

Fig. 12 Schematic of Backscatter Geometries

Again under the assumption of single scattering the albedo of a cloud can be found from the transport equation and is presented in Fig. 13; the albedo is plotted as a function of optical thickness, $\alpha_e R$, for different values of α_s/α_e. For a non-absorbing medium, $\alpha_s/\alpha_e = 1$, the albedo approaches 1 whereas if α_a is finite the albedo rapidly approaches an asymptotic value <1. The latter implies that multiple scattering effects rapidly decrease.

With this brief description of transmittance and backscatter, we will now consider contrast.

3.3.3 Contrast

The contrast concepts discussed here cover the visible and infrared spectral regions where the possible impact of thermal effects will be examined. Since the infrared region includes thermal viewers where the scene information is displayed such systems are considered.

3.3.3.1 Reflected Radiation

The attenuation of target and background radiation is only necessary but not sufficient to describe the effect on an target acquisition system of an obscuring medium in a line of sight; that is, the observed image contrast is a significant parameter.

By definition the inherent contrast, at zero range, between a target and its immediate background is expressed here by the equation,*

$$C_o = \frac{N_T - N_B}{N_B} \qquad (3.24)$$

*This definition of contrast (Blackwell) is used by this writer as part of his target acquisition routines for CARMONETTE.

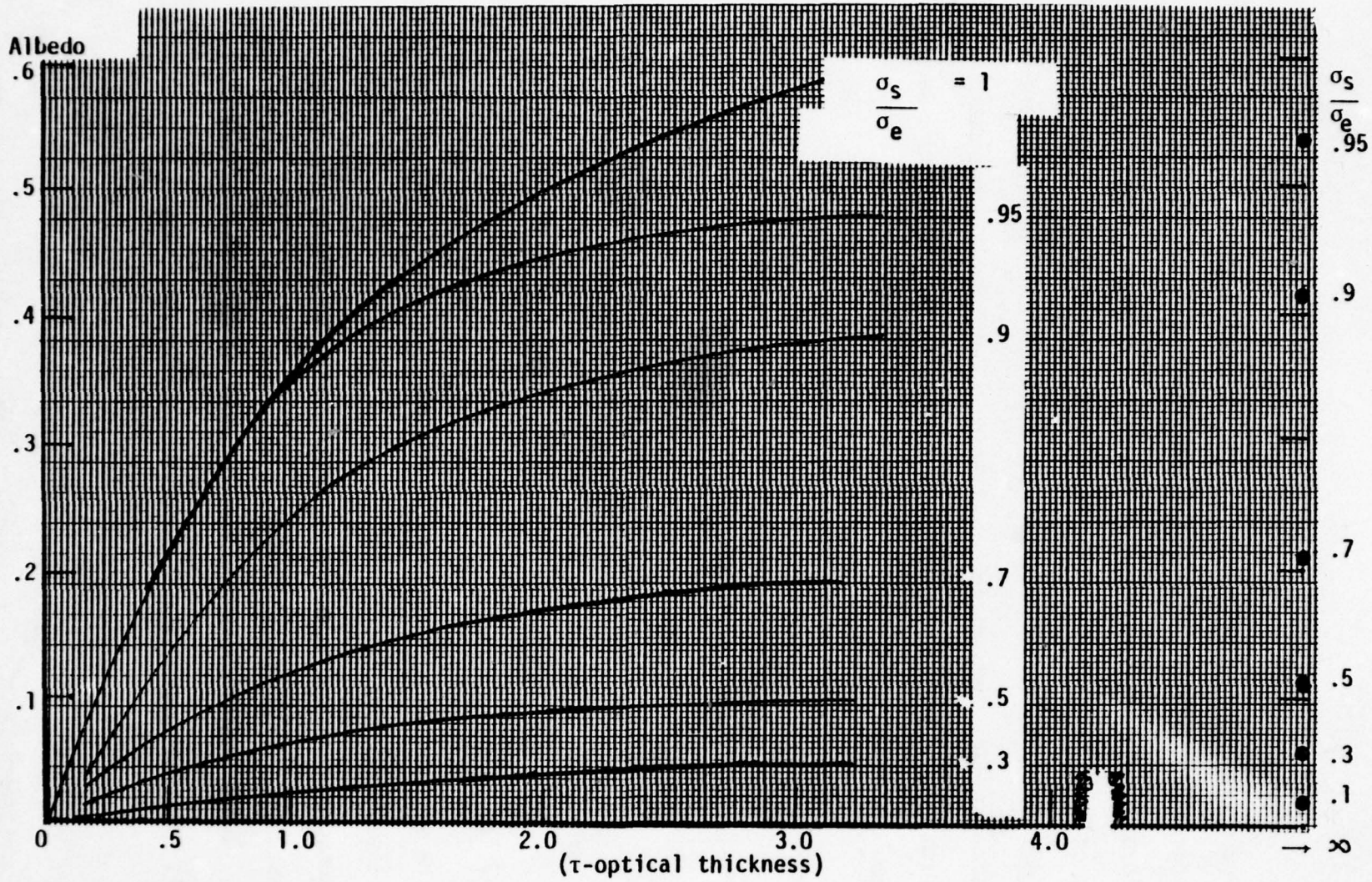

Fig. 13 Albedo vs Optical Thickness, τ

where N_T = target radiance, and

N_B = background radiance

The observed or apparent contrast at range, R, has been defined as

$$C_R = C_o \left[1 + \frac{1 - e^{-\alpha_s R}}{0.5(1 + R_g)e^{-\alpha_e R}(R_B)} \right]^{-1} \qquad (3.25)$$

where R_g = ground reflectance and

R_B = background reflectance.

A definition for apparent contrast[1] given by Middleton (after Duntley)(14) is

$$C_R = C_o \left[1 + \frac{S_K}{G_d} (e^{+\alpha_e R} - 1) \right]^{-1} \qquad (3.26)$$

where S_K/G_d = sky-ground ratio.

This ratio varies with ground conditions, cloud cover, and scattering conditions of the atmosphere. Generally for a cloudy sky, the ratio is $\simeq\beta^{-1}$ and $0.2\ \beta^{-1}$ for a clear sky where $\beta = \bar{R}_g$, the average ground reflectance.

For daytime conditions, and visual systems, C_τ, the threshold contrast[2] (50% probability of detection level) has been assumed to be ~2% and, the maximum visual range (visibility) V is found from the expression

---

[1] A simple derivation can be given as follows; if G is glare, then

$$C_R = \frac{(N_T - N_B)e^{-\alpha_e R}}{N_B e^{-\alpha_e R} + G} = C_o[1 + \frac{G}{N_B}\ e^{\alpha_e R}]^{-1}$$

[2] Sawyer, K.F., Thorpe's Dictionary of Applied Chemistry, 4th Ed. (1950) reports on an experiment with smoke. The objective was to establish the liminal value of contrast. Results indicate that the curve had the same shape as Blackwell's except the required threshold contrast was a factor of two greater.

(14) Middleton, W.E.K., Vision through the Atmosphere, University of Toronto Press, Canada (1952).

$$C_\tau = e^{-\alpha_e \cdot V} ; \qquad (3.27)$$

$$V = 3.912/\alpha_e$$

If α_e is defined in units of km^{-1}, V is in kms.

Duntley's expression omits several factors such as sun angle and geometrical relation of viewer to target. Hruschke, Rand Corp., has developed an algorithm for the determination of the sky/ground ratio for different conditions. This algorithm is now presented.

He defines the ratio by an expression

$$\frac{S_K}{G_d} = F_\delta(SG_\beta + SG_\varepsilon + SG_V)/3 \qquad (3.28)$$

where $SG_\beta = \exp(-1.15 \ln \beta - .75)$; β = ground albedo

$SG_\varepsilon = \exp(-3.4 \sin \varepsilon + 2.7)$; ε = solar elevation (°)

$SG_V = \exp(-0.5 \ln V + 1.5)$; V = visibility (km)

and, δ = the receiver depression angle.

(1) First, for cloud cover >4/8s, $\varepsilon = 25$.

(2) To compute F_δ one must determine a set of indices for different values of δ, ε, β, and V see Table 9.

Table 9. - Values of Indices j_1, j_2, j_3, j_4 as Functions of δ, ε, ρ, V

j_1	δ (deg)	j_2	ε (deg)	j_3	ρ	j_4	V (km)
1	$\delta \geq 82$	1	$\varepsilon \leq 10$	1	$\rho \geq .5$	1	$V \geq 10$
2	$50 > \delta \geq 30$	2	$10 < \varepsilon \leq 30$	2	$.5 > \rho \geq .15$	2	$10 > V$
3	$30 > \delta \geq 12$	3	$30 < \varepsilon \leq 55$	3	$.15 > \rho$		
4	$12 > \delta$	4	$50 < \varepsilon$				

(3) With the established values of the indices enter Table 10 and find F_δ.

Table 10

VALUES OF F_δ AS FUNCTION OF INDICES j_1, j_2, j_3, j_4 [a]

j_1	j_2	j_3	j_4	F_δ	j_1	j_2	j_3	j_4	F_δ	j_1	j_2	j_3	j_4	F_δ	j_1	j_2	j_3	j_4	F_δ
1	1	1	1	2	2	1	1	1	1	3	1	1	1	1.2	4	1	1	1	1.2
1	1	1	2	2	2	1	1	2	1.2	3	1	1	2	2	4	1	1	2	0.8
1	1	2	1	2	2	1	2	1	1	3	1	2	1	1.5	4	1	2	1	1.5
1	1	2	2	2	2	1	2	2	1.2	3	1	2	2	2.5	4	1	2	2	1
1	1	3	1	2	2	1	3	1	1.2	3	1	3	1	2.5	4	1	3	1	2.5
1	1	3	2	2	2	1	3	2	2	3	1	3	2	3.5	4	1	3	2	1
1	2	1	1	1.5	2	2	1	1	1	3	2	1	1	1.2	4	2	1	1	1.2
1	2	1	2	1.5	2	2	1	2	1.2	3	2	1	2	1.7	4	2	1	2	0.8
1	2	2	1	1.5	2	2	2	1	1	3	2	2	1	1.2	4	2	2	1	1.2
1	2	2	2	1.5	2	2	2	2	1.2	3	2	2	2	2	4	2	2	2	0.8
1	2	3	1	1.5	2	2	3	1	1.2	3	2	3	1	2	4	2	3	1	2
1	2	3	2	1.5	2	2	3	2	1.5	3	2	3	2	3	4	2	3	2	1
1	3	1	1	1.5	2	3	1	1	1	3	3	1	1	1	4	3	1	1	1.2
1	3	1	2	1.5	2	3	1	2	1.2	3	3	1	2	1.2	4	3	1	2	0.7
1	3	2	1	1.5	2	3	2	1	1	3	3	2	1	1.2	4	3	2	1	1.2
1	3	2	2	1.5	2	3	2	2	1.2	3	3	2	2	1.5	4	3	2	2	0.8
1	3	3	1	1.5	2	3	3	1	1.2	3	3	3	1	1.5	4	3	3	1	1.5
1	3	3	2	1.5	2	3	3	2	1.5	3	3	3	2	2	4	3	3	2	0.8
1	4	1	1	1	2	4	1	1	1	3	4	1	1	0.7	4	4	1	1	1
1	4	1	2	1	2	4	1	2	1	3	4	1	2	1	4	4	1	2	0.5
1	4	2	1	1	2	4	2	1	1	3	4	2	1	1	4	4	2	1	1
1	4	2	2	1	2	4	2	2	1	3	4	2	2	1.2	4	4	2	2	0.7
1	4	3	1	1	2	4	3	1	1	3	4	3	1	1	4	4	3	1	1
1	4	3	2	1	2	4	3	2	1.2	3	4	3	2	1.5	4	4	3	2	0.7

[a] For $82 > \delta \geq 50$, $F_\delta = 1$.

At this point we consider in particular the smoke layer which produces in most instances "glare." To handle this induced background we consider as a first approximation that (1) the ground plane reflectance is replaced by the smoke layer reflectance and (2) the Duntley form (eq. 3.26) or the Hruschke algorithm can be applied. In either case, the albedo, β, of the cloud layer is defined by Fig. 13 and when the visibility, V, is required then the ambient (unsmoked) atmosphere is considered as the propagation medium.

Let us now consider the contrast modulation which is given by the expression

$$C_M = \frac{N_T - N_B}{N_T + N_B} = \frac{C}{2+C} \tag{3.29}$$

where C, the contrast, is defined above. By analogy to the above treatment in "footnote, p 48", we can write eq. (3.29) as

$$(C_M)_r = (C_M)_o \left[1 + \frac{1}{2+C} \cdot \frac{G}{N_B} e^{\alpha_e R} \right]^{-1} \tag{3.30}$$

Since $0 \leq C$ and $C \sim 1$ is a high conspicuity value then we assume $(1/2+C) \approx 0.4$ and $G/N_B = \beta^{-1}$. Hence we may write for $(C_M)_R$

$$(C_M)_R = (C_M)_o \left[1 + \frac{.4}{\beta} e^{\alpha_e R} \right]^{-1} \tag{3.31}$$

Let $\beta = .4$ and $\sigma_t R = 1$ then the contrast modulation is reduced to about 27% of the original value, a serious reduction in spatial frequency content making the recognition task difficult. It should be stated that the above is an illustrative example and estimate. An exact calculation should be made when necessary.

3.3.4 Thermal Contrast

Of particular interest for the thermal viewer there are several factors, in addition to attenuation, which may affect picture contrast. These factors are the following:

1. Channel Crosstalk - contrast loss due to scattering within the smoke cloud by the aerosol constituents;
2. Temperature - temporal history of the smoke cloud temperature;
3. Emission - temporal history of the particulate emission; and

4. Radiance Modulation - spatial variations of radiance due to hot spots when WP-like material is used and/or concentration inhomogeneities of particulates.

The several factors are germane to staring, i.e., the DC type thermal viewers, whereas the factors (1) and (4) are particularly troublesome to the current viewers (AC type). We will now consider each of the above factors.

1. Channel Crosstalk

Let ϕ be the system instantaneous field of view (IFOV) in milliradians then the effect of smoke could be such that a portion of the background radiation will impinge on the target signal resolution element. Conversely, some target radiation can fall on the adjacent cell, see Fig. 14.

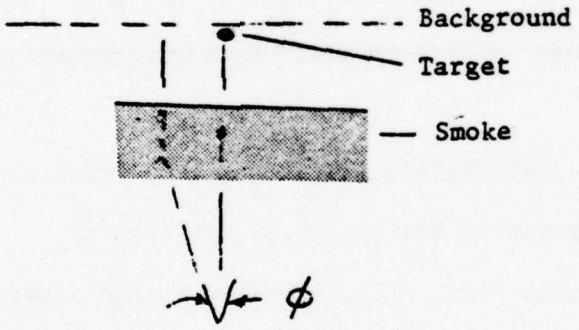

Fig. 14 Schematic of Scattering Effect

In a similar manner, some background radiance will fall on the target resolution element. We describe the resultant radiance difference between the target cell (N_S) and background cell (N_B) as

$$\Delta N = [N_S(0) + N_B(\phi_1)] - [N_B(0) + N_S(\phi_1)] \qquad (3.32)$$

where $N_i(\phi_1)$ is the scattering contribution. Rewriting eq. (3.32) we obtain

$$\Delta N = [N_S(0) - N_B(0)]\left\{1 - \frac{N_S(\phi_1) - N_B(\phi_1)}{N_S(0) - N_B(0)}\right\}$$

If we identify $(\Delta T)_o \equiv \Delta N(0)$, the effect of scattering is

$$\left\{1 - \frac{\Delta N(\phi_1)}{\Delta N(0)}\right\} \tag{3.33}$$

We will now tacitly assume that single scattering will occur and this is reasonable. That is, for a WP screen (.02 gm/m^3) the attenuation length is ~0.144 kms and, for a diesel fog dispersal (.005 gm/m^3) the attenuation length is ~4.34 kms. The latter two numbers bracket the overall spectrum of values. Since the likelihood is small that a translucent smoke layer will be thicker than ≥150 meters the assumption is reasonable.

We can now calculate $N_S(\phi_1)$, $N_B(\phi_1)$ by the use of simple diffraction theory. The reason is that $\phi_1 \leq 0.50$ milliradian.

The scattered flux, $F(\theta)$, is given by the equation

$$F(\theta) = F(0)e^{-\alpha_e L} \cdot D(\theta)$$

where for a monodispersed aerosol

$$D(\theta) = \frac{N\rho^2 d^2}{4}\left(\frac{J_1^2(z)}{z^2}\right)$$

the parameters are

N = particle concentration/km^3

$\rho = \pi d/\lambda$ (d = diameter)

$z = \rho\theta$ (kilometer-radian)

J_1 = Bessel Function of the first kind

Substituting the appropriate values for an instantaneous field of view = 0.25 mrad we obtain the values of $\Delta N(\phi)/\Delta N(0) = 0.03$ or, the reduced ΔT $\sim 0.97\Delta T_o$. Hence crosstalk can be dismissed as a problem.

2. Temperature

In Section 3.2 we presented an exposition of the thermal history of the smoke cloud and, showed $\Delta T \leq 2.8°C$ x concentration for a relative humidity ≤80%. These values of ΔT are not detrimental with the possible exception of a high performance DC system with MRT ~.01.

3. Particle Emission

The conversion of chemical compositions to smoke is normally an exothermic reaction producing particulates that may range in the 200°C to 500°C. In the specific case of phosphorus there is an exothermic reaction that converts the oxide particle to phosphoric acid droplets. The initial conversion energy is transferred to the early phase of the smoke cloud whereas for phosphoric acid the droplet remains hot ~several hundred degrees for a finite time. The question is how long will it be hot.

The temperature history at r, along radius of a spherical particle (radius = a) at an uniform temperature, T_o, is given by (15) as

$$T(r,t) = \frac{T_o}{K+1} - \frac{2KaT_o}{3r} \sum_{n=1,2..} e^{-k\alpha_n^2 t} \times f(\alpha_n, r)$$

where α_n = roots of $\tan a\alpha = 3a\alpha/3+ka^2\alpha^2$

K = ratio of medium heat capacity to particle heat capacity and,

k = thermal conductivity

When $kt/a^2 \geq 0.16$ then $T(r) = T_o/K+1$. Substituting appropriate values

[15] Carslaw, H.S., and Jaeger, J.C., Conduction of Heat in Solid, Oxford, 1947.

into the former we obtain $t \simeq 1.6 \times 10^{-6}$ sec which is due to the small particle radius, a, being only ~1 μm. To estimate K we consider a smoke concentration ~1 gm/m^3 then $K \simeq 300$ and the particles will have equilibrated with the air in the smoke cloud since we have shown earlier that $\Delta T \simeq 2.8°C$ at a concentration of 1 gm/m^3. This appears to be consistent with observations; that is, except for early times (C·L large) the particle emission is not significant. Hence for C·L ≥ system threshold, particle emission is a non-contributory factor to system performance degradation.*

4. Radiance Modulation

For the present we will only discuss the mechanism in a qualitative manner as a detail analysis is beyond the scope of this study. In the above we have considered the smoke cloud density to be uniform or locally isotropic except in the regions of overlap. Similarly in the gaussian approach no local homogeneities exist. Hence neither approach provides for local small scale eddies arising from atmospheric shear or terrain features. In the latter case the effects are localized and are comparable to or ~ 2X the size of the terrain feature. If the thermal viewer system resolution provides 0.3 meter at the smoke cloud then the inhomogeneities will be confined to the ground level. Other inhomogeneities at practical times would be comparable to a major fraction of the cloud dimension or, significantly larger than thermal resolution elements.

Hence, local hot spots from munition fragments, burning wicks or spatially distributed smoke pots may cause serious problems. Also whenever an overlap condition occurs there may be occasions that these

*NOTE: This is not to be confused with (1) hot "chunks" at t ≃ 0 secs or (2) hot smoking chunks which can cause target blockage.

overlaps may give rise to $\Delta T(s)$ comparable to a target's ΔT when the target is detected through the smoke cloud. In this general category the vertical stratification may cause a problem in the vicinity of the peak (for stable or inversion conditions). Similarly, the observed fluctuations in lateral concentration due to axial wind fluctuations may under special circumstances lead to a signal modulation problem in time and space coordinate.

To summarize, we suggest that operational modelled experiments be performed to examine conclusively if circumstances exist where the smoke cloud contains regions that can appear as clutter. For modelling we propose to use the several expressions for contrast and transmission germane to the proposed model.

First, the initial obscuration is induced by the cloud opacity, namely high attenuation. The transmission over the range, R, between target and observer is given by

$$T = (1 + \alpha_e^s \cdot \ell D) \exp -\left[(\alpha_e^{air} (R-\ell) + \alpha_e^s \ell)\right] \qquad (3.34)$$

where ℓ and α_e^s are the smoke path length and linear extinction coefficient of smoke respectively. The value of ℓ is a function of observer-target orientation with respect to plume axis and, is discussed in Appendix F.

The second effect is contrast reduction of D.C. systems by the glare or backscatter from the plume.

Hence we propose as a first order approximation to utilize the following expression for the perceived contrast through smoke, C_{rs}.

$$C_{rs} = C_r \cdot T_s \cdot \left[1 + a/\beta(e^{\alpha_s R^*} - 1)\right]^{-1} \qquad (3.35)$$

where C_r = contrast without smoke

T_s = transmittance through smoke

a = constant (1, 0.2 for non-sunny and sunny conditions respectively)

R* = range from cloud edge

α_s = smoke cloud scattering coefficient

To obtain a precise backscatter estimate the phase function may be used.

In Volume 2 we have assembled the model details into a formal structure.

4. VALIDATION

In this section we present the results of a validation of the material described in the earlier section; that is, on the basis of the agreement between the model formulated earlier and results from several field tests we conclude that the proposed model can provide reasonable prediction of the smoke cloud history and the obscuring effects of smoke. We now present the results on cloud rise, cloud width and then actual obscuration effects.

4.1 Cloud Rise

A significant parameter of cloud dynamics is the rate of cloud rise as a function of munition fill material, namely exothermic (phosphorus) and other smokes. Specifically, we evaluate the impact of rate of heat release on cloud height, since the cloud height affects cloud volume magnitude.

For the purpose of validation we selected the results of a number of munitions tested at the Jefferson Proving Ground (10). The comparative analysis is given below.

(a) 60mm Mortar

Fill - .75 # white phosphorus, burn time = 1 sec

Relative humidity - 62%

Pasquill Cat C

Mean Windspeed - 2 m/sec

With the above conditions, we first applied the appropriate expression for the cloud rise, $z(t)$ as given in Table 7. This result is shown in Fig. 15. We then calculated the increment, Δh, due to the use of WP,

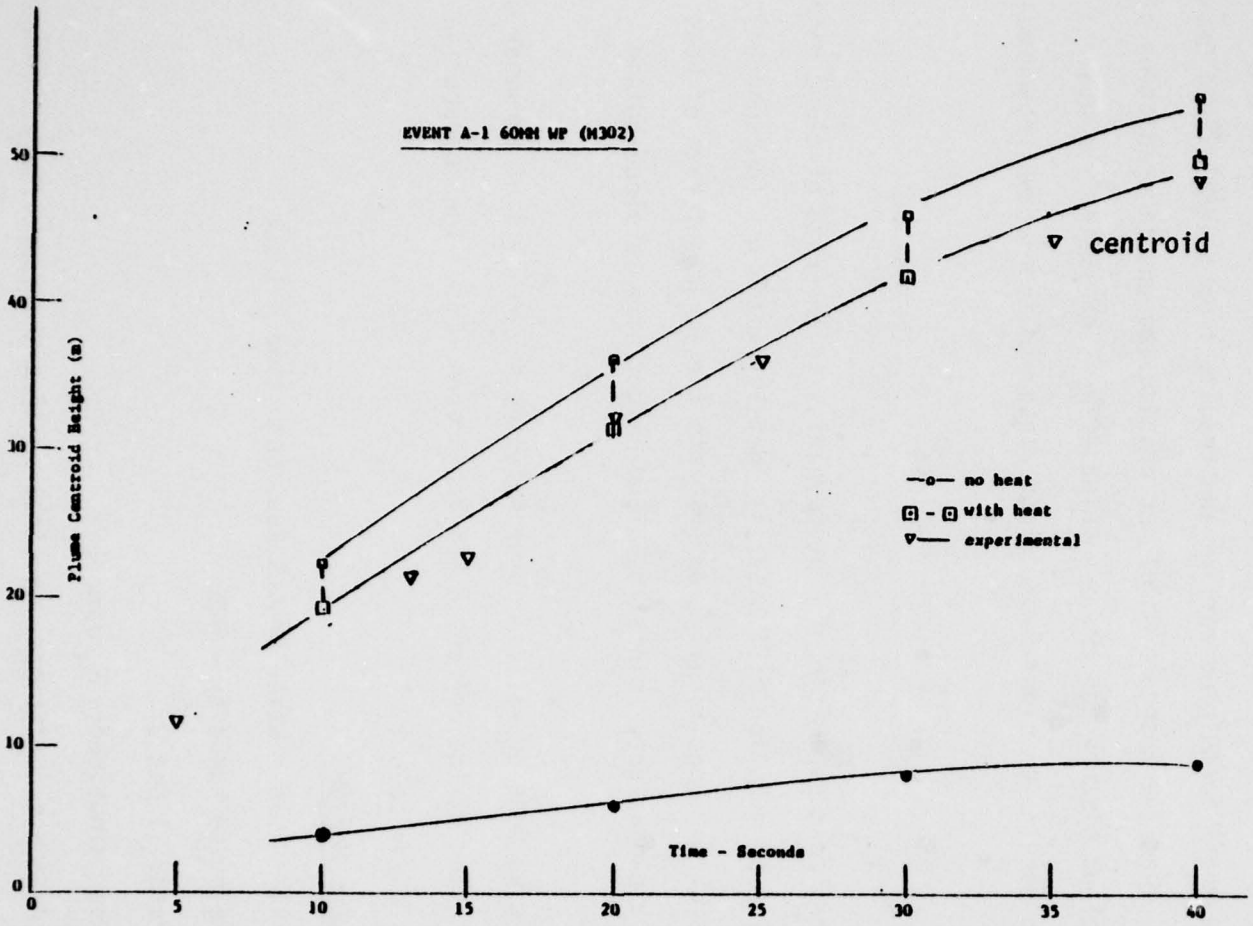

Fig. 15 Cloud Rise History

using eq. (3.15). The total cloud height, Z(t), is compared with the observed values where the effect of the variation in $\bar{u}$ is included.

The agreement between the computed and observed results is excellent. This and subsequent results support the need and method of including thermal effects into the formalism proposed here.

(b) 81mm Mortar

Fill - 1.75 # white phosphorus, burn time = 1 sec

Relative humidity = 92%

Pasquill Category = A

Mean Windspeed = .5-1.0 m/sec

In Fig. 16, we present the comparative result for the 81mm mortar. The agreement is satisfactory at later times. Uncertainty in the wind speed makes a precise correlation difficult.

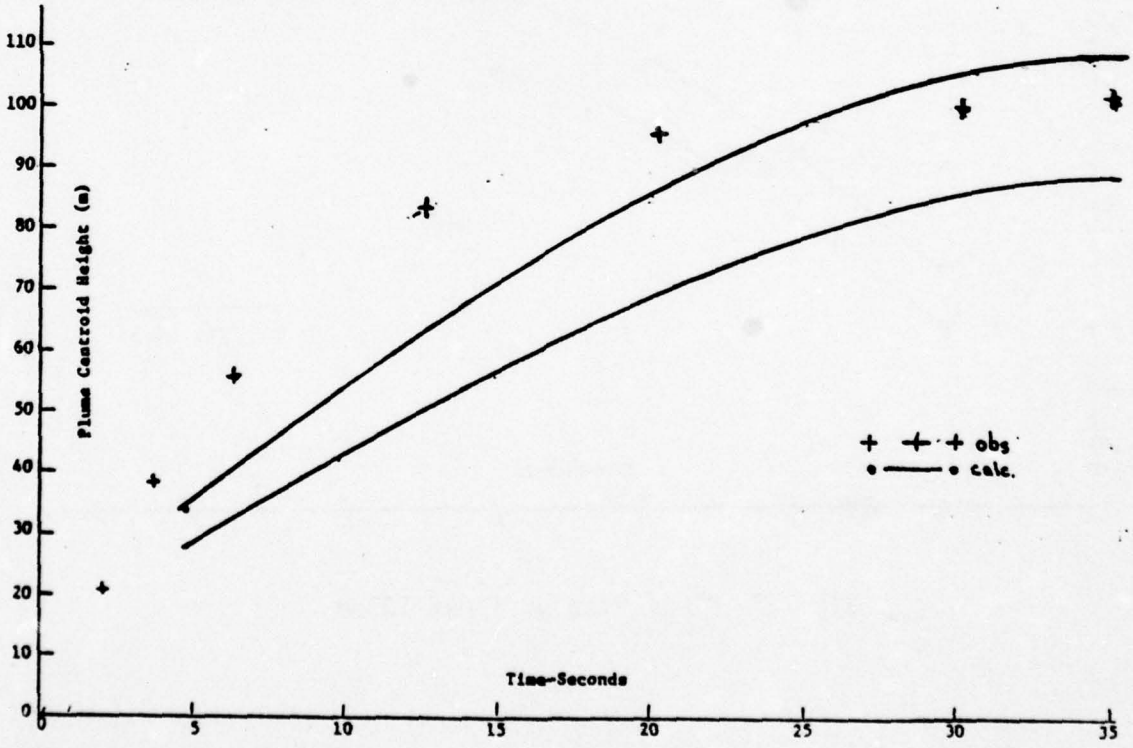

Fig. 16 Plume Rise vs Time: 81mm

(c) 105mm

Fill - 3.83 # white phosphorus, burn time = 1 sec

Relative humidity = 92%

Pasquill category = A/B

Mean windspeed - 1.0-2 m/sec

The results are given in Fig. 17 and show good agreement.

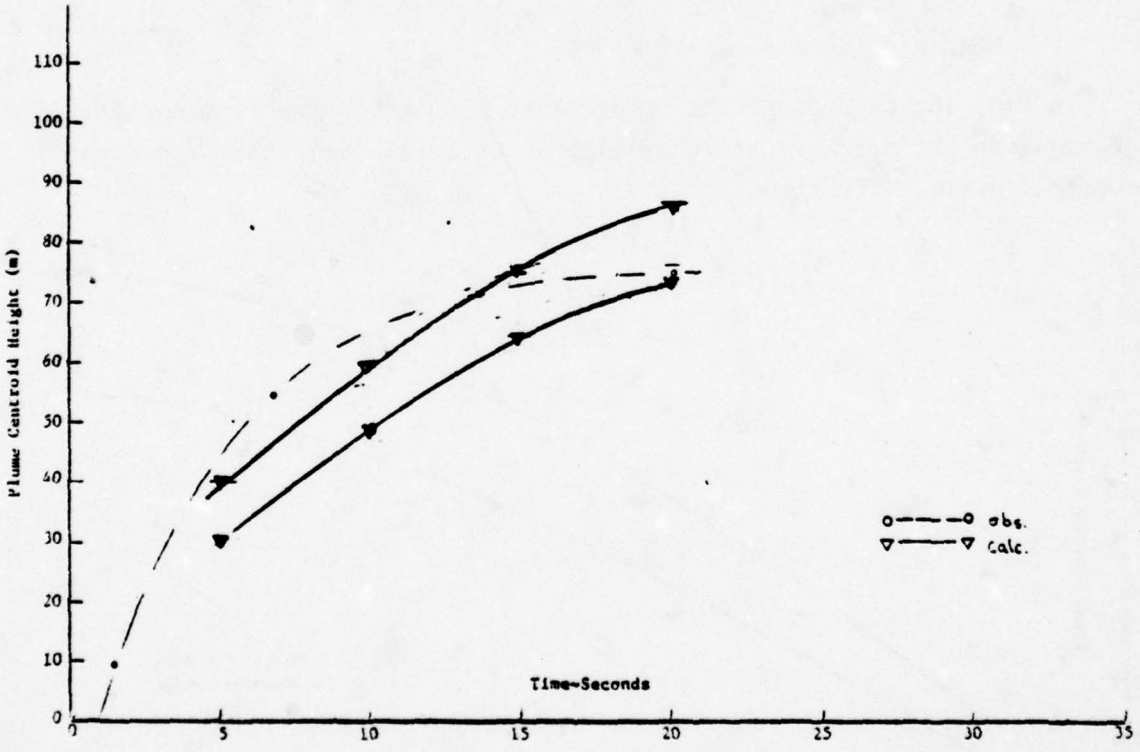

Fig. 17 Plume Rise vs Time: 105mm

(d) 155mm

Fill = 25.84 # 155 HC

Relative Humidity: 92%

Pasquill Category: B/C

Mean windspeed: 1.2-2.5 m/sec

In Fig. 18 we present the comparative results and again with good agreement.

An item of significance is the fact that the cloud approaches an asymptotic value as discussed in eqs. (3.15).

Hence we can state that the plume rise algorithms including the effect of cloud buoyancy is valid.

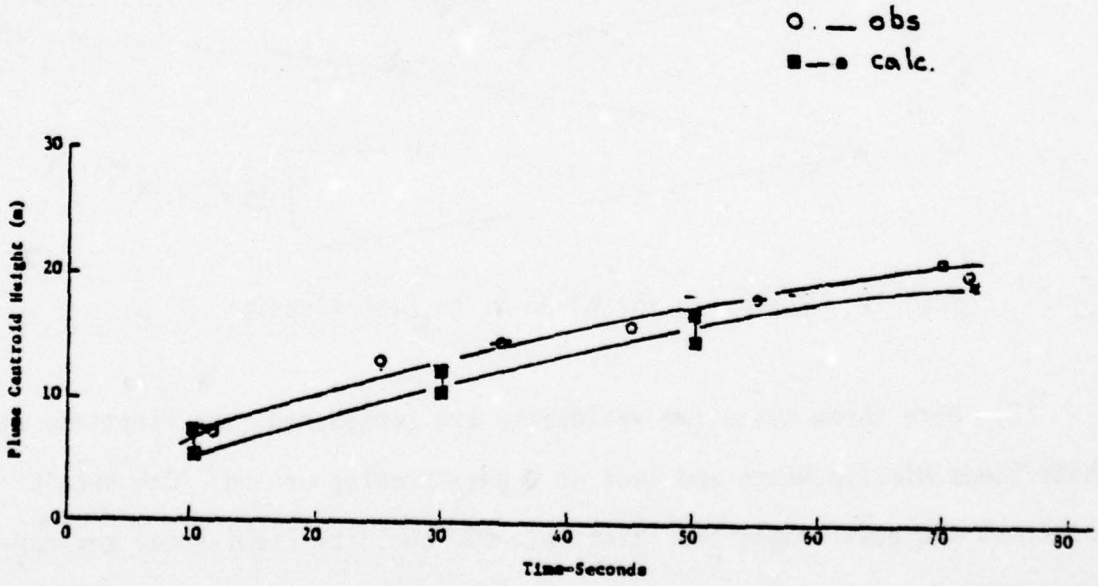

Fig. 18 Plume Rise vs Time: 155mm HC

4.2 CLOUD WIDTH AND OBSCURATION EFFECTS

(1) The effects of the smoke cloud on electrooptical systems are, as noted earlier, dependent upon the product (concentration x smoke path length). Hence the ability to calculate the concentration along the line-of-sight is basic to any model. In the validation tests to follow, the line-of-sight is established a'priori since it is the line which contains the particle density sampling devices.

(2) The cloud width is defined in Table 7 for single smoke munitions. To determine the total cloud width, L, as a function time for several collinear munitions one may add to the initial width at time zero the width, $y(t)$, from Table 7, see Fig. 19.

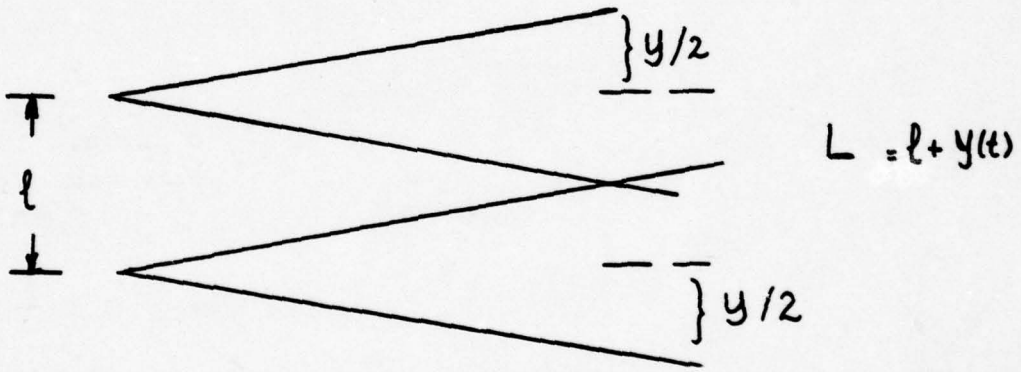

Fig. 19. Schematic for Cloud Width Determination

(3) Here three tests for validation are considered; the first two at White Sands Missile Range and last at Dugway Proving Ground. One should note that the test ranges are relatively low humidity (semi-arid) environments and, the ground is relatively smooth. For example at Dugway the relative humidity ~35%. This fact tends to suppress the thermal effects.

Validation (#1) - WMSR Test 9, WP-3, 20 July 1977

The first test was to compare the results obtained from the static detonation of 5 - 4.2" WP rounds. The input data were relative humidity - 31%,wind speed = 3.4 m/sec, wind direction 250° and Pasquill Category B-C. The geometrical configuration and surface cloud history are shown in Fig. 20. The calculated width is ~80m whereas the observed width is ~83 m.

In Fig. 21 we present a comparison of the calculated and measured (CxL) as a function of time where the five rounds are treated as five individual events neglecting the effect of overlap zones and considered the volume to be ellipsoidal. The agreement is fair since we have omitted fluctuations in the wind speed, however the calculated mean (CxL) would have accurately predicted the effect on a thermal system. In addition, an estimate of the atmospheric transmission τ in the 8-12μm region corresponding to CxL values is depicted in Fig. 21.

Let us now consider the detail shape of the CxL curve. From later results we find that the time mean wind speed, $\bar{u}$, provides the mean concentration; however, any fluctuations may be significant. Since we are interested in fluctuations on the order of seconds with sampling times ~1 sec and these data are unavailable we can only suggest that <u>in part</u> these fluctuations are responsible. The reason is that the overlapping may contribute additional turbulence.

In Fig. 22 we have reproduced the observed temporal history of concentration at the three aerosol samplers. We note that the two exterior samplers are similar whereas the center sampler's behavior is entirely different but consistent with the overlap zones. The observed gaps in concentration may be due to wind fluctuations.

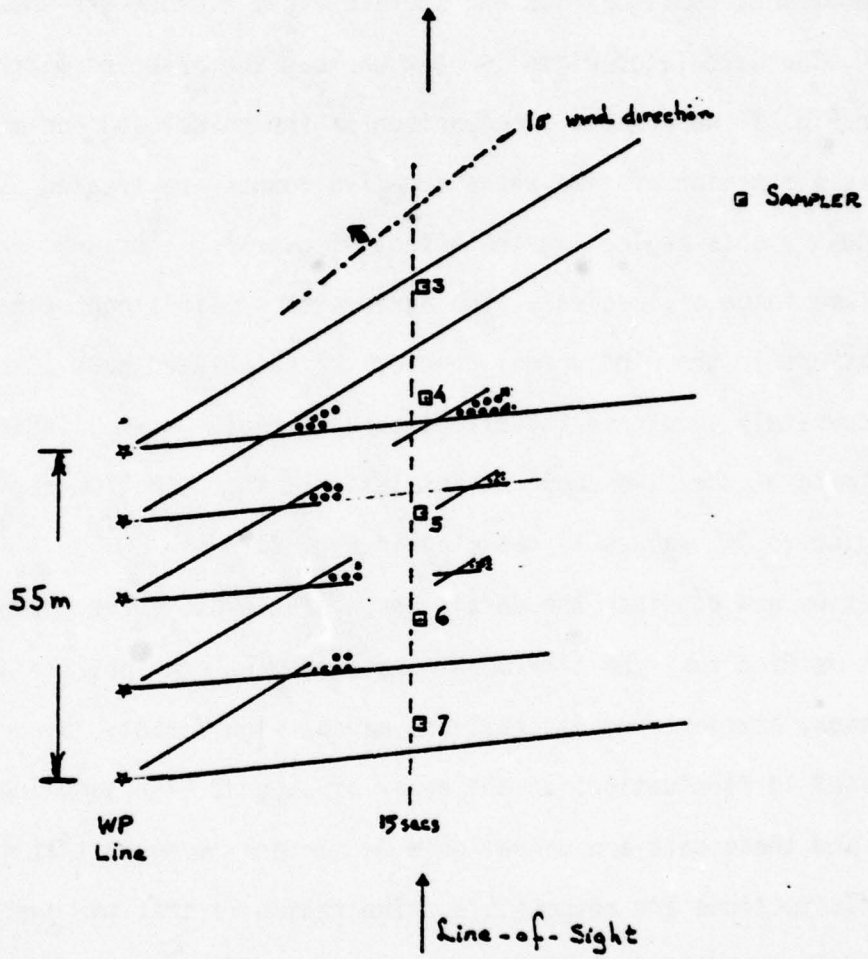

Fig. 20 Geometrical Configuration of Validation #1

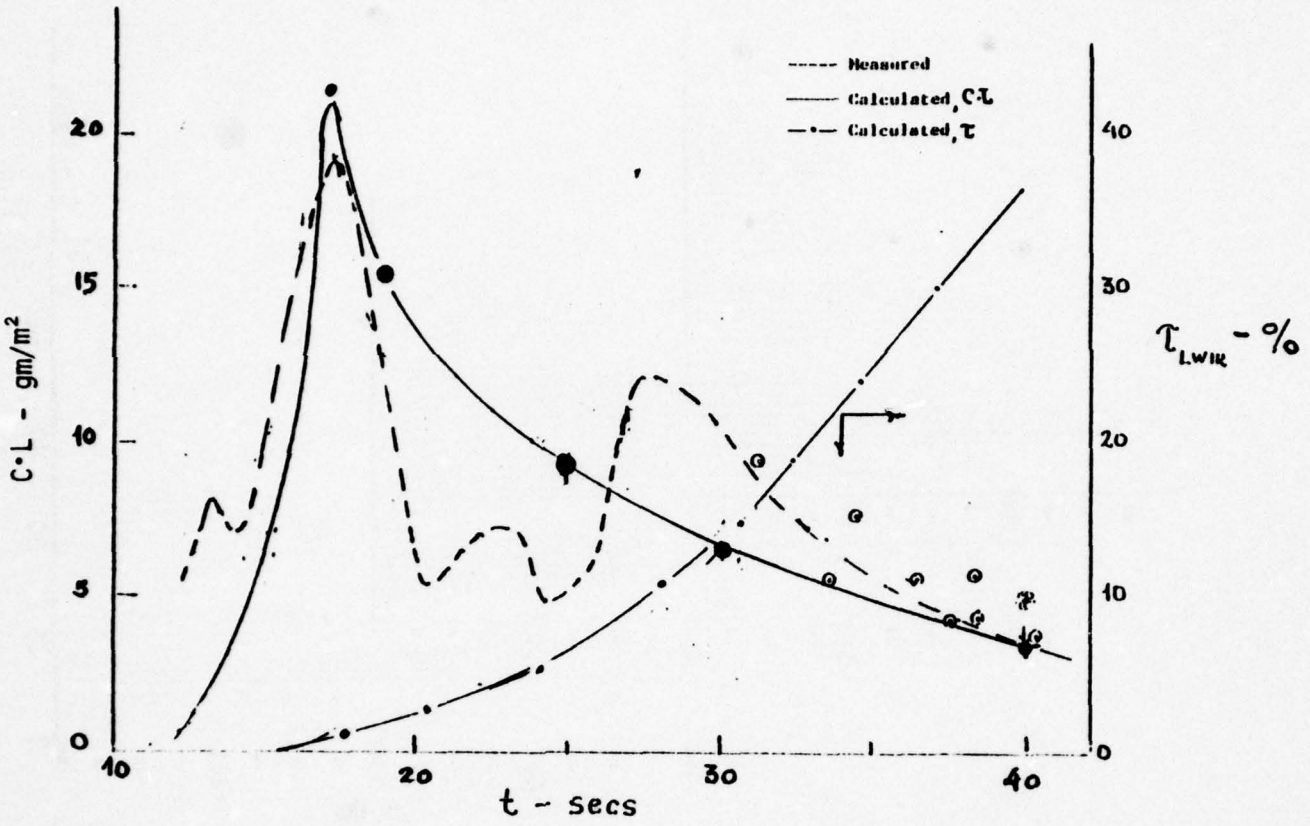

Fig. 21 C·L History for 5-4.2" WP Mortars

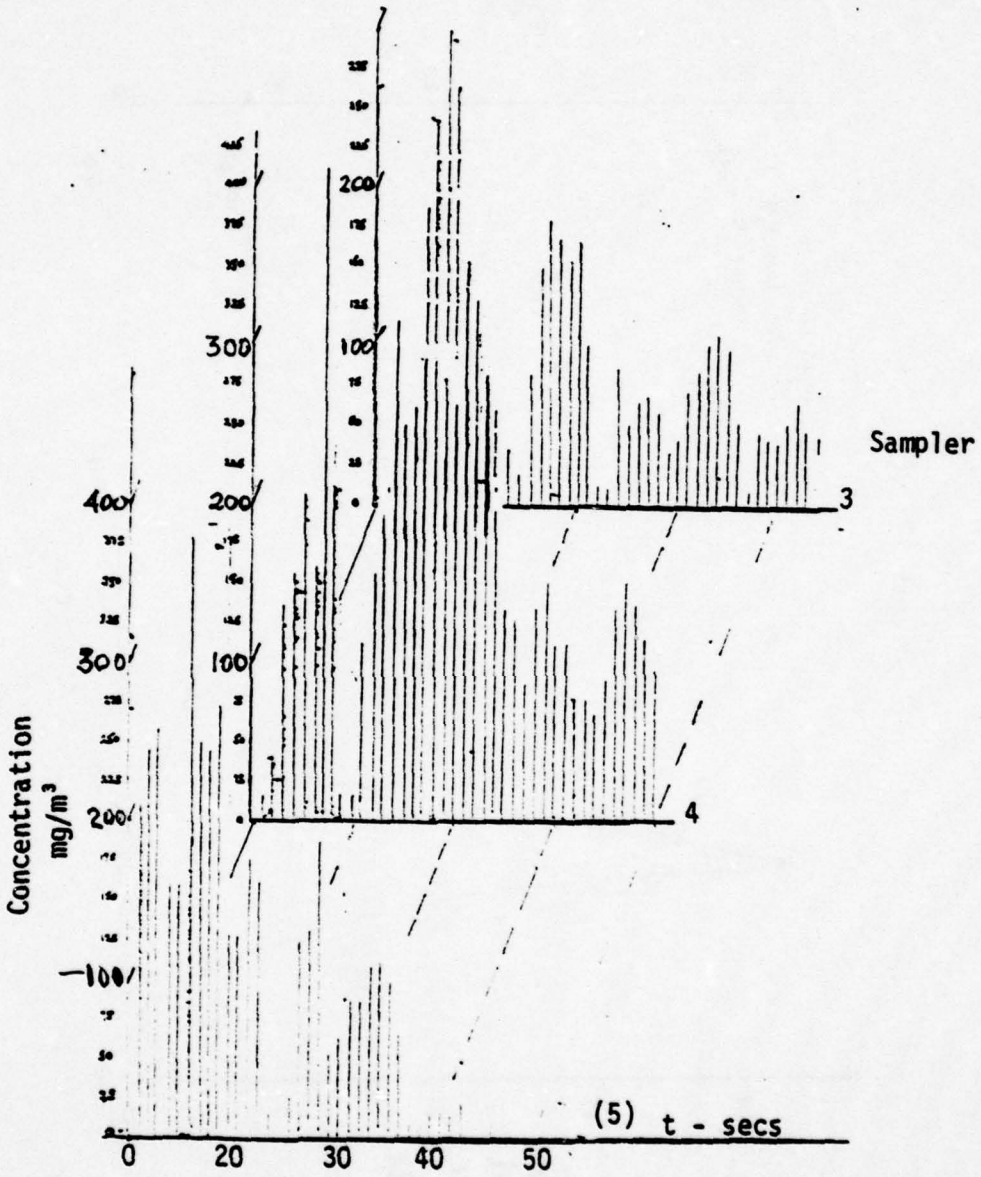

Fig. 22 Spatial-Temporal History of Concentration

One should note that the above estimate is of practical value; however, an improved methodology is required to treat the overlap region. The reason is that the outer layers are optical thinner than the inner core and, the effects on radiation transfer may be different than for an uniform concentration along a line-of-sight, e.g., when considering backscatter.

Validation (#2) - WSMR Test 12, WPW-2, 21 July 1977

The second validation is more complex and represents a non-steady state continuous line array. Here 13- 2.75" rocket heads were detonated in a static mode. Each head contains 12 white phosphorus wicks (WPW) and the total weight of white phosphorus/head is 1.682 kg. The meteorological conditions were relative humidity - 36% and mean wind speed - 3.7 m/sec. The Pasquill stability category was stated to be B.

In Fig. 23 is the geometric layout of the smoke material. We assume in the absence of any distribution data, that the source is three lines where the centerline (~75 m from sampler line) contains 50% of source strength and 50% is equally distributed $\pm$ 20 m from the centerline.

First we note that the effect of the WP is insignificant since each wick has only ~140 gms of slow burning phosphorus. Hence the width increase and height of the cloud are defined by Table 7. The values at 15, 20, and 25 secs, arrival times from the three lines to sampling line, are y = 27.1, 33.4 and 39.5 and z = 8.8, 10.98 and 13.2 m respectively.

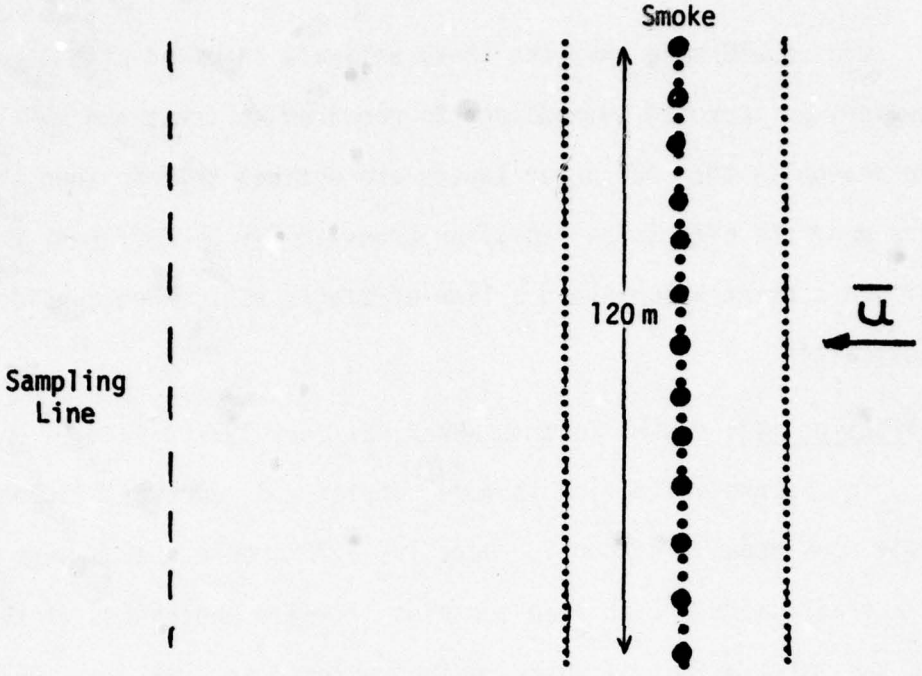

Fig. 23 Sensor/Smoke Layout

From the above the maximum width is $\ell + y = (120 + 39.4)m \sim 160m$. The observed maximum width ~150 meters.

We now compute the concentration in steps, i.e., from each source line separately. The concentration at the sampling line is given by

$$C(x,t) = \left(\frac{Q \cdot Y}{t \cdot \ell}\right) \frac{1}{\sqrt{\frac{\pi}{2}}\,\bar{u}\, Z(x,t)(1+k)} \qquad (3.36)$$

where Q = smoke material wt (gms)

Y = yield

t = burn time (sec)

ℓ = length of smoke material (m)

$\bar{u}$ = mean speed (m/sec)

$z(x,t)$ = smoke cloud height at x

k = [smoke width (y) at x]/ℓ

Substituting the values for constants in (3.36) @ 14.9 secs to obtain

$$C(x,t) = \frac{(5.46 \times 10^3)(3)}{(240)(120)} \quad \frac{1}{\frac{\pi}{12}(3.7)(8.8)(1.22)}$$

$$= .055 \text{ g/m}^3 \text{ @ } \underline{14.9 \text{ secs}}.$$

At 20.2 secs, the smoke from the 2nd line arrives and the smoke from the 3rd line arrives at 25.6 secs. The individual concentrations are found directly from (3.36)

$$C(x,20) \simeq .055 \times 2 \times \frac{8.8}{11} = .088 \text{ g/m}^3,$$

and

$$C(x,25.6) \simeq .055 \times 1 \times \frac{8.8}{13.2} = .037 \text{ g/m}^3$$

The parameter (C•L) = concentration x smoke thickness and the individual contributions are

(1) $C(x,15) \simeq .055 \times 147 = 8.10 \text{ gm/m}^2$

(2) $C(x,20) \simeq .088 \times 153 = 13.5 \text{ g/m}^2$ or, @20 sec = 21.6 g/m^2

(3) $C(x,25) \simeq .037 \times 160 = 5.9 \text{ g/m}^2$ or @25 sec = 27.5 g/m^2

At later times we assert that the mean concentration drops as M(t)/V(t) and therefore, we obtain the following values at 40 and 120 secs, namely ~17.54 g/m^2 and ~9.4 gm/m^2, see Fig. 24.

The oscillatory character of the "C•L" curve clearly depends on the turbulence spectra of atmosphere during the test; that is $\bar{u}$ is the mean speed whereas the actual speed is $u = \bar{u} + u'$ where u' is the fluctuations. To appropriately find the variance of the wind speed we need sampling times ~1 sec for a sampling period of ~10 mins i.e. $t_o \pm 5$ mins.

An examination of the wind speed at 2 and 7 meters sampled every 60 secs indicated that a minimum occurred at +150 secs and a peak occurred at ~210 secs an excursion of ~1.75 to 2 in $\bar{u}$. The standard deviation is ~30%; however, the excursion of a factor of 2 can reduce or increase the C•L by a factor of 2. The reason is that the concentration $\propto \bar{u}^{-1}$. The mean value and the standard deviation are shown in Fig. 24.

Further validation has been obtained from a comparison between predicted and observed system outage but omitted for classification reasons.

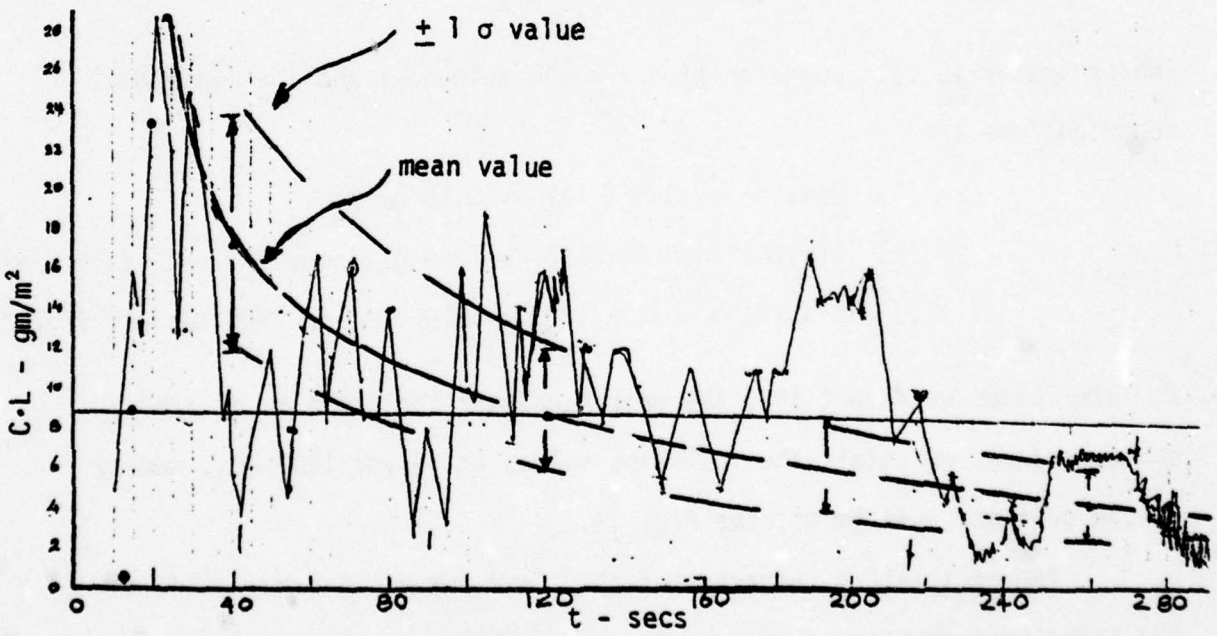

Fig. 24 C•L History for 13 - 2.75" Heads:
(—) measured; (---) calculated

Validation (#3) - Dugway Test DPI-002-T-34, 19 Nov 1977

Here we consider the static test firing of six (6) 155 mm (M110E2) white phosphorus shells spaced 3.7 meters apart. The input data are as follows: mean speed - 4.9 m/sec at 20° to horizontal axis; relative humidity - 35%; and Pasquill category - D.

Before presenting any calculational results let us briefly discuss the experimental details. The close proximity of such large shells raises the question on the interactive effects and the dispersal of the smoke source material. Further the size of the phosphorus particles is uncertain and, in turn the burn time.

The test data include the cloud size at time of detonation: height ≈7 m; width ≈25 m; and length ≈22 m. Hence, the phosphorus material was dispersed over the area 25 x 22 m^2. Interestingly, since the original width is 18.5 m the additional linear spread was only ~6.5 m. If we now consider an individual round and apply the appropriate Δh equation* we find $x^* = 4.4$ m and $\Delta h \rightarrow 23$ m in several seconds. Thereafter the plume will rise gently by momentum exchange.

Since the phosphorus cannot burn long enough to be treated as a continuous source we assume that source is approximately instantaneous.

The (C•L) result is shown in Fig. 25 for the Sampling Line at x ~76 m. For comparison we show the measured C•L at x ~137 m and we note that the two C•L values as a function of time are approximately similar. The latter is an inherent assumption of the model, namely uniform concentration.

*For category D, eq. (3.15c).

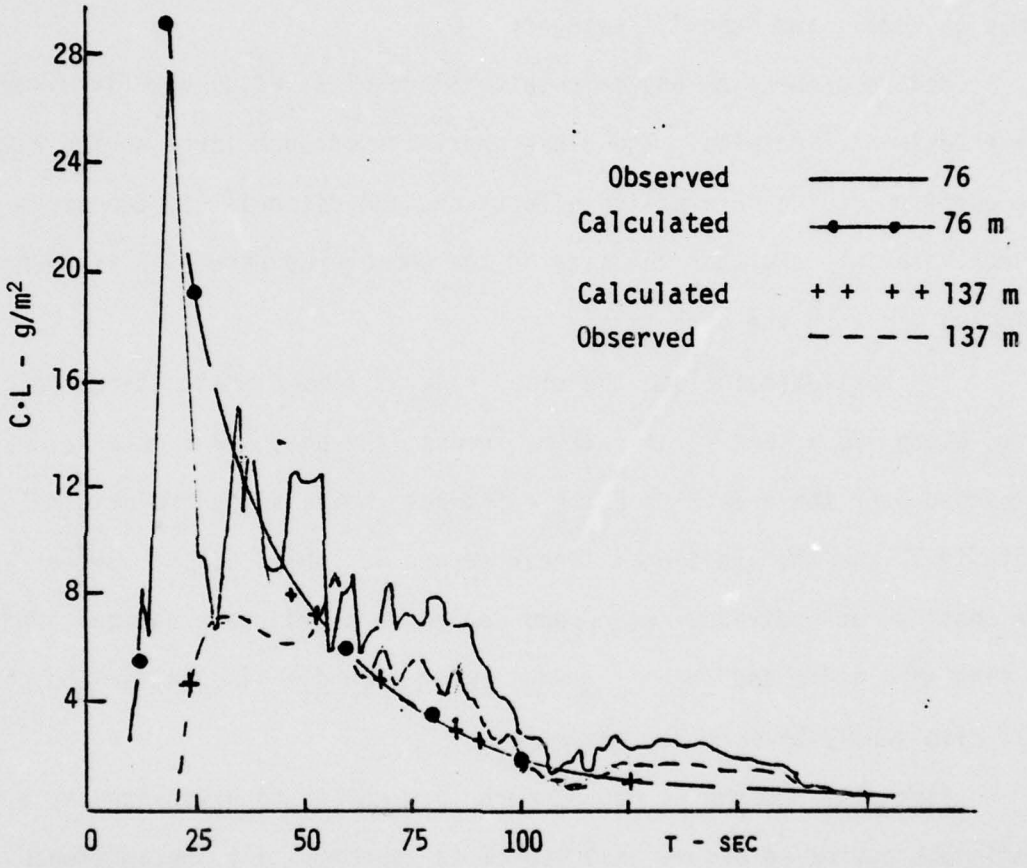

Fig. 25 C·L History of 6-155mm WP Shells

Appendix A

MUNITIONS CHARACTERISTICS

Table A1

TYPES OF FILL AND FILL WEIGHTS FOR SMOKE MUNITIONS

SYSTEM	AMMUNITION	FILL TYPE	FILL WEIGHT (LBS)
Hand Grenade, Smoke[1]	AN-M8(STD.A)	HC	1.2
Hand Grenade, Smoke	M15(STD.C)	WP	0.9
Hand Grenade, Smoke	M18(STD.A)	Colored Smoke	0.71
Hand Grenade, Smoke	M34(STD.A)	WP	0.94
Rifle Grenade, Smoke[1]	M19A1(STD.C)	WP	0.53
3.5 inch Rocket[1]	M30(C&T)*	WP	2.23
40 mm[2]	M675(E25) (STD.B)	Red Smoke	0.21
40 mm	XM676(L.P.)**	Yellow Smoke	0.13
57 mm Cannon[2]	M300A1(C&T)	WP	0.37
60 mm Mortar[2]	M302A1(C&T)	WP	0.75
	M302(C&T)	WP	0.75
75 mm Rifle[2]	M311, M311A1(C&T)	WP	1.35
76 mm Gun[2]	M361A1(STD.A)	WP	1.38
81 mm Mortar	M57(Obsolete)	FS	4.59
	M57, M57A1(STD.C)	WP	4.06

Table A1 (Cont'd)

TYPES OF FILL AND FILL WEIGHTS FOR SMOKE MUNITIONS

SYSTEM	AMMUNITION	FILL TYPE	FILL WEIGHT (LBS)
81 mm Mortar (Cont)	M370(STD.B)	WP	1.60
	M375(STD.B)	WP	1.75
	M375A1(STD.B)	WP	1.75
	M375A2(STD.A)	WP	1.75
90 mm Tank Gun	M313C(STD, STD.B)	WP	1.97
105 mm Tank Gun	M416(STD.A)	WP	6.00
105 mm Howitzer	M60(STD.A)	WP	3.83
	M84B1, M84(STD.A)	HC	7.50
	M84BE Yellow	HC	4.92
	Red	HC	5.21
	Green	HC	5.13
	Violet	HC	5.13
	M84E1(LP)	HC	12.30
155 mm Gun	M104(STD.B)	WP	15.60
Howitzer	M110E2 Smoke Projectile	WP	15.60
Howitzer	M110(STD.A)	FS	17.47
Howitzer	M116(STD.B)	HC	25.84
Howitzer	M116B1 (any color)	HC	17.19
120 mm Gun	M357 Projectile	WP	7.2

Table A1 (Cont'd)

TYPES OF FILL AND FILL WEIGHTS FOR SMOKE MUNITIONS

SYSTEM	AMMUNITION	FILL TYPE	FILL WEIGHT (LBS)
4.2 inch Mortar[2]	M2A1 Smoke Cartridge	WP	7.50
	"	PWP	7.50
	M328(STD.B)	WP	7.50
	M328A1(STD.A)	WP	8.14
	M2(STD.B)	WP	7.50
	M2(Obsolete)	FS	7.50
5 inch Gun[2]	5-inch/38-cal. Projectile	WP	7.10
	5-inch/54-cal. Projectile	WP	8.34
100-lb Smoke Bomb[3]	AN-M47A4	WP	100.00
		PWP	74.00
100-lb-TI Smoke Bomb[4]	M84A1(C&T)	Red Smoke	72.0
200-lb-TI " "	M91(STD.)		
250-lb-TI " "	M91(STD.)	Red Smoke	16.6
		Green	18.8
		Yellow	13.9

Table A1 (Cont'd)

TYPES OF FILL AND FILL WEIGHTS FOR SMOKE MUNITIONS

SYSTEM	AMMUNITION	FILL TYPE	FILL WEIGHT (LBS)
250-lb-T1 Smoke Bomb	M100(STD.)	Red-Green Smoke Yellow-Green Red-Yellow	70.1 66.1 58.9
250-lb-T1 " "	M09(C&T)	Red Smoke Green Yellow	63.4 71.8 56.7
250-lb-T1 " "	M90(C&T)	Red Smoke Green Yellow	59.3 66.1 53.0
250-lb-T1 " "	M98(C&T)	Red Smoke Green Yellow	32.2 35.9 28.8
CBU-11A[3]	261 BLU-16/B Smoke Bombs	HC	Cluster 265.00 Bomb 1.00
CBU-12/A	261 BLU-17/B Smoke Bombs	WP	Cluster 315.00 Bomb 1.20

Table A1 (Cont'd)

TYPES OF FILL AND FILL WEIGHTS FOR SMOKE MUNITIONS

SYSTEM	AMMUNITION	FILL TYPE	FILL WEIGHT (LBS)
CBU-12A/A***	213 BLU-17/B Smoke Bombs	HC	Cluster 256.00 Bomb 1.20
CBU-13/A	130 BLU-16/B	HC	Cluster 130.00 Bomb 1.00
	131 BLU-17/B Smoke Bombs	WP	Cluster 158.00 Bomb 1.20

*Contingency & Training
**Limited Production
***Adapted for F-4 Aircraft

(1) "Logistics Complete Round Charts, Grenades, Mines, Pyrotechnics, Rockets, Rocket Motors, Demolition Material," AMCP 700-3-5, March, 1970.
(2) "Logistics Complete Round Charts. Artillery Ammunition. "AMCP 700-3-3, Nov., 1970
(3) JHLH Effectiveness Manual (Air-To-Surface) Weapons Characteristics Handbook, 1965
(4) "Logistics. Complete Round Charts, Bombs "AMCP 700-3-4, Dec., 1968

NOTE: FM3-50 notes a MK12 Mod 0 Smoke Tank (Navy) which can produce a 360 meter screen in 30 secs with a duration of 5-15 minutes.

Table A2

Some Smoke Generators and Pots

Smoke	Type	Fill	Fill Wt/Flow Rate
Smoke Generator	M3	Fog Oil	25-50 gals/hr
Smoke Pot	AN-M7	Fog Oil (SGF)	–
	AN-M7A1	Fog Oil (SGF)	–
Smoke Pot	M1	HC	10.0
	ABC-M5	HC	3.0
Air Smoke Pot	M4A2		

Table A3

U.K. Grenades

Smoke Screen Type	Range (m)	Burn Time (sec)	Source	Smoke	Time (sec)	Fill
L5A1,2,3,4	70 (grd)	55-75	Point ground	White	8	
L7A1	70 (grd)	30-50	Point ground	Green		
XL7E2	120 (grd)	30-50	Point ground	Green		
XL8E1 (Curtain) L8A1	30	60-90	8 m air, ground	-	2	RP+ butyl rubber
XL18E1 (for L8A1 practice)	120		10 m air, ground			T_iCl_4+ silica
XL19E1	110	8-10		Green		

Appendix B

DISCUSSION OF SMOKE YIELD

DISCUSSION OF SMOKE YIELD

The yield of smoke/obscurants, particular white phosphorus, is uncertain. Johnson and Forney[1] published a set of data which has been reduced here in algebraic form:

$$Y(WP) = 3.8 + .003\ (RH\% - 10)^{1.67}$$

$$Y(ZnCl_2) = 1 + .051\ (RH\% - 5)^{.85}$$

$$Y(AlCl_3/H_2SO_4) = 2.8 + .016\ (RH\% - 20)^{1.25}$$

$$Y(\text{Fog Oil}) = 1$$

Other data indicate that yield for white phosphorus can be defined by the expression, eq. 2.2.

$$Y(WP) = 2.9 + .003\ (RH\% - 40)^{1.67}$$

The other obscurant yields have adjusted accordingly. This difference is significant and can seriously alter the validation of a model; that is, the spatio-temporal history of the aerosol concentration and radiation transfer.

Another impact of the yield is the effect on ΔT (eq 3.13). Since the parameter ν relates the liquid fraction to the total mass we may also write $\nu = (Y-k)/Y$. If $k = 2.9$ or 3.8 the value of ν will change accordingly and similarly ΔT, see Fig. 5.

---

[1] Johnson, M.C. and Forney, P.D., "The Effectiveness of Obscuring Smokes," ORG, Edgewood Arsenal, 1972 (unpublished).

Appendix C

A STABILITY CLASSIFICATION BASED ON HOURLY AIRPORT OBSERVATIONS

A STABILITY CLASSIFICATION BASED ON HOURLY AIRPORT OBSERVATIONS *

This system of classifying stability on an hourly basis for research in air pollution is based upon work accomplished by Dr. F. Pasquill of the British Meteorological Office (see reference 1 of text). Stability near the ground is dependent primarily upon net radiation and wind speed. Without the influence of clouds, insolation (incoming radiation) during the day is dependent upon solar altitude, which is a function of time of day and time of year. When clouds exist, their cover and thickness decrease incoming and outgoing radiation. In this system insolation is estimated by solar altitude and modified for existing conditions of total cloud cover and cloud ceiling height. At night, estimates of outgoing radiation are made by considering cloud cover. This stability classification system has been made completely objective so that an electronic computer can be used to compute stability classes. The stability classes are as follows: (A) Extremely Unstable, (B) Unstable, (C) Slightly Unstable, (D) Neutral, (E) Slightly Stable, (F) Stable, (G) Extremely Stable. Table A-1 gives the stability class as a function of wind speed and net radiation. The net radiation index ranges from 4, highest positive net radiation (directed toward the ground), to -2, highest negative net radiation (directed away from the earth). Instability occurs with high positive net radiation and low wind speed, stability with high negative net radiation and light winds, and neutral conditions with cloudy skies or high wind speeds.

The net radiation index used with wind speed to obtain stability class is determined by the following procedure:

---

* The following explanation of the Pasquill Stability classification has been extracted from an article by D. Bruce Turner in the February 1964 Journal of Applied Meteorology

(1) If the total cloud cover is 10/10 and the ceiling is less than 7000 feet, use net radiation index equal to 0 (whether day or night).

(2) For nighttime (night is defined as the period from one hour before sunset to one hour after sunrise):

a. If total cloud cover $\leq 4/10$, use net radiation index equal to -2.

b. If total cloud cover $>4/10$, use net radiation index equal to -1.

(3) For daytime:

a. Determine the insolation class number as a function of solar altitude from Table A-2.

b. If total cloud cover $\leq 5/10$, use the net radiation index in Table A-1 corresponding to the insolation class number.

c. If cloud cover $>5/10$, modify the insolation class number by following these six steps:

(1) Ceiling <7000 ft., subtract 2.

(2) Ceiling ≥ 7000 ft. but <16000 ft., subtract 1.

(3) Total cloud cover equal 10/10, subtract 1. (This will only apply to ceilings ≥ 7000 ft. since cases with 10/10 coverage below 7000 ft. are considered in item 1 above).

(4) If insolation class number has not been modified by steps (1), (2), or (3) above, assume modified class number equal to insolation class number.

(5) If modified insolation class number is less than 1, let it equal 1.

(6) Use the net radiation index in Table A-1 corresponding to the modified insolation class number.

TABLE A-1 STABILITY CLASS AS A FUNCTION OF NET RADIATION AND WIND SPEED

WIND SPEED (KNOTS)	NET RADIATION INDEX 4	3	2	1	0	-1	-2
0, 1	A	A	B	C	D	F	G
2, 3	A	B	B	C	D	F	G
4, 5	A	B	C	D	D	E	F
6	B	B	C	D	D	E	F
7	B	B	C	D	D	D	E
8, 9	B	C	C	D	D	D	E
10	C	C	D	D	D	D	E
11	C	C	D	D	D	D	D
≥ 12	C	D	D	D	D	D	D

TABLE A-2 INSOLATION AS A FUNCTION OF SOLAR ALTITUDE

SOLAR ALTITUDE (a)	INSOLATION	INSOLATION CLASS NUMBER
60° < a	Strong	4
35° < a ≤ 60	Moderate	3
15° < a ≤ 35	Slight	2
a ≤ 15°	Weak	1

AD-A062 862 GENERAL RESEARCH CORP MCLEAN VA F/G 19/1
AN OBSCURING AEROSOL DISPERSION MODEL. VOLUME I. DEVELOPMENT AN--ETC(U)
DEC 78 R ZIRKIND DAAK02-76-C-0366
UNCLASSIFIED CR-231-VOL-1 NL

2 OF 2
ADA
062862

END
DATE
FILMED
3 79
DDC

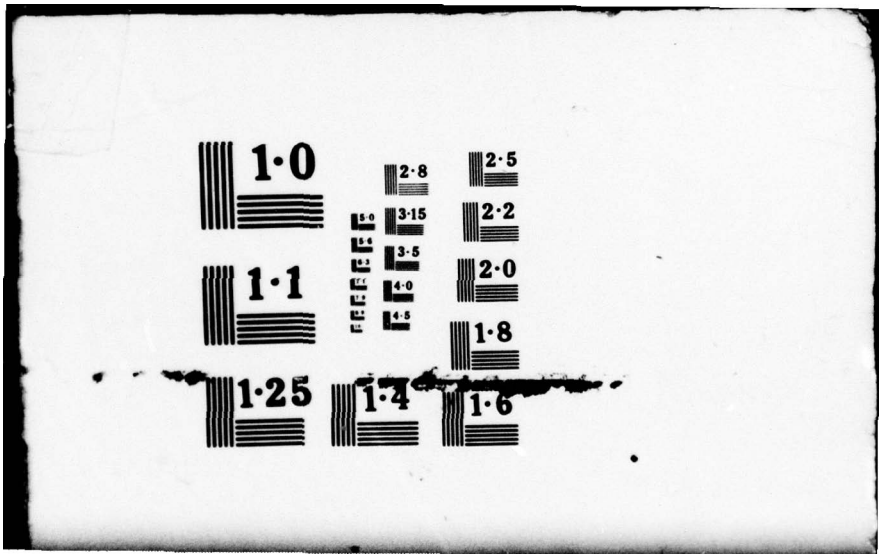
1·0
1·1
1·25
2·8
3·15
3·5
4·0
1·4
2·5
2·2
2·0
1·8
1·6

Appendix D

DESCRIPTION OF A COMPUTER MODEL FOR DISPERSION OF MULTIPLE SOURCES

DESCRIPTION OF ATDL COMPUTER MODEL FOR DISPERSION FROM MULTIPLE SOURCES *

Steven R. Hanna

Air Resources Atmospheric Turbulence and Diffusion Laboratory
National Oceanic and Atmospheric Administration
Oak Ridge, Tennessee

In order to estimate surface concentrations of pollutants in regions containing many sources, it is convenient to place the emissions into two categories: area sources (*e.g.*, home heating or small industries) and point sources (*e.g.*, power plants or large industries). In previous reports,[1,2] simple methods of calculating concentrations due to area sources were derived and verified. We have devised a straightforward computer model for accounting for point sources as well as area sources. This model has been applied to many regions, including Rockwood-Harriman, Tennessee,[3] and Knoxville, Tennessee.[4] It is the purpose of this paper to outline the ATDL computer program in detail so that others may use it.

CALCULATION OF SURFACE CONCENTRATIONS DUE TO AREA SOURCES

Most source emission inventories distribute the area sources in an urban region into a square grid pattern, with grid distances of about 5 km, where it is assumed that the area source strength in any grid square is uniform across that square. Gifford's[5] "reciprocal plume" concept is employed in order to estimate the surface concentration $\chi(\mu g/m^3)$ due to area sources upwind of the receptor point:

$$\chi = \int_0^D \sqrt{\frac{2}{\pi}} \frac{Q_A}{U\sigma_z} \, dx \qquad (1)$$

where $Q_A(\mu g/m^2 sec)$ is source strength, D(m) is the distance to the edge of the urban area, U(m/sec) is the wind speed, and σ_z(m) is the vertical dispersion parameter. Smith[6] suggests the following empirical form for σ_z:

$$\sigma_z = ax^b, \text{ (x in meters)} \qquad (2)$$

*Noll, K.E., (ed), Industrial Air Pollution Control, Ann Arbor Science Publishers Inc., 1975.

Sunny day	a = .40	b = .91
Cloudy day	a = .15	b = .75 (also applies to yearly averages)
Night	a = .06	b = .71

If the receptor is at the center of grid block "0," with grid distance Δx, and the wind blows in only one direction, then equation 1 can be written as the summation over grid squares upwind of the receptor square:

$$\chi = \sqrt{\frac{2}{\pi}} \frac{(\Delta x/2)^{1-b}}{Ua(1-b)} \left[Q_{A0} + \sum_{i=1}^{4} Q_{Ai} \left[(2i+1)^{1-b} - (2i-1)^{1-b} \right] \right] \quad (3)$$

The source strengths $Q_{A0}, Q_{A1}, Q_{A2}, \ldots$, apply to the grid square in which the receptor is located, the grid square upwind of the receptor square, and so on, respectively. The integration is arbitrarily terminated after four grid squares. If the frequency with which the wind blows from the 16 major directions is known, then equation 3 becomes the double summation:

$$\chi = \sqrt{\frac{2}{\pi}} \frac{(\Delta x/2)^{1-b}}{Ua(1-b)} \left[Q_A(0,0) + \sum_{i=\pm1}^{\pm4} \sum_{j=\pm1}^{\pm4} Q_A(i,j)\, f(i,j) \left[(2r+1)^{1-b} - (2r-1)^{1-b} \right] \right] \quad (4)$$

where r is the number of grid blocks that square (i,j) is away from the central receptor square. For example, r equals one for the "ring" of eight squares adjacent to the central receptor square. When the 16 point wind direction frequency distribution is input to the program, the parameters f (i,j) and $(2r+1)^{1-b} - (2r-1)^{1-b}$ are calculated within the program, using techniques explained by Gifford and Hanna.[1]

In the program, therefore, each element C(i,j) of a 9 by 9 matrix of coefficients is multiplied by the corresponding element $Q_A(i,j)$ of the source matrix to obtain the concentration χ in the central square. Thus, it is necessary to expand the source matrix by 4 squares on all sides, entering small, background source strengths in these squares, so that the 9 by 9 coefficient matrix will "fit" over the source grid along the edges of the given urban area.

These techniques are straightforward and do not necessarily require a digital computer. We have often made them using a slide rule or desk calcula-

tor. However, the point source calculations, described in the next section, are sufficiently complicated that a digital computer should be used.

CALCULATION OF SURFACE CONCENTRATIONS DUE TO POINT SOURCES

The basic Gaussian plume formula described by, for example, Slade[7] is used to estimate surface concentrations due to point sources. For a 16 point wind direction frequency distribution, the surface concentration χ of a pollutant emitted at strength Q_p (μg/sec) is given by the formula:

$$\chi = \sqrt{\frac{2}{\pi}} \frac{fQ_p}{\sigma_z r U \frac{2\pi}{16}} e^{-\frac{H^2}{2\sigma_z^2}} \quad (5)$$

where H(m) is the effective source height, r(m) is the distance of the receptor point from the source, and f is the frequency with which the wind blows towards the sector of interest. (This formula is equivalent to Slade's[7] equation 3.144.) The effective source height H is the sum of the stack height h_s and the plume rise h_p, which is calculated using the formula proposed by Briggs:[8]

$$h_p = 2.9 \left\{ w_o R_o^2 \left[T_{po} - T_{eo} \right] / \left[U\left(\frac{\partial T_e}{\partial z} + .01^\circ C/m \right) \right] \right\}^{1/3} \quad (6)$$

where g, T, w_o, and R are the acceleration of gravity, absolute temperature, initial plume vertical speed, and stack radius, respectively. The subscripts p and e refer to plume and environment variables, respectively.

Equation 5 can be used in order to estimate the average concentration in the grid square in which the point source is located. The source is assumed to be located in the center of the square, and the average concentration in the circle with radius $\Delta x/2$ is assumed to equal the average in the square with side Δx. Also since there is only one wind direction sector for the source square, the fraction $2\pi/16$ in equation 5 becomes 2π, and the frequency f equals one.

$$\bar{\chi}_{\text{source square}} = \frac{1}{\pi\left(\frac{\Delta x}{2}\right)^2} \int_0^{2\pi} d\theta \int_0^{\Delta x/2} \sqrt{\frac{2}{\pi}} \frac{Q_p}{a r^b U 2\pi} e^{-\frac{H^2}{2a^2 r^{2b}}} dr \quad (7)$$

This equation is integrated numerically by the computer, given the input parameters Δx, Q_p, a, b, H, and U. It is found that the average concentration due to a ground level (H = 0) point source located in the middle of the grid square is equal to the average concentration due to a uniform area source in that grid square, provided that Q_p equals $Q_A (\Delta x)^2$; *i.e.*, the total emissions in the square are equal. The average concentration $\overline{\chi}$ in grid squares other than the source grid square is assumed to equal the concentration in the center of the square calculated using equation 5. Gifford's[5] reciprocal plume concept is then used to estimate the total surface concentration in a grid square due to contributions from the given distribution of point sources by superimposing a 9 by 9 matrix over the source grid, and multiplying term by term. This is done in the program by classes of effective stack height, H.

PROGRAM DESCRIPTION

Input

The computer program, written in FORTRAN IV for use on an IBM 360/65 computer, performs the above calculations using the following input parameters. Maximum permissible dimensions and units are given.

Card 1; (2F10.2,4I5)
- DX: grid distance (m)
- BX: rural or background source strength ($\mu g/m^2 sec$)
- NR: number of rows, including an extra 4 rows on the top & bottom
- NC: number of columns, including an extra 4 columns on either side
- Nϕ: number of corrections to area source strengths (if no corrections, put Nϕ = 1. If no area sources, put Nϕ = 0.)
- NH: number of effective source height classes

Card 2; (16I5); NN: number of stability classes

Card 3; (8F10.2); RX(10): parameters a in $\sigma_z = ax^b$

Card 4; (8F10.2); PX(10): parameters b in $\sigma_z = ax^b$

Card 5; (8F10.2); U: wind speed (m/sec)

Card 6; (8F10.2); F(16): wind direction frequency distribution beginning with NNE and going clockwise

Card 7; (20A4); ITIT1: description of area sources

Card 8; (20A4); ITIT2: description of point sources

Card 9; (20A4); ITIT3: description of concentration patterns

Card 10; (16I5); ID(30): row number of area source correction. If no correction, ID(1) = 1

Card 11; (16I5); JD(30): column number of area source correction. If no correction, JD(1) = 1

Card 12; (8F10.2); ST(30): area source corrections ($\mu g/m^2 sec$). If no correction, ST(1) = .0

Card 13; (8F10.2); S(30,30): area source strengths ($\mu g/m^2 sec$)

Card 14; (8F10.2); H(20): effective source heights (m)
Card 15; (16I5); NP(20): number of point sources in each source height class
Card 16; (16I5);IC(10,30): row number of point source
Card 17; (16I5);JC(10,30): column number of point source
Card 18; (8F10.2); QEC(10,30): point source strength (μg/sec)
If no point sources, put NH = 1, H(1) = 1, NP(1) = 1, IC(1,1) = 1, JC(1,1) = 1, QEC(1,1) = 0.0

Output

Maximum permissible dimensions are given.

1. (8F10.2); F(16): wind direction frequency distribution, beginning with NNE and going clockwise
2. (8F10.2): FU(9,9): 9 by 9 matrix of direction frequency distribution, divided by wind speed
3. NR (number of rows), NC (number of columns), Nϕ (number of area source corrections), NH (number of effective source height classes)
4. DX (grid distance [m]), BX (rural source strength [μg/m^{2}sec]), U (wind speed [m/sec])
5. R, B: current values in $\sigma_z = Rx^B$, applying to the following numbers 6-13
6. C(9,9): matrix of coefficients for area sources
7. A(30,30): concentrations (μg/m^3) due to area sources
8. H(20): current effective source height, applying to numbers 9-11
9. IC(10,30), JC(10,30), QEC(10,30): current location and magnitude of point sources
10. SS(9,9): matrix of coefficients for current point sources
11. AA(30,30): concentrations (μg/m^3) due to current point sources
12. AC(30,30): concentrations (μg/m^3) due to all sources
13. RAT(30,30): ratio of concentration due to area sources to concentration due to all sources

EXAMPLE OF OUTPUT OF PROGRAM

Consider the town of Moonshine, Tennessee (population 603), a square town which has been divided into a square grid system consisting of four 5 km by 5 km grids. Each grid square has an area source emission of 1 μg/m^{2}sec. A point source, with effective source height, H = 30m, and source strength 10^7 μg/sec, is in the center of the southwest block. The wind blows with equal frequency from all directions; *i.e.*, F(1) = F(2) . . . = F(16) = 0.67. Assume that the wind speed U equals 5 m/sec. Consider only the stability class applicable to average yearly conditions: NN = 1, RX(1) = .15, PX(1) = .75.

Other input parameters are then: DX = 5000., BX = .0, NR = 10, NC = 10, Nϕ = 1, NH = 1, ID(1) = 1, JD(1) = 1, ST(1) = .0, S(5,5) = S(5,6) = S(6,5) = S(6,6) = 1., NP = 1, IC(1,1) = 6, JC(1,1) = 5, QEC(1,1) = 10^7.

The predicted surface concentrations due to area and point sources are listed in Table 3. These numbers can be used by anyone to check whether or not they are using the program correctly.

Table 3: Source Data and Predicted Surface Concentrations at Moonshine, Tennessee

Grid Square	Area Source $\mu g/sec\ m^2$	Point Source $10^7\ \mu g/sec$	Surface Concentration Due to Area Sources $\mu g/m^3$	Surface Concentration Due to Area Sources $\mu g/m^3$
NW	1.0	0.0	34.64	0.58
NE	1.0	0.0	34.64	0.33
SW	1.0	1.0	34.64	3.70
SE	1.0	0.0	34.64	0.58

APPENDIX: PROGRAM LISTING

```
      DIMENSION S(30,30),FU(30,30),C(30,30),A(30,30),QE(30,30),D(30,30),
     1SS(30,30),AA(30,30),AC(30,30),IC(10,30),JC(10,30),QEC(10,30), ID(3
     20),JD(30),ST(100),BX(10),PX(10),ITIT1(20),ITIT2(20),ITIT3(20),N(20
     3),NP(20),AAB(30,30),HAT(30,30),F(16)
  100 FORMAT(2F10.2,4I5)
  105 FORMAT(8F10.2)
  110 FORMAT(20A4)
  163 FORMAT(16I5)
      READ(5,100) DX,BX,NR,NC,NO,NH
      DO 300 I=1,NR
      DO 300 J=1,NC
  300 S(I,J)=BX
      READ(5,163) NH
      READ(5,105) (BX(I),I=1,NH)
      READ(5,105) (PX(I),I=1,NH)
      READ(5,105) U
      READ(5,105) (F(I),I=1,16)
      READ(5,110) ITIT1
      READ(5,110) ITIT2
      READ(5,110) ITIT3
      READ(5,163) (IC(I),I=1,NO)
      READ(5,163) (JD(J),J=1,NO)
      READ(5,105) (ST(J),J=1,NO)
      JI=NC-4
      IJ=NR-4
      READ(5,105) ((S(I,J),J=5,JI),I=5,IJ)
      READ(5,105) (N(I),I=1,NH)
      READ(5,163) (NP(I),I=1,NH)
      DO 860 I=1,NH
      NNP=NP(I)
      READ(5,163) (IC(I,J),J=1,NNP)
      READ(5,163) (JC(I,J),J=1,NNP)
      READ(5,105) (QEC(I,J),J=1,NNP)
```

```
860 CONTINUE
    WRITE(6,794)  (F(I),I=1,16)
794 FORMAT(2X,9HWIND ROSE/(8F10.4))
    DO 789 I=1,9
    DO 789 J=1,9
789 FU(I,J)=.0
    E=1./8
    FU(5,5)=E
    DO 790 I=1,4
    FU(5-I,5+I)=F(2)*E
    FU(5+I,5+I)=F(6)*E
    FU(5+I,5-I)=F(10)*E
    FU(5-I,5-I)=F(14)*E
    FU(5-I,5)=F(16)*E
    FU(5,5+I)=F(4)*E
    FU(5+I,5)=F(8)*E
790 FU(5,5-I)=F(12)*E
    FU(4,5)=FU(4,5)+E*(F(1)+F(15))
    FU(5,6)=FU(5,6)+E*(F(3)+F(5))
    FU(6,5)=FU(6,5)+E*(F(7)+F(9))
    FU(5,4)=FU(5,4)+E*(F(11)+F(13))
    DO 791 I=1,2
    FU(1+I,6)=F(1)*E
    FU(4,6+I)=F(3)*E
    FU(6,6+I)=F(5)*E
    FU(6+I,6)=F(7)*E
    FU(6+I,4)=F(9)*E
    FU(6,1+I)=F(11)*E
    FU(4,1+I)=F(13)*E
791 FU(1+I,4)=F(15)*E
    FU(1,7)=F(1)*E
    FU(3,9)=F(3)*E
    FU(7,9)=F(5)*E
    FU(9,7)=F(7)*E
    FU(9,3)=F(9)*E
    FU(7,1)=F(11)*E
    FU(3,1)=F(13)*E
    FU(1,3)=F(15)*E
    WRITE(6,9)  ((FU(I,J),J=1,9),I=1,9)
  9 FORMAT(2X,37HIMPCT WIND SPEED AND FREQUENCY MATRIX/(9F10.5))
    WRITE(6,670)  NP,NC,NO,NH
670 FORMAT(2X,9HNO. ROWS=,I5,3X,12HNO. COLUMNS=,I5,3X,3HNO=,I5,3X,21HN
   10 EFFECT SOURCE HTS=,I5)
    WRITE(6,10)  DX,BX,G
 10 FORMAT(2X,9HDX IN M =,F6.0,3X,23HRURAL SOURCE STRENGTHS=,F5.1,3X,1
   11HWIND SPEED=,F10.3,5HM/SEC)
    DO 600 I=1,NR
    DO 600 J=1,NC
600 QE(I,J)=.0
    DO 167 K=1,NO
    I=ID(K)
    J=JD(K)
167 S(I,J)=ST(K)
    WRITE(6,200)  ITIT1,((S(I,J),J=1,NC),I=1,NR)
200 FORMAT(2X,20A4/(10F10.2))
    DO 162 II=1,NH
    B=BX(II)
    A=AX(II)
    WRITE(6,119)  B,A
119 FORMAT(2X,43HNEW SET OF POWER LAW PARAMETERS FOR SIGMA Z/3X,2HB=,F
   15.3,3X,2HA=,F5.3)
    IF(NO)  160,160,150
150 CONTINUE
    DO 1 I=1,9
    DO 1 J=1,9
  1 C(I,J)=.0
    BB=((DX/2.)**(1.-B))/(E*(1.-B))
    CC=9.**(1.-B)-7.**(1.-B)
    DD=.80*BB*CC
    DO 2 J=1,9,2
    C(1,J)=DD*FU(1,J)
  2 C(9,J)=DD*FU(9,J)
    DO 3 I=3,7,2
    C(I,1)=DD*FU(I,1)
  3 C(I,9)=DD*FU(I,9)
    CC=7.**(1.-B)-5.**(1.-B)
    DD=.80*BB*CC
```

```
      C(8,8)=DD*FU(8,8)
      C(2,2)=DD*FU(2,2)
      C(2,8)=DD*FU(2,8)
      C(8,2)=DD*FU(8,2)
      DO 4 J=4,6
      C(2,J)=DD*FU(2,J)
    4 C(8,J)=DD*FU(8,J)
      DO 5 I=4,6
      C(I,2)=DD*FU(I,2)
    5 C(I,8)=DD*FU(I,8)
      CC=5.**(1.-B)-3.**(1.-B)
      BB=.80*BB*CC
      DO 6 J=3,7
      C(3,J)=BB*FU(3,J)
    6 C(7,J)=BB*FU(7,J)
      DO 7 I=4,6
      C(I,3)=BB*FU(I,3)
    7 C(I,7)=BB*FU(I,7)
      CC=3.**(1.-B)-1.
      DD=.80*BB*CC
      DO 8 J=4,6
      C(4,J)=DD*FU(4,J)
    8 C(6,J)=DD*FU(6,J)
      C(5,4)=DD*FU(5,4)
      C(5,6)=DD*FU(5,6)
      C(5,5)=.80*BB*FU(5,5)
      WRITE(6,11)  ((C(I,J),J=1,9),I=1,9)
   11 FORMAT(2X,39HMATRIX OF COEFFICIENTS FOR AREA SOURCES/(9F10.5))
      DO 500 I=5,IJ
      DO 500 J=5,JI
      A(I,J)=.0
      DO 500 K=1,9
      DO 500 L=1,9
  500 A(I,J)=C(K,L)*S(I-5+K,J-5+L)+A(I,J)
      WRITE(6,95)
   95 FORMAT(2X,34HCONCENTRATIONS FROM GROUND SOURCES)
      WRITE(6,110)  ITIT3
      WRITE(6,700)  ((A(I,J),J=5,JI),I=5,IJ)
  700 FORMAT(8F10.4)
  160 IF(QEC(1,1))  162,162,161
  161 CONTINUE
      WRITE(6,202)
  202 FORMAT(2X,16HELEVATED SOURCES)
      WRITE(6,110)  ITIT2
      DO 899 I=5,IJ
      DO 899 J=5,JI
  899 AAE(I,J)=.0
      DO 880 NI=1,NN
      DO 874 KL=1,NE
      DO 874 KE=1,NC
  874 QE(KL,KE)=.0
      WRITE(6,871)  H(NI)
  871 FORMAT(2X,26HEFFECTIVE SOURCE HEIGHT = ,F10.3)
      WRITE(6,872)
  872 FORMAT(10X,6HROW NO.,3X,9HCOLUMN NO.,4X,25HEMISSION(MICROGM PER SEC)
     1)
      NNP=NP(NI)
      WRITE(6,873)  ((IC(NI,K),JC(NI,K),QEC(NI,K)),K=1,NNP)
  873 FORMAT(2I12,F20.5)
      DO 164 K=1,NNP
      I=IC(NI,K)
      J=JC(NI,K)
  164 QE(I,J)=QEC(NI,K)
      DO 81 L=1,9
      DO 81 K=1,9
   81 D(I,K)=0.0
      II=H(NI)**2./2.
      P=EXP(-II/(B**2.*((DX/2.)**(2.*B))))
      PA=B*((DX/2.)**(B+1.))
      IIBT=.0
      DDP=.0
      II2=DX/2.
      DO 948 IJJ=1,100
      IF(IJJ-10)  952,952,953
  952 DB=100.
      GO TO 954
```

```
953 DR=1000.
954 DDDR=DDR+DR/2.
    DDR=DDR+DR
    XYZ=XY/(R**2.*(DDDR**(2.*B)))
    IF(XYZ-20.) 960,960,961
960 XINT=XINT+DR*EXP(-XYZ)/(DDDR**B)
961 CONTINUE
    IF(XX2-DDR) 955,955,948
955 IJJ=100
948 CONTINUE
    D(5,5)=XINT/(8.*R*XX2**2.)
    DO 71 L=1,4
    E=2*L
    EP=E**(2.*B)
    XP=1.*E
    PE=XP**(2.*B)
    Z=P**(1./EP)/(PA*(E**(B+1.)))
    IF(L-1) 950,950,949
949 D(5,5+L)=Z
    D(5,5-L)=Z
    D(5+L,5)=Z
    D(5-L,5)=Z
    GO TO 951
950 D(5,6)=Z/3.
    D(5,4)=Z/3.
    D(6,5)=Z/3.
    D(4,5)=Z/3.
951 Z=P**(1./PE)/(PA*(XP**(B+1.)))
    D(5+L,5+L)=Z
    D(5-L,5+L)=Z
    D(5+L,5-L)=Z
 71 D(5-L,5-L)=Z
    DO 72 L=1,2
    QQ=2*L+2
    QQ=1.1*QQ
    G=QQ**(2.*B)
    Z=P**(1./G)/(PA*(QQ**(B+1.)))
    D(4-L,6)=Z
    D(4-L,4)=Z
    D(6+L,4)=Z
    D(6+L,6)=Z
    D(4,4-L)=Z
    D(6,4-L)=Z
    D(4,6+L)=Z
 72 D(6,6+L)=Z
    Z=P**(.125**(2.*B))/(PA*(8.**(B+1.)))
    D(1,3)=Z
    D(1,7)=Z
    D(3,1)=Z
    D(3,9)=Z
    D(7,1)=Z
    D(7,9)=Z
    D(9,3)=Z
    D(9,7)=Z
    DO 91 K=1,9
    DO 91 L=1,9
 91 SS(K,L)=2.0*D(K,L)*FU(K,L)
    WRITE(6,92) ((SS(I,J),J=1,9),I=1,9)
 92 FORMAT(2X,33HCOEFFICIENTS FOR ELEVATED SOURCES/(9F12.11))
    DO 510 I=5,IJ
    DO 510 J=5,JI
    AA(I,J)=.0
    DO 410 K=1,9
    DO 410 L=1,9
    ADD=SS(K,L)*QE(I-5+K,J-5+L)
    AA(I,J)=AA(I,J)+ADD
410 AAB(I,J)=AAB(I,J)+ADD
510 CONTINUE
    WRITE(6,96) H(NI)
 96 FORMAT(2X,50HCONCENTRATIONS FROM ELEVATED SOURCES WITH HEIGHT =,F1
   10.3)
    WRITE(6,110) ITITJ
    WRITE(6,700) ((AA(I,J),J=5,JI),I=5,IJ)
880 CONTINUE
    IF(NO) 166,162,166
```

```
166 CONTINUE
    IF(NN) 169,162,169
169 CONTINUE
    DO 520 I=5,IJ
    DO 520 J=5,JI
    AC(I,J)=A(I,J)+AAB(I,J)
520 RAT(I,J)=A(I,J)/AC(I,J)
    WRITE(6,97)
 97 FORMAT(2X,31HCONCENTRATIONS FROM ALL SOURCES)
    WRITE(6,110) ITITJ
    WRITE(6,700) ((AC(I,J),J=5,JI),I=5,IJ)
    WRITE(6,890)
890 FORMAT(2X,65HRATIO OF CONCENTRATION DUE TO AREA SOURCES TO TOTAL C
   1ONCENTRATION)
    WRITE(6,700) ((RAT(I,J),J=5,JI),I=5,IJ)
162 CONTINUE
    STOP
    END
```

REFERENCES

1. Gifford, F. A., Jr., and S. R. Hanna, 1970: Urban air pollution modelling, presented at 1970 Meeting of the Int. Union of Air Poll. Prev. Assoc., Washington, Dec. 11, 1970, 17 pp + 7 figs.
2. Hanna, S. R., 1971: A simple method of calculating dispersion from urban area sources, *J. Air Poll. Control Assoc., 21*, 774-777.
3. Hanna, S. R. and S. D. Swisher, 1970: Air Pollution Meteorology of the Rockwood-Harriman, Tennessee, Industrial Corridor. Atm. Turb. and Diff. Lab. Rept. 40, Box E, Oak Ridge, Tennessee, 21 pp.
4. Hanna, S. R., 1972: An Air Quality Model for Knox County, Tennessee. Atm. Turb. and Diff. Lab., Rept. 55, Box E, Oak Ridge, Tennessee, 34 pp.
5. Gifford, F. A., 1959: Computation of pollution from several sources. *Int. J. of Air Poll., 2*, 109-110.
6. Smith, M. E. (Editor), 1968: Recommended guide for the prediction of the dispersion of airborne effluents, ASME., ix and 85 pp.
7. Slade, D. (Editor), 1968: *Meteorology and Atomic Energy, 1968*, USAEC Rept. No. TID-24190, x and 445 pp.
8. Briggs, G. A., 1969: *Plume Rise*, USAEC Rpt. No. TID-25075, vi + 82 pp.

Appendix E

SPECTRAL EXTINCTION COEFFICIENTS FOR SOME SMOKES

The appended curves are reproduced from the following two reports:

(1) Milham, M.E. et al, "New Findings on the Nature of WP/RP Smokes," USARRADCOM TRARSCL-TR-77067, July 1977: Figs. D-1, D-2.

(2) Milham, M., "A Catalog of Optical Extinction Data for Various Aerosols/Smokes," Edgewood Arsenal Special Pub., ED-SP-77002; June 1976.

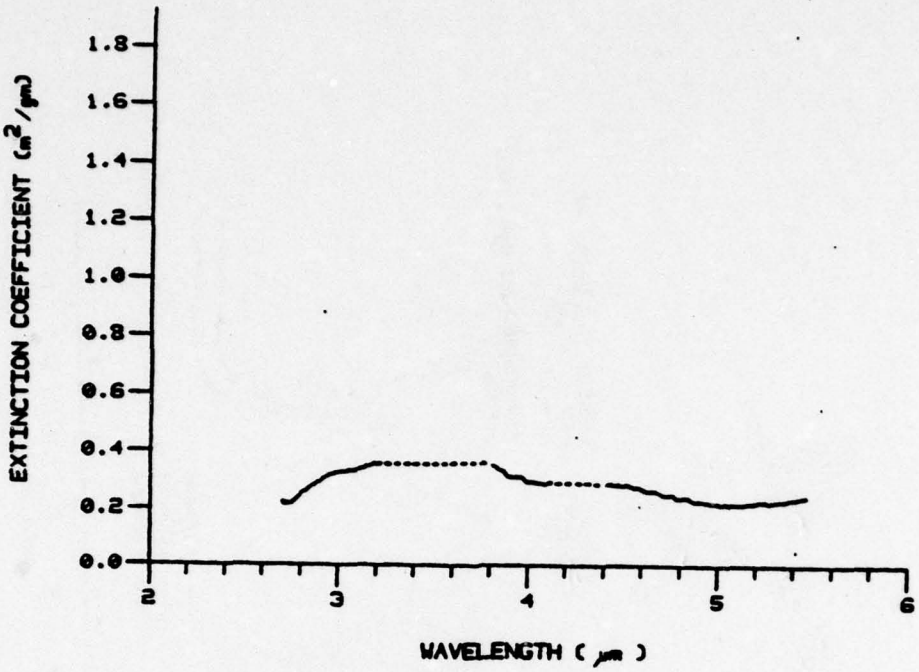

Fig. D-1 . Experimental Low Relative Humidity WP/RP Spectrum
(3- to 5-μm region)

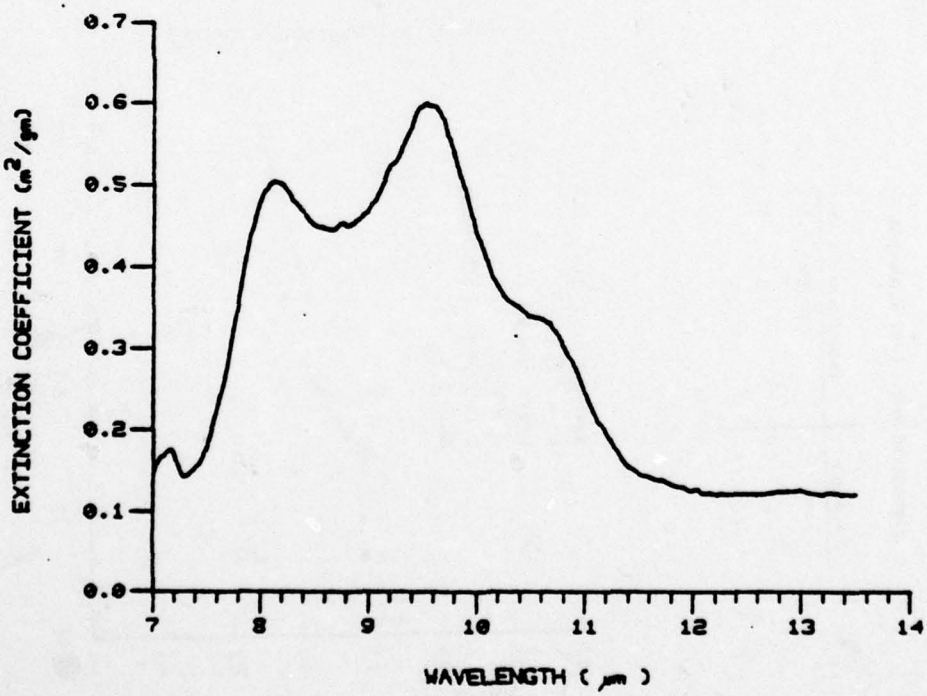

Fig. D-2 Experimental Low Relative Humidity WP/RP Spectrum
(7- to 14-μm region)

Fig. D-3 Red Phosphorus Smoke, 3 to 5 μm and 8 to 13 μm, Test Date: 20 November 1975.

Experimental Data: Laser Wavelengths

Wavelength	Extinction coefficient
μm	m^2/gm
.63	1.8
1.06	1.5

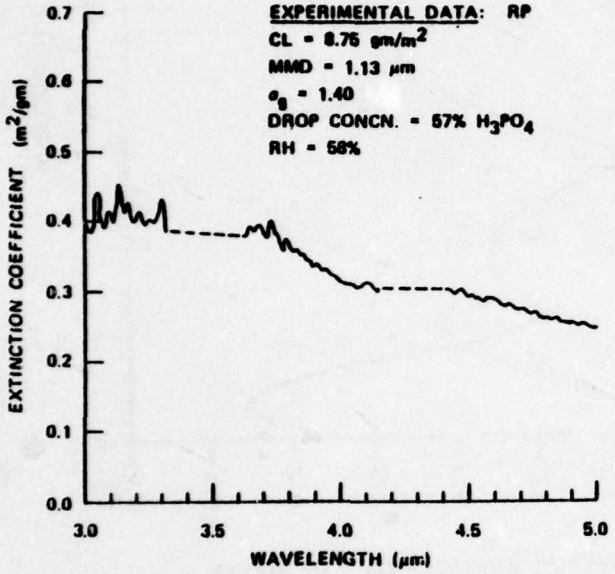

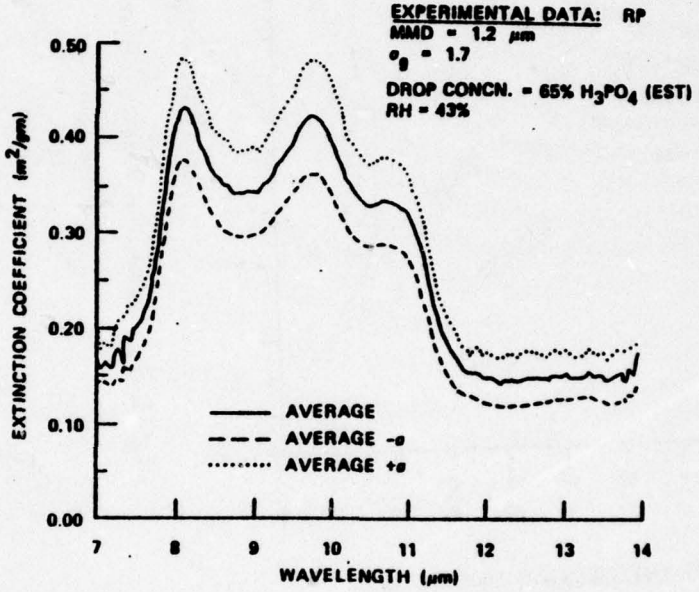

Fig. D-4 FS Smoke, 3 to 5 μm and 8 to 13 μm, Test Date: 19 November 1975.

Experimental Data: Laser Wavelengths

Wavelength	Extinction coefficient
μm	m^2/gm
.63	4.5
1.06	2.0

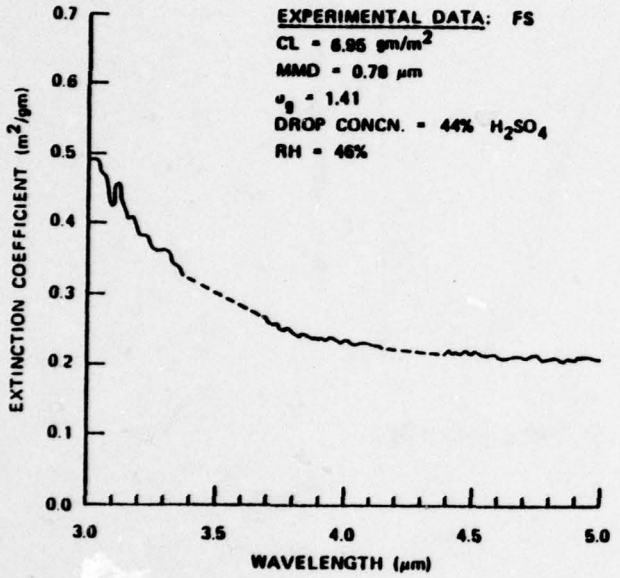

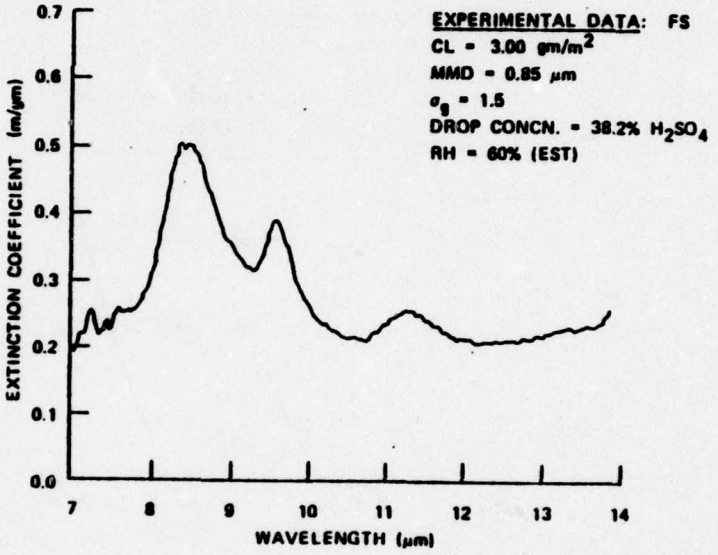

Fig. D-4 Cont'd

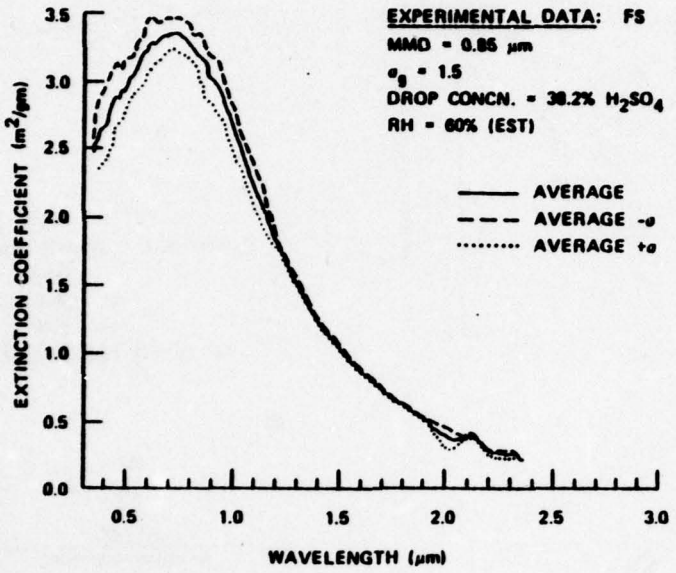
EXPERIMENTAL DATA: FS
MMD = 0.85 μm
σ_g = 1.5
DROP CONCN. = 38.2% H_2SO_4
RH = 60% (EST)
AVERAGE
AVERAGE -σ
AVERAGE +σ
EXTINCTION COEFFICIENT (m^2/gm)
WAVELENGTH (μm)
0.0
0.5
1.0
1.5
2.0
2.5
3.0
3.5

Fig. D-5 HC SMOKE (ZINC OXIDE, ALUMINUM, HEXACHLOROETHANE) EXPERIMENTAL DATA. 3 to 5 μm AND 8 to 13 μm, Test Date: 19 November 1975.

Experimental Data: Laser Wavelengths

Wavelength	Extinction coefficient
μm	m^2/gm
.63	1.4
1.06	1.5

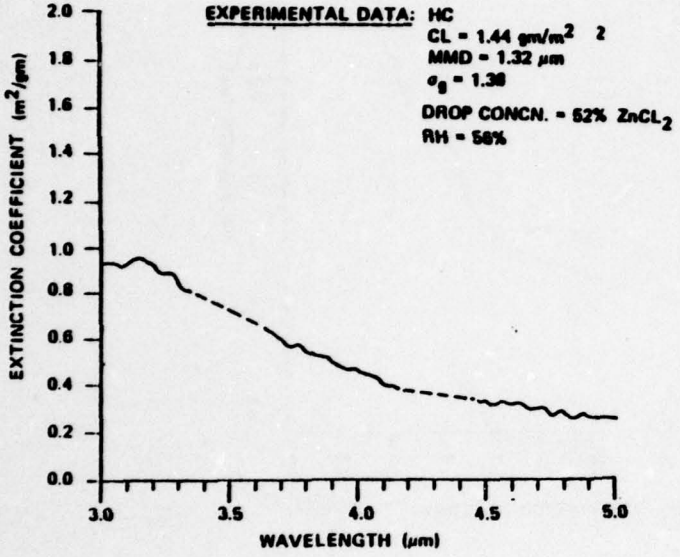

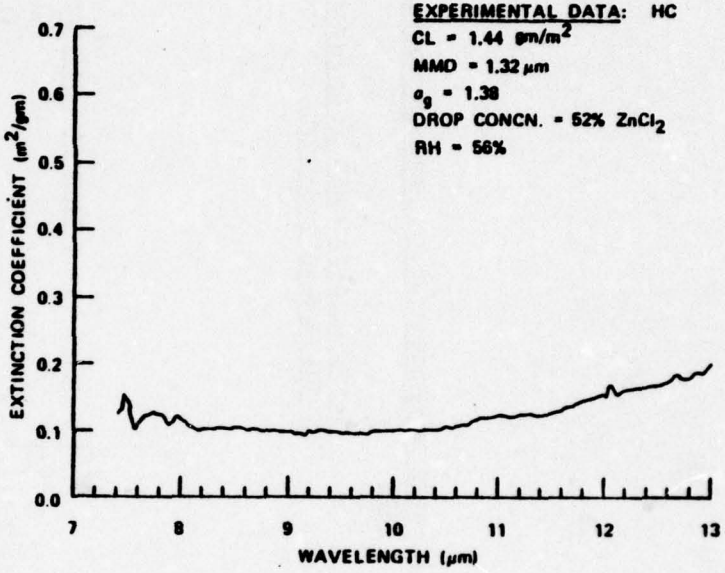

Fig. D-6 FOG OIL SMOKE (LOW-VOLATILITY HYDROCARBON DISTILLATE) EXPERIMENTAL DATA.

1. Fog Oil Smoke, 0.4 to 2.4 μm, 3 to 5 μm, and 8 to 13 μm (IMBIBER BEAD DEVICE). Test Date: 2 December 1975.

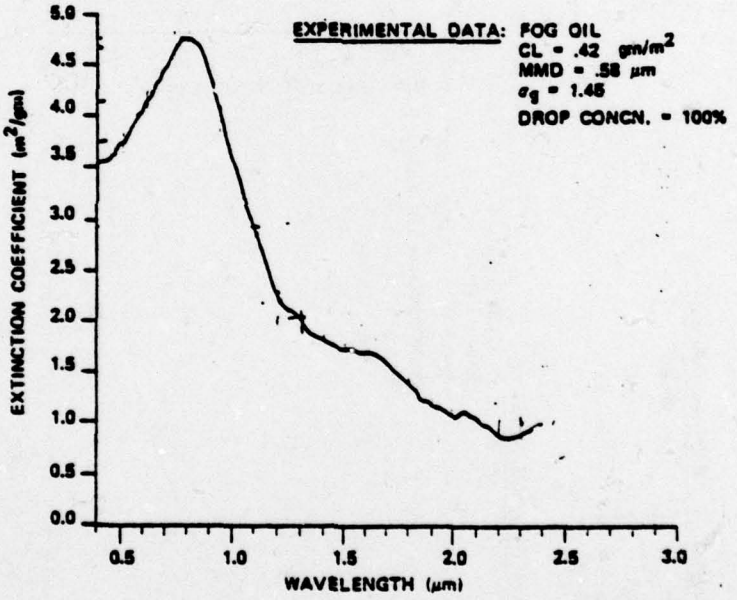

Fig. D-6 Cont'd

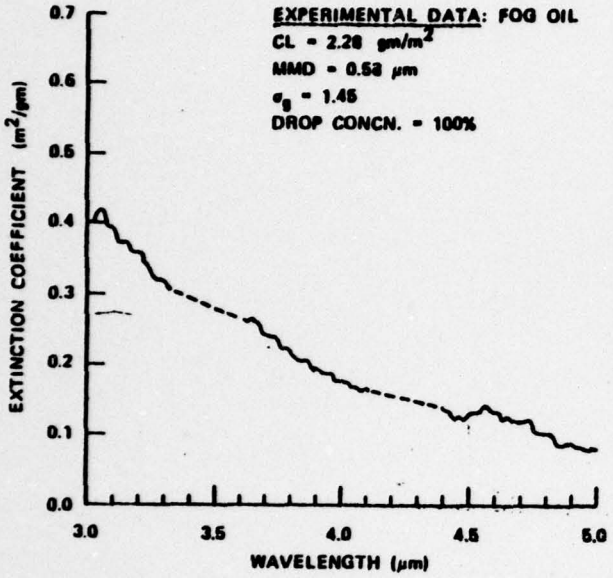
EXPERIMENTAL DATA: FOG OIL
CL = 2.28 gm/m²
MMD = 0.58 μm
σg = 1.45
DROP CONCN. = 100%
EXTINCTION COEFFICIENT (m²/gm)
0.0
0.1
0.2
0.3
0.4
0.5
0.6
0.7
3.0
3.5
4.0
4.5
5.0
WAVELENGTH (μm)

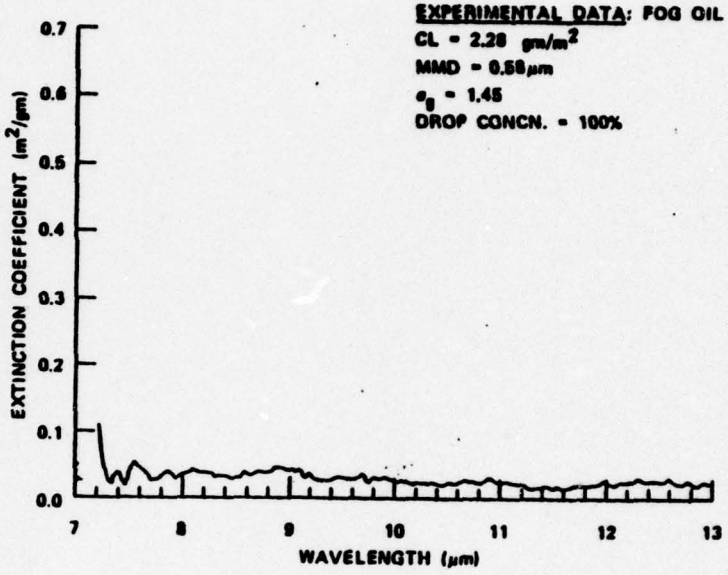
EXPERIMENTAL DATA: FOG OIL
CL = 2.28 gm/m²
MMD = 0.58 μm
σg = 1.45
DROP CONCN. = 100%
EXTINCTION COEFFICIENT (m²/gm)
0.0
0.1
0.2
0.3
0.4
0.5
0.6
0.7
7
8
9
10
11
12
13
WAVELENGTH (μm)

Appendix F

SMOKE PATH LENGTH

For illustrative purposes, we present here, a brief discussion of the geometry of the path through a smoke cloud.

Consistent with the model of a right cone we will derive some expressions for the path length, L, through the smoke plume.

We consider the smoke source to be the origin of coordinates (o,o,o) and consider the observer and target coordinates to be (x_o,y_o,o) and (x_t,y_t,o) respectively. See Fig. E-1

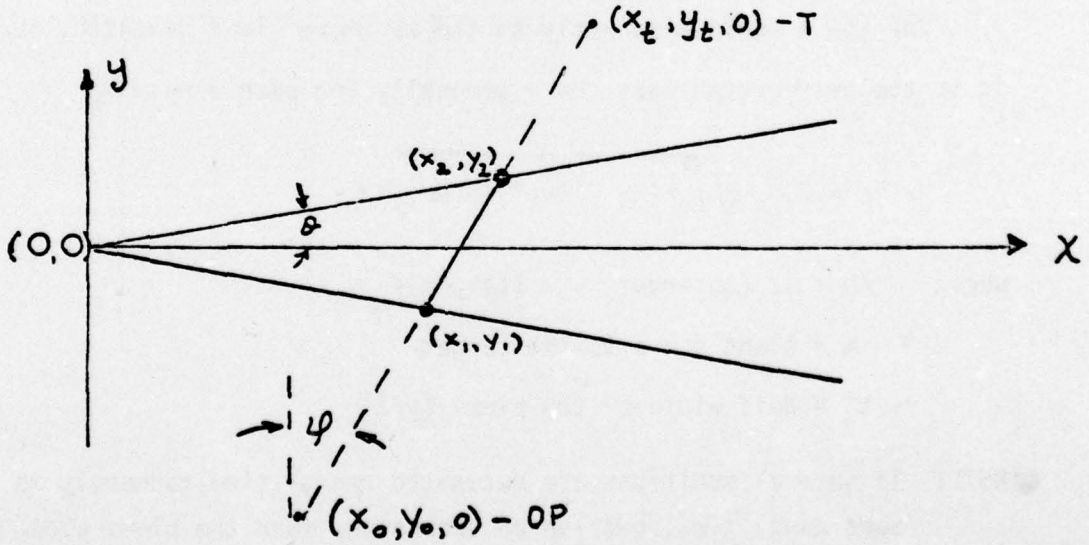

Fig. E-1 Geometrical Arrangement

From Fig. E-1 we can write the following for the coordinates of the segment through the plume

$$x_1 = (y_o + y_o \tan\phi)/(\text{Cot}\ \phi + \tan\theta)$$

$$y_1 = -\tan\theta \cdot x_1$$

$$x_2 = (y_o + x_o \tan\phi)/(\text{Cot}\ \phi + \tan\theta)$$

$$y_2 = \tan\theta = (9.1 + Ax)/2x$$

and, its length, L, is

$$L = 2(y_o + x_o\ \text{Cot}\ \phi)(\text{Cot}\ \phi + \theta)/(\text{Cot}^2\theta \cdot \text{Cot}^2\phi - 1)^{\frac{1}{2}}$$

where $\tan\theta = (9.1 + Ax)/2x$

It should be noted that in the limit, $\lim_{x\to\infty} \text{Cot}\ \theta = 2/A$.

When OP-T is normal to the x-axis then $L = 2x_o\ \text{Cot}\ \theta$.

The above would also apply to the WP smoke cloud geometry, i.e., it is the near ground case. More generally the path length is

$$L = 2\,\frac{R}{\Delta h}\sqrt{r_2^2(t) - [h(T)-h(\overline{OP})]^2}$$

where $\Delta h = |Z\ (\text{observer}) - Z\ (\text{target})|$

R = slant range to the target

$r_2(t)$ = half width of the plume (y/2)

NOTE: If several munitions are detonated nearby simultaneously in the same zone, i.e., overlap on expansion, then the plume width and concentration can be treated as additive provided the spatio temporal history is accounted for correctly.

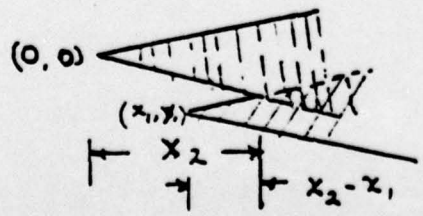

$$x_2 = x_1 + \bar{u}(t_2 - t_1)$$

Appendix G

PLUME HEIGHT

In Table 7 we have defined the vertical rise as $2.93 + A \cdot x$ where A depends upon Pasquill category. For modelling purposes we have proposed a fixed value for each category. Actually the parameter "A" varies continuously with mean wind speed, $\bar{u}$, for values ≤ 5 m/sec. Although smoke normally is not discharged in $\bar{u} \leq 2$ m/sec because of the horizontal coverage is low, for completeness we present the value of A for $0.5 \leq u < 5$ m/sec. The latter will cover stability categories A, B, and C.

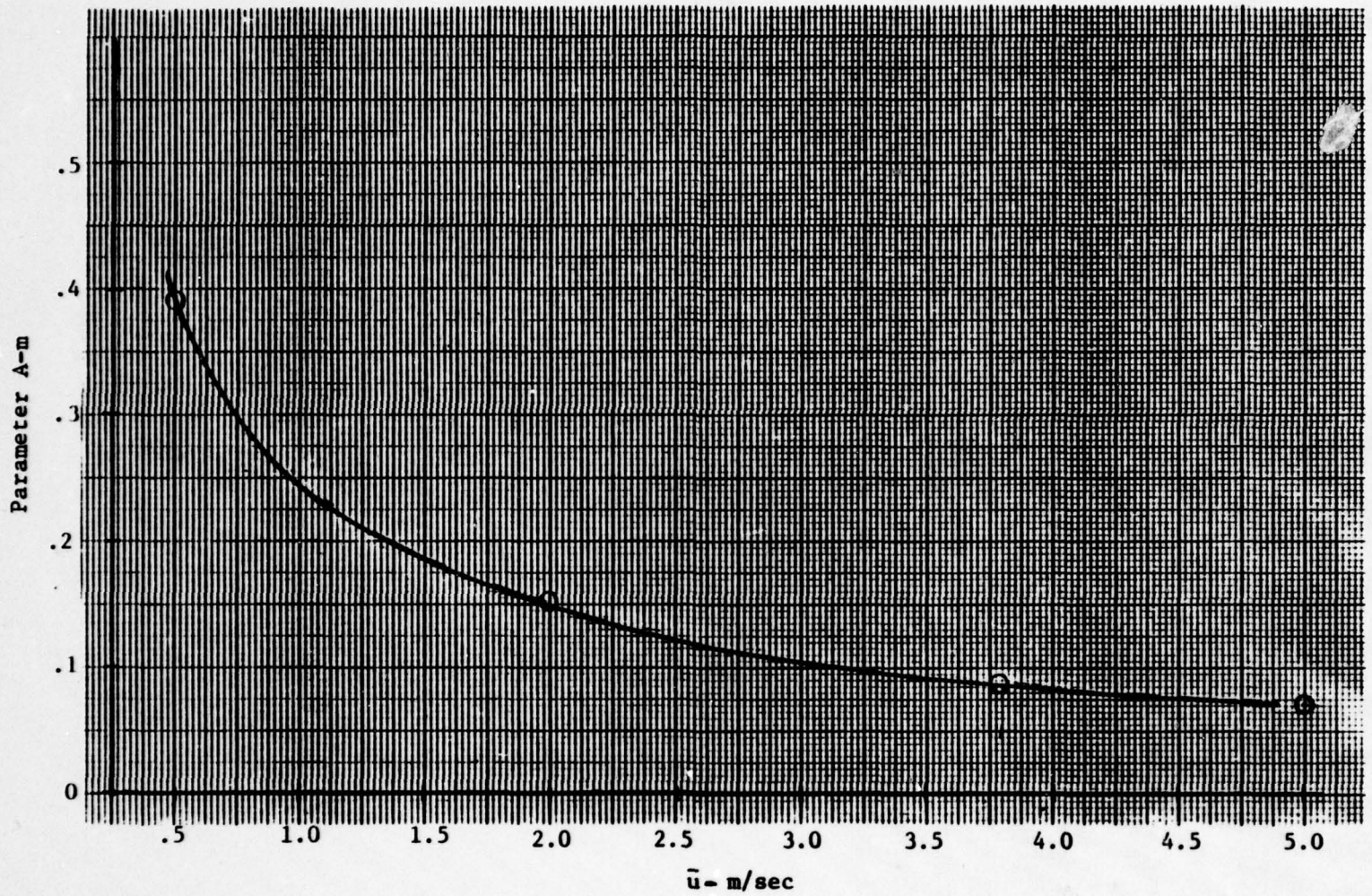

Fig. G.1 Plume Rise at Low Wind Speeds
$z(t) = 2.73 + A(\bar{u}t)$

DISTRIBUTION LIST

ORGANIZATION	COPIES
Deputy Under Secretary of the Army (Operations Research) ATTN: Mr. Woodall, Dr. Fallin HQ, Department of the Army Washington, DC 20310	2
HQ DA ODCSOPS ATTN: DAMO-RQD (LTC T. Hamilton) Washington, DC 20310	1
Commander US Army Material Development and Readiness Command ATTN: DRCBSI (BG Moore) 5001 Eisenhower Avenue Alexandria, VA. 22333	1
Director Defense Intelligence Agency ATTN: DT-1A (Mr. Berler) Pentagon Washington, DC 20310	1
Director Night Vision & Electro-Optics Laboratory ATTN: DELNV-D (John Johnson) DELNV-VI (Joseph Moulton, Frank Shields, Dr. Jim Ratches, Luanne Obert, Tom Cassidy, Rich Bergemann) Ft. Belvoir, Virginia 22060	7
Defense Documentation Center Cameron Station Alexandria, Virginia 22314	2
Commander US Army Training & Doctrine Command ATTN: ATCD-TEC (Dr. M.P. Pastel) Ft. Monroe, VA. 23651	1

Commander 4
US Army Combined Arms Combat Developments
Activity
ATTN: ATCA-CAP-B (Mr. K. Pickett)
ATCA-CAT (Mr. Robert Dekinder, Jr.)
ATCA-TSM-K (LTC Enlow)
ATC-TSM-K (LTC Douglass Bacon)
Ft. Leavenworth, KS 66027

Commander 5
US Army Material Systems Analysis Facility
ATTN: DRXSY-LA (Paul Frosell), DRXSY-CSD (Tom Dolce)
DRXSY-GI (Dan Kirk)
DRXSY-GI (Sid Gerard)
DRXSY-GP (Fred Campbell)
Aberdeen Proving Ground, MD 21005

PM Smoke/Obscurants 3
ATTN: DRCPM-SMK-T (COL Shelton)
DRCPM-SMK-T (Joe Steedman)
DRCPM-SMK-T (Gene Bowman)
Bldg 324
Aberdeen Proving Ground, MD 21005

Commander 1
US Army Ballistics Research Laboratories
ATTN: DRDAR-BLB (A. LaGrange)
Aberdeen Proving Ground, MD 21005

Commander 4
USAARRADCOM
Chemical Systems Laboratory
ATTN: DRDAR-CLY-A (R.O. Pennsyle)
DRDAR-CLB-PS (J. Vervier)
DRDAR-CLB-PS (Dr. Steubing)
DRDAR-CLN (T. Tarnove)
Aberdeen Proving Ground, MD 21010

Commander 2
US Army Ordnance and Command Center
and School
ATTN: ATSL-CL (Dr. Welch)
ATSL-CLC-C (MAJ Colclasure)
Aberdeen Proving Ground, MD 21010

Commander 1
US Army Test and Evaluation Command
ATTN: DRSTE-AD-M (Warren Baity)
Aberdeen Proving Ground, MD 21005

Commander 2
US Army Dugway Proving Ground
ATTN: STEDP-PA (Dr. L. Solomon)
STEDP-PP (Mr. E. Peterson)
Dugway, UT 84022

Commander 6
Atmospheric Sciences Laboratory
ATTN: DELAS-AE-E (Dr. L. Duncan), DELAS-BE (Fred Horning)
DRSEL-BL-MS-A (Dr. Gomez)
DRSEL-BL-MS-A (J. Lindberg)
DRSEL-BL-MS-A (F. Niles)
DELAS-EO (James B. Mason)
White Sands Missile Range, NM 88002

Commander 8
US Army TRADOC Systems Analysis Activity
ATTN: ATAA-D (Dr. Wilbur Payne)
ATTA-TDB (Dr. Stadtlander)
ATTA-TDB (Mr. Dominquez)
ATTA-TDB (Mr. Bustillos)
ATTA-DBB (Doyle Banks)
ATAA-TA (Mr. Maceo Scott)
ATAA-TGP (Anita Oniveras)
ATAA-TEM (Mr. Hugh McCoy)
White Sands Missile Range, NM 88002

Commander 3
US Army Missile Research and Development Command
ATTN: DRDMI-CGA (Dr. B. Fowler)
DRDMI-REW (Mr. Widenhofer)
DRDMI-TEG (Mr. Howard Race)
Redstone Arsenal, AL 35809

Commander 1
US Army Missile Research &
Development Command
OPM-GLD MIRADCOM
ATTN: DRCPM-LDT (Mr. S.E. Thomas)
Redstone Arsenal, AL 35809

Commanding Officer 1
US Army Electronic Proving Ground
ATTN: STEEP-MT-SI (Mr. Bell)
Ft. Huachuca, AZ 85613

Commander 1
US Army Electronics Command
ATTN: DRDEL-AP-OA-FM (Mr. Hank Olson)
Ft. Monmouth, NJ 07703

Commander
Harry Diamond Laboratories
ATTN: DELHD-RAC (Dr. Z. Sztankay)
DELHD-RAC (Robert Humphrey)
DRXDO-RAF (Dr. Giglio)
DELHD-SD (Dr. W. Pepper)
2800 Powder Mill Road
Adelphi, MD 20783 — 4

Commander
US Army Mobility Equipment Research
& Development Command
ATTN: DRXFB-RCT (Fred Kezer, Rick Berg)
Ft. Belvoir, VA 22060 — 2

Commandant
US Army Infantry Center and School
ATTN: ATSH-CD-CS (OR/SA)(Dr. Dyer)
Ft. Benning, GA 31905 — 1

Commandant
US Army Field Artillery School
ATTN: ATSF-G-RA (MAJ John Kehres)
Ft. Sill, OK 73503 — 1

Commandant
US Army Armor School
ATTN:: ATZK-CD-SB (MAJ Brinkley, Mr. Gene Hilkenmeyer)
Ft. Knox, KY 40121 — 2

Commander
President US Army Armor and Engineer Board
ATTN: ATZK-AE-AR (MAJ Sanford)
Ft. Knox, KY 40121 — 1

Commander
US Army Aviation Center and School
ATTN: ATZQ-ASH-SSG-RO (LTC Brown)
ATCQ-D (Mr. Maccabe)
Ft. Rucker, AL 36360 — 2

Commander
US Army Engineer Waterways
Experimental Station
ATTN: Mr. Gerry Lundien
Vicksburg, Miss. 39180 — 1

Commander
Concepts Analysis Agency
ATTN: MOCA-SM (COL W. Spilker, H. Hock, E. Rose)
8120 Woodmont Avenue
Bethesda, MD 21004 — 3

Project Manager, AAH
ATTN: DRCPM-AAH-TM-S (Mr. Reago)
St. Louis, MO 63166 — 1

Project Manager
XM1 Tank System
ATTN: DRCPM-GCM-SI (Mr. Carson)
MAMP, Bldg 1
Warren, MI 48090 — 1

US Army ITAC
FANX III
National Security Agency
ATTN: Mr. Bob Wooldridge
Washington, DC — 1

DRSRDA
Pentagon
ATTN: LTC Dave Click
Rm. 3E433
Washington, DC 20310 — 1

US Air Force Airstaff
Directorate of Concepts
Pentagon
ATTN: MAJ E. Duff
Rm. 1E388
Washington, DC 20310 — 1

US Air Force Airstaff
Directorate of Concepts & Analysis
Pentagon
ATTN: Special Assistant for Weather (MAJ E. Kolczynski)
Rm. 1D380B
Washington, DC 20310 — 1

Commander
Wright-Patterson AFB
ATTN: AFAL-WRP-3 (Paul Huffman)
Dayton, OH 45433 — 1

Commander
Eglin Air Force Base
ATTN: AFATL-DCMT (Mr. Burnett)
Eglin AFB, FL 32542 — 1

Commander
Naval Weapons Support Center
ATTN: Code 5042 (Dr. Karl Dinerman, Dr. Duane Johnson)
Crane, IN 47522 — 2

Commander 2
Naval Weapons Center
ATTN: Code 3522 (Dr. Wade Swinford)
Code 2173 (Dr. Alex Shlanta)
China Lake, CA 93555

Commander 1
Naval Air Systems Command
ATTN: Code Air-e10C (Dr. H. Rosenwasser)
Washington, DC 20361

Commanding Officer 1
Naval Intelligence Support Center
ATTN: NISC (Code 433)(H.F. St. Aubin)
4301 Suitland Road
Suitland, MD 20390

Commander 1
Naval Surface Weapons Center
ATTN: Diane L. Shamblin
Code DG-302
Dahlgren, VA 22448

Commanding General 1
Marine Corps Development Center
ATTN: Firepower (Code D092)(CPT Dennis Morga)
Quantico, VA 22134

Director 1
Advanced Research Projects Agency
ATTN: Dr. Jim Tegnelia
1400 Wilson Blvd.
Arlington, VA 22209

Director 1
Oklahoma State Field Office
ATTN: Dr. Marv Smith
Eglin Air Force Base, FL 32542

The Rand Corporation 1
ATTN: Mr. Ralph Huschke
1700 Main Street
Santa Monica, CA 90406

CIA 1
ATTN: OSR-CIR (Mr. L. Blackwell)
Washington, DC 20505

CRDV/DREV 1
CP880 ATTN: Robert Corriveau
Courcelette, Quebec
Canada
GOA-IRO

Institute of Defense Analysis 2
Science and Technology Division
ATTN: Mr. L. Biberman
Dr. R. Roberts
400 Army-Navy Drive
Arlington, VA. 22202